IMPACT OF TITANIUM DIOXIDE NANOPARTICLES ON THE NUTRITIONAL COMPOSITION OF *Haematococcus pluvialis*

MANISHAA SRI A/P MAHENDRAN

MASTER OF SCIENCE

FACULTY OF SCIENCE

UNIVERSITI TUNKU ABDUL RAHMAN

MAY 2023

IMPACT OF TITANIUM DIOXIDE NANOPARTICLES ON THE NUTRITIONAL COMPOSITION OF *Haematococcus pluvialis*

By

MANISHAA SRI A/P MAHENDRAN

A dissertation submitted to Faculty of Science

Universiti Tunku Abdul Rahman

in partial fulfillment of the requirements for the degree of

Master of Science

May 2023

ABSTRACT

IMPACT OF TITANIUM DIOXIDE NANOPARTICLES ON THE NUTRITIONAL COMPOSITION OF *Haematococcus pluvialis*

MANISHAA SRI A/P MAHENDRAN

Haematococcus pluvialis (*H. pluvialis*) is farmed worldwide due to its nutrient-rich properties and provides multiple benefits to human health. However, the wide usage of titanium dioxide nanoparticles (TiO_2 NPs) causes nano pollution of water bodies due to the presence of TiO_2 NPs residue in domestic and industrial wastes which may affect the nutritional quality of *H. pluvialis*. Hence, this study aimed to investigate the interaction and accumulation of TiO_2 NPs on *H. pluvialis* and determine the changes in biomass and nutritional value of *H. pluvialis* due to the exposure to TiO_2 NPs. The cellular interaction and accumulation of TiO_2 NPs on *H. pluvialis* were examined through Fourier transformed infrared (FTIR) spectroscopy and Scanning electron microscope (SEM). The loss in biomass together with the macromolecules, pigments, and phenolic compounds of *H. pluvialis* was investigated upon treating with various concentrations of TiO_2 NPs (5, 10, 25, 50 and 100 µg/mL) for 24, 48 72 and 96 h. The Energy dispersive X-ray (EDX) analysis confirmed the surface accumulation of TiO_2 NPs on *H. pluvialis* cells, while SEM images evidenced the surface alterations and damage of the treated cells. The functional groups such as hydroxyl, amine, methyl, amide I, amide II, carboxyl, carbonyl, and phosphate groups from the cell wall of the *H.*

pluvialis were identified to be possibly involved in the interaction of TiO_2 NPs with *H. pluvialis*. The results showed that the treatment of *H. pluvialis* with TiO_2 NPs caused a dose and time-dependent reduction in biomass, macronutrients, pigments, and phenolic compounds. The highest detrimental effects were found at 96 h with the reported values of 43.29 ± 2.02%, 67.05 ± 0.99%, 48.67 ± 0.18% and 44.22 ± 0.49% reduction in biomass, proteins, carbohydrates and lipids, respectively, along with 39.31 ± 2.54%, 34.92 ± 0.84%, 34.24 ± 0.36%, and 42.66 ± 0.94% loss in chlorophyll-a, carotenoids, astaxanthin, and total phenolic compounds of *H. pluvialis* for 100 µg/mL of TiO_2 NPs. Hence, the study confirmed that the exposure of TiO_2 NPs is detrimental to *H. pluvialis* where the interaction and accumulation of TiO_2 NPs on *H. pluvialis* caused reduction in biomass, macromolecules, pigments, and total phenolic compounds. The finding on how TiO_2 NPs affect nutrient microalga *H. pluvialis*'s nutritional qualities will be helpful in evaluating the environmental effect of TiO_2 NPs in waterways. The data will also aid in the development of methods for screening TiO_2 NPs contamination in microalgae which may otherwise pose delirious effects to the consumers.

ACKNOWLEDGEMENT

The accomplishment of this project required a lot of guidance and assistance, and I am extremely fortunate enough to have got this throughout the study. Firstly, I would like to thank God the Almighty for all the blessings being poured on me and the guidance throughout my life. Heartful thanks to my parents, Mr. Mahendran, and Mrs. Kanageswari for providing me such privileges in studies and for making my future better. Next, I would like to express my appreciation to my supervisor, Dr. Anto Cordelia Tanislaus Antony Dhanapal for all her guidance, support, trust and assistance for the completion of this study. I would like to thank my co-supervisor, Dr. Sinouvassane Djearamane, for his guidance, support and advice, throughout the work. I have learned a lot from my supervisors and have broadened my perspective in this studied area. This research was supported by Universiti Tunku Abdul Rahman (Grant no: IPSR/RMC/UTARRF/2020-C1/A05). I would like to express this appreciation to the university UTAR for providing this opportunity to complete my project with sufficient facilities and equipment.

I would also not forget to remember my friends Sharolynne Liang Xiao Tong, Harshyini Maheswaran and Hemaroopini Subramaniam for their moral support and guidance during the research. I would like to send my warm and heartiest appreciation to those who have contributed to the successful completion of this

project. A million thanks to those who involved themselves directly and indirectly in all aspects to complete this study.

DECLARATION

I MANISHAA SRI A/P MAHENDRAN hereby declare that the dissertation is based on my original work except for quotations and citations which have been duly acknowledged. I also declare that it has not been previously or concurrently submitted for any other degree at UTAR or other institutions.

(MANISHAA SRI A/P MAHENDRAN)

Date: 23 May 2023

APPROVAL SHEET

This dissertation entitled "**IMPACT OF TITANIUM DIOXIDE NANOPARTICLES ON THE NUTRITIONAL COMPOSITION OF *Haematococcus pluvialis***" was prepared by and submitted as partial fulfillment of the requirements for the degree of Master of Science at Universiti Tunku Abdul Rahman.

Approved by:

_____

(Dr. Anto Cordelia Tanislaus Antony Dhanapal) Date: 23 May 2023
Supervisor
Department of Chemical Science
Faculty of Science
Universiti Tunku Abdul Rahman

_____

(Dr. Sinouvassane Djearamane) Date: 23 May 2023
Co-Supervisor
Department of Allied Health Science
Faculty of Science
Universiti Tunku Abdul Rahman

FACULTY OF SCIENCE

UNIVERSITI TUNKU ABDUL RAHMAN

Date: 23 May 2023

SUBMISSION OF DISSERTATION

It is hereby certified that **MANISHAA SRI A/P MAHENDRAN** (ID No: **20ADM00763**) has completed this dissertation entitled "IMPACT OF TITANIUM DIOXIDE NANOPARTICLES ON THE NUTRITIONAL COMPOSITION OF *Haematococcus pluvialis*" under the supervision of Dr. Anto Cordelia Tanislaus Antony Dhanapal (Supervisor) from the Department of Chemical Science, Faculty of Science, Dr. Sinouvassane Djearamane (Co-Supervisor) from the Department of Allied Health Science, Faculty of Science.

I understand that the University will upload softcopy of my dissertation in pdf format into UTAR Institutional Repository, which may be made accessible to UTAR community and public.

Yours truly,

_____

(MANISHAA SRI A/P MAHENDRAN)

TABLE OF CONTENTS

LIST OF TABLES

LIST OF FIGURES

LIST OF ABBREVIATIONS

Ag	Silver
Ag NPs	Silver Nanoparticles
$AgNO_3$	Silver nitrate
ANOVA	Analysis of variance
Au	Gold
BBM	Basal Bold Medium
BSA	Bovine serum albumin
$CaCl_2 \cdot 2H_2O$	Calcium chloride dihydrate
CeO_2	Cerium (IV) oxide
Co NPs	Cobalt nanoparticles
$CoCl_2 \cdot 6H_2O$	Cobalt (II) chloride hexahydrate
$Co(NO_3)_2 \cdot 6H_2O$	Cobalt (II) nitrate hexahydrate
Cr	Chromium
Cu	Copper
CuO	Copper (II) oxide
CuO NPs	Copper oxide nanoparticles
$CuSO_4 \cdot 4H_2O$	Copper (II) sulfate tetrahydrate
$CuSO_4 \cdot 5H_2O$	Copper (II) sulfate pentahydrate
CPI	Revised Nanotechnology Consumer Products Inventory
DBW	Dry biomass weight
DW	Dry weight
EC_{50}	Half maximal effective concentration
EDX	Energy dispersive X-ray
FCR	Folin-Ciocalteu phenol reagent
$FeCl_3 \cdot 6H_2O$	Iron(III) chloride hexahydrate
$FeSO_4 \cdot 7H_2O$	Iron(II) sulfate heptahydrate

FTIR	Fourier transform infrared
H_2SO_4	Sulfuric acid
H_3BO_3	Boric acid
HCl	Hydrochloric acid
ICP-OES	Inductively coupled plasma-optical emission spectroscopy
IR	Infrared
K^+	Potassium ion
KOH	Potassium hydroxide
K_2HPO_4	Dipotassium hydrogen phosphate
KH_2PO_4	Potassium dihydrogen phosphate
Mg NPs	Magnesium nanoparticles
$MgSO_4 \cdot 7H_2O$	Magnesium sulfate heptahydrate
$MnCl_2 \cdot 4H_2O$	Manganese (II) chloride tetrahydrate
MNMS	Manmade nanomaterials
MNPs	Metallic nanoparticles
MoO_3	Molybdenum trioxide
MRI	Magnetic resonance imaging
Na^+	Sodium ion
Na_2CO_3	Sodium carbonate
$Na_2EDTA \cdot 2H_2O$	Disodium ethylenediaminetetraacetate dihydrate
$Na_2MoO_4 \cdot 2H_2O$	Sodium molybdate dihydrate
NaCl	Sodium chloride
$NaHCO_3$	Sodium bicarbonate
NaK tartrate$\cdot 4H_2O$	Potassium sodium tartrate tetrahydrate
$NaNO_3$	Sodium nitrate
NaOH	Sodium hydroxide
NiO NPs	Nickel oxide nanoparticles
nm	Nanometre

NPs	Nanoparticles
PBS	Phosphate buffered saline
PCPs	Personal care products
PEC	Predicted Environmental Concentrations
POD	Peroxidase
PRINT	Particle replication in non-wetting templates
Pt	Platinum
PUFAs	Polyunsaturated fatty acids
ROS	Reactive oxygen species
Se	Selenium
SEM	Scanning electron microscope
SEM-EDX	Scanning electron microscope-energy dispersive X-ray
SOD	Superoxide dismutase
TEM	Transmission electron microscope
Ti	Titanium
TiO_2 NPs	Titanium dioxide nanoparticles
UV	Ultraviolet
WWTPs	Wastewater treatment facilities
XPS	X-ray photoelectron spectroscopy
XRD	X-ray diffractometry
Zn	Zinc
ZnO NPs	Zinc oxide nanoparticles
$ZnSO_4 \cdot 7H_2O$	Zinc sulfate heptahydrate

CHAPTER 1

INTRODUCTION

1.1 Background of Research

Nanotechnology focuses on the understanding and application of atoms and molecules smaller than 100 nanometres (nm). The word "nanometre" was first created by 1925 Nobel laureate in Chemistry Richard Zsigmondy expressly to define particle size. Eventually, the idea of influencing matter at the atomic level was proposed by Richard Feynman, the Physics Nobel Prize winner in the year 1965. A rapidly expanding and active subject of research is nanotechnology, with applications across all the other scientific disciplines such as wound dressings, wood flooring, electronics, biological sensors, water treatments, and also cosmetic industries. The wide applications and unique features of nanoparticles (NP) clearly explain the huge market potential for nanoparticles (Banerjee and Roychoudhury, 2019). The global nanomaterials market size was predicted to be $9.68 billion in 2021, and the demand for nanomaterials will likely increase due to the growing usage of NPs. Precedence Research (2022) estimated that the global market for nanomaterials would be valued at $43.1 billion by 2030, growing at a spectacular compound annual growth rate of 18.05% between 2022 and 2030.

Metallic nanoparticles are used in a variety of commercial and consumer goods (Miao et al., 2009). Approximately 1814 consumer items made with NPs in 32 countries are included in the Revised Nanotechnology Consumer Products Inventory (CPI), which was published in 2013. Around 762 (42%) of the listed goods are in the health and fitness categories, which also include 39% of the products, personal care items including toothbrushes, hair products, and lotions for the skin (Vance and Marr, 2015). The primary nanomaterial composition mentioned in the CPI is made up of metals and metal oxide nanoparticles. Titanium dioxide nanoparticles (TiO_2 NPs) and zinc oxide nanoparticles (ZnO NPs) are the most commonly produced nanomaterials with an estimated global output ranging from 10,000 to 88,000 tons per year. TiO_2 is the second most frequently utilized nanomaterial in a wide range of consumer products, following silver nanoparticles. Because of their unique physical and chemical properties, such as brightness, high refractive index, and resistance to discoloration, TiO_2 NPs are frequently used as white pigments in a variety of products, including paints (lacquers and varnishes), paper, and plastics (Yu et al., 2011). About 70% of all TiO_2 NPs produced as pigments are used in household products like paints, glazes, enamels, plastics, paper, and food, as well as cosmetic products such as toothpaste, ultraviolet (UV) sunscreens, shampoos, deodorants, and shaving creams (Botelho et al., 2014). Inorganic UV filters, air and water purification catalysts, antibacterial agents, and other uses for TiO_2 NPs are also included (Janer et al., 2014).

Due to its high refractive index and brilliant white pigment, TiO_2 NPs are a perfect material for whitening agents utilised in various applications. The use of TiO_2 NPs in self-cleaning goods as well as improving sterilisation and deodorising procedures has been made possible by the discovery of its photocatalytic and super-hydrophilicity capabilities. In recent years, TiO_2 NPs have also been used extensively in medical applications. These NPs have the potential for enhancing and attenuating the effects of chemotherapy to improve the effectiveness and focus of cancer treatment (Wang et al., 2015; You et al., 2016). Additionally, a wide range of goods including doughnuts, gum, candies, and many others include food-grade TiO_2 NPs toothpaste, sunscreen, shaving foam, shampoo, conditioner, deodorant, and other personal care items using food-grade TiO_2 NPs (Weir et al., 2012a).

As the use of engineered nanomaterials becomes more widespread, NPs will likely contaminate the land, waterways, and even groundwater, according to studies conducted by (Lohse et al., 2017; Lone et al., 2013a). Reports suggest that NPs primarily enter aquatic environments through two pathways: wastewater treatment plant effluents and waste incineration (Li and Lenhart, 2012; Liang et al., 2022b). The use of TiO_2 NPs is particularly common, leading to their significant release into sewage. TiO_2 NPs have been found in raw sewage from ten typical wastewater treatment facilities in the United States, with Ti concentrations ranging from 181-1233 μg/L. (Kiser et al., 2009) discovered that a wastewater recycling plant in central Arizona contained 100-3000 μg/L of titanium in its raw sewage, while the effluent contained 5-15 μg/L. The concentration of TiO_2 NPs in sewage is likely to

increase with the growing use of TiO_2 NP-based products (Yuan et al., 2021). According to Boxall et al. (2007) and Gottschalk et al. (2015), TiO_2 NPs have the highest values in terms of concentration in surface water, with a mode of 3 and 0.30 ng L^{-1} for freshwater and saltwater, respectively. According to Predicted Environmental Concentrations (PEC), in sediments, the highest values for TiO_2 NPs occur in freshwater and marine settings, with concentrations of 1200 and 390 μg kg^{-1}, respectively showing these values. TiO_2 NPs have been found to be harmful to a variety of species, including yeast, bacteria, algae, crustaceans, nematodes, and fish, with LC_{50} values ranging from 10 to 100 mg/mL^{-1} (Kahru and Dubourguier, 2010). The transport and subsequent accumulation of NPs in higher aquatic species through the food chain may be facilitated by the ingestion of NPs by lower trophic organisms (Croteau et al., 2011; Miao et al., 2010; Zhao et al., 2016). Thus, the ecosystem as a whole will likely be influenced by TiO_2 NPs within lower trophic organisms (Burchardt et al., 2012).

Haematococcus pluvialis is a species of tiny, aquatic, photosynthetic microorganisms that exist as single cells, possessing a green colouration, and have the ability to move due to the presence of two hair-like appendages called flagella. Its size ranges from 20-50 μm in diameter and 8-12 μm in length. This microalga contains various essential components, including carotenoids, astaxanthin, fatty acids, proteins, carbohydrates, and minerals (Burchardt et al., n.d.; Chekanov et al., 2014). *H. pluvialis* is recognized as the topmost natural source of astaxanthin, which is well-known for its properties as an antioxidant, anti-inflammatory, and anti-cancer agent (Hong et al., 2016;

Matos et al., 2017). Furthermore, farmed fish, such as salmon, sea bream, trout, ornamental fish, and prawns have been fed with *H. pluvialis* as part of their diet (Dore & Cysewski, 2003). The greatest natural source of this very valuable carotenoid pigment is *H. pluvialis*, which can collect astaxanthin up to 5% dry weight (DW) (Wayama, 2013). Dietary supplements containing *H. pluvialis* astaxanthin have been proven safe for humans and have been commonly used as a nutraceutical supplement for over 15 years without harmful side effects of their supplementation (Yang, 2013). In 2014, Paula Pérez-López stated that natural astaxanthin sourced from *H. pluvialis* appears to be a more desirable option than its synthetic counterpart for communities seeking environmentally friendly alternatives, due to its composition, purpose, utilization, and safeguarding. However, the presence of NPs during the nutrient microalgae's growth in water bodies may result in physiological and biochemical alterations that reduce the nutritional value of the nutrient rich microalgae, thereby causing deleterious impacts in its nutritional quality and food chain (Lone et al., 2013a).

Titanium dioxide is abundantly produced and massively used in a wide range of consumer products (Banerjee and Roychoudhury, 2019). A substantial danger of environmental contamination of NPs, particularly aquatic ecosystems including ground water, emerges from such extensive use (Lohse et al., 2017). Water bodies contaminated with NP pollution can lead to changes in the biochemical and physiological processes of microalgae. This, in turn, can negatively affect the nutritional value of these microalgae (Lone et al., 2013a). The fresh water microalga *H. pluvialis* grows in water bodies and has

an inherent capacity to effectively accumulate metals and metallic NPs in biomass (Dazhi et al., 2003; Al-Dhabi, 2013; Comotto et al., 2014; Zinicovscaia et al., 2016; Djearamane et al., 2018). The negative impacts of nanoparticles on *H. pluvialis'* nutritional value, however, have not yet been shown. This study aims to assess the negative effects of TiO_2 NPs on the nutritional qualities of *H. pluvialis* by analyzing the accumulation of NPs in its cells and the resulting changes in its carbohydrate, protein, lipid, carotenoid, astaxanthin, and total phenolic contents. The results of this research will assist to develop and offer customers high-quality nutritional supplements with intact nutritional properties by enabling the detection of TiO_2 NPs contamination in the nutrient microalga *H. pluvialis*. In other words, eating nutritional microalgae polluted with NPs would reduce the amount of anticipated nutrients and may also put customers at risk for health problems because of the NPs that have collected. Having an understanding of how TiO_2 NPs impact the nutritional microalgae *H. pluvialis* could be advantageous for promoting *H. pluvialis* products to customers without compromising their nutritional value.

1.1 Research Objectives

This study aimed to assess the impacts of TiO_2 NPs on the nutritional qualities of *H. pluvialis* by analyzing the interaction and accumulation of TiO_2 NPs in *H. pluvialis* cells, as well as observing changes in biomass, macromolecules (proteins, carbohydrates, lipids), pigments (chlorophyll-a, carotenoids, astaxanthin), and phenolic compounds. Therefore, the primary objectives of this research were to examine the harmful effects of TiO_2 NPs on the nutritional properties of *H. pluvialis*. The key objectives of this investigation include:

1) To study the cellular interaction and cellular accumulation of TiO_2 NPs in *H. pluvialis* and the subsequent morphological alterations of *H. pluvialis* with the presence of TiO_2 NPs.

2) To evaluate the alterations in the biomass of *H. pluvialis* owing to the existence of TiO_2 NPs at varied concentrations and time intervals.

3) To explore the impact of TiO_2 NPs on macromolecules, pigments, and phenolic compounds of *H. pluvialis* at varied concentrations and time intervals.

CHAPTER 2

LITERATURE REVIEW

2.1 Microalgae

Microalgae are tiny organisms that rely on light and carbon dioxide to create organic carbon. They have a fast growth rate and can multiply rapidly in ideal environmental conditions (Devi et al., 2014). Microalgae produce various types of compounds such as polysaccharides, lipids, pigments, proteins, vitamins, bioactive substances, and antioxidants. These compounds can be used to make biofuels, dietary supplements, medicines, and cosmetics (Das et al., 2011). Additionally, microalgae can be utilized to purify wastewater and decrease atmospheric CO_2 (Khan et al., 2018). Microalgae have been consumed by humans for over a thousand years due to their high nutritional value, containing essential minerals (potassium, iron, magnesium, calcium, and iodine), proteins, vitamins (A, B1, B2, B6, B12, C, and E), and other nutrients (Koyande et al., 2019; Molino et al., 2018). The Chinese have been documented to have used *Nostoc* during a famine over 2000 years ago, and indigenous peoples have also consumed microalgae for generations (Wang et al., 2021). Several types of commonly used microalgae with excellent nutritional values include *Spirulina platensis*, *Dunaliella terticola*, *Chlorella* sp., *Dunaliela saline*, *Skeletonema*, *Nannochloris*, *Nitzschia*, *Schizochytrium*, *Tetraselmis*, *Haematococcus*, *Botryococcus*,

Phaeodactylum, *Porphyridium*, *Chaetoceros*, *Crypthecodinium*, and *Isochrysis* (Sathasivam et al., 2019). Particularly in Asian nations like China, Japan, and Korea, microalgae with a high amount of critical nutrients have emerged as a significant source of food (Jibri et al., 2016). Most types of microalgae contain high levels of protein, and a few of them have been utilized for creating food proteins and nutritional supplements. For instance, the chlorophyceae *Chlorella* sp. and *Scenedesmus obliquus*, as well as the cyanobacteria *Arthrospira* sp., are examples of microalgae that have been used for this purpose (Wang et al., 2021).

2.2 *Haematococcus pluvialis*

The taxonomy of *H. pluvialis* is presented in Table 2.1.

Table 2.1: Taxanomical categorization of *H. pluvialis* (M. M. R. Shah et al., 2016).

Kingdom	**Plantae**
Subkingdom	**Viridiplantae**
Infrakingdom	**Chlorophyta**
Division	**Chlorophyta**
Subdivision	**Chlorophytina**
Class	**Chlorophyceae**
Order	**Chlamydomonadales**
Family	**Haematococcaceae**

Genus	**Haematococcus**
Species	***Haematococcus pluvialis***

The freshwater unicellular biflagellate green microalgae *H. pluvialis* Flotow can be found in the class Chlorophyceae, order Volvocales, and family Haematococcaseae. It goes by other names such as *Sphaerella lacustris* or *Haematococcus lacustris*. Haematococcus was initially described by J. Von Flotow in 1844, while Tracy Elliot Hazen gave a detailed account of its biology and life cycle in 1899. *H. pluvialis* is present in various ecosystems worldwide, particularly in small, temporary freshwater bodies like rain puddles, man-made pools, natural and artificial ponds, and birdbaths. This microalga has been discovered in different parts of the world, including Europe, Africa, North America, and Himachal Pradesh in India, and is commonly found in temperate regions of the world (M. M. R. Shah et al., 2016).

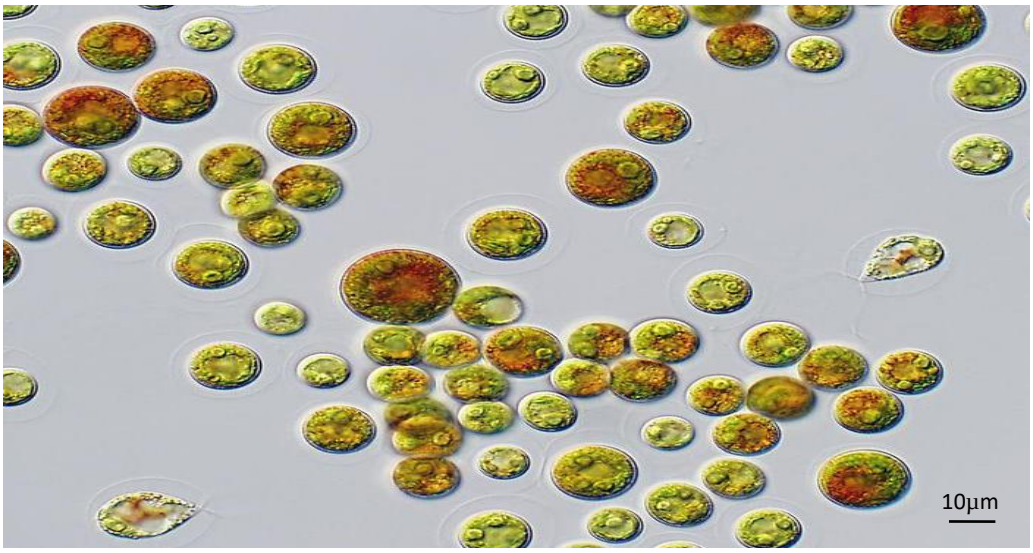

Figure 2.1: Light microscopic image of *H. pluvialis* (Nordic Microalgae, 2019)

H. pluvialis, like most other unicellular green algae in the Volvocalean group, has a similar cell structure. Its life cycle involves four different types of cellular morphologies: macrozooids (zoospores), microzooids, palmella, and hematocysts (aplanospores), which are illustrated in Figure 2.1 (M. M. R. Shah et al., 2016). The cultivation of *H. pluvialis* can be divided into two stages: the initial green stage and the subsequent red stage. Microalgae first divide into daughter cells when conditions such as temperature, pH, nitrate, metal, or light wave length and intensity are optimal. Cells often cease dividing in reaction to stressful situations. Accumulation of carotenoids, primarily astaxanthin, is a result of stress. During the green period, the temperature should vary between 25 and 30 °C (Han et al., 2013).

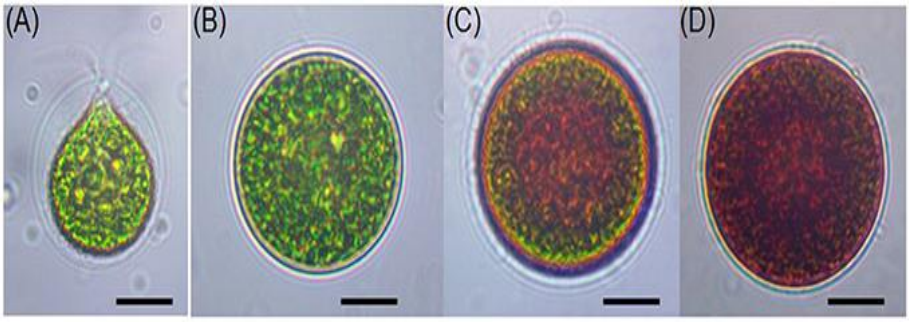

Figure 2.2: ***H. pluvialis*** **cells life cycle under light microscope from A) Macrozooids, B) Microzooids, C) Palmella, to D) Hematocysts (M. Shah et al., 2016).**

The media KM1, BBM, Z8, BG- 11, OHM, and their modified variations are most often utilised for the development of *H. pluvialis*. For autotrophic cultures, BBM and Z8 are employed, whilst KM1 medium is appropriate for heterotrophic cultures. In a mixotrophic culture, sodium acetate or another organic carbon source may be added to BBM media (Tripathi et al., 1999). In a photoautotrophic mode, light is required for microalgae to utilise it as an energy source and an inorganic component as a source of carbon. Nevertheless, in the photoheterotrophic mode, light is not necessary but might be employed as an energy source, and the supply of carbon is organic. A source of energy and carbon in a heterotrophic mode are both organic. When growing microalgae, the mixotrophic method makes use of both organic and inorganic sources of carbon and energy (Prokop et al., 2015).

The metabolic profile of the cell changes as it develops and progresses through several phases of its life cycle. The majority of the green cells found in *H. pluvialis* contain a significant amount of protein, ranging from 29-45% of their weight when they are in a dry state. The red cells, on the other hand, have a protein content ranging from 21-23% when dry, but it drops to 36% when they turn into palmella. The cell's ability to withstand prolonged stress is due to its starch-type carbohydrates. The content of carbohydrates increases from 15-17% when the cells are green to 60-74% when they are in the red cyst stage. According to (Recht et al., 2012) study, the total carbohydrate content may increase rapidly on the first day of stress exposure, reaching up to 63% when dry. However, it may decrease to 41% when dry the following day and remain at this level until the end of the cultivation.

2.3 Nutritional Properties of *Haematococus pluvialis*

H. pluvialis is a type of single-celled microalgae found in freshwater that could be a valuable source of beneficial substances such as proteins, carotenoids, and fatty acids. Among these compounds, astaxanthin stands out as a potent antioxidant. Compared to other microalgae, *H. pluvialis* is known for its ability to accumulate high levels of astaxanthin, making it one of the most economically viable sources of natural astaxanthin (M. M. R. Shah et al., 2016). Subjecting *H. pluvialis* to stress results in the production of astaxanthin, which is also known as 3,3'-dihydroxy-ß-carotene-4,4'-dione, as a secondary carotenoid with a bright blood red (Mularczyk et al., 2020). Throughout the cell cycle of *H. pluvialis*, structural modifications occur, leading to a change

from green to red. Additionally, alterations in the chemical constituents of cellular matter also occur.

During the "green phase," the dry biomass weight (DBW) shows that up to 1% lutein is present, and the overall lipid content ranges from 20 to 25. In the "red phase," however, there is a significant increase in lipid content, ranging from 32 to 37%, with the deposition of 1-5% astaxanthin (Oslan et al., 2021a). As a cell progresses through various stages of its life cycle, its metabolic profile changes. If the cell matures under optimal conditions, *H. pluvialis* strains typically exhibit protein content ranging from 29% to 45% of their dry weight during the green stage (Mularczyk et al., 2020). The protein levels of *H. pluvialis* may drop to 36% during its palmella phase. Furthermore, research revealed that proteins accounted for 21-23% of the cell content during the red stage of *H. pluvialis* cultivation (M. M. R. Shah et al., 2016). The red stage had a total amino acid content of 10.02/100 mg, and the majority of the amino acids present were aspartic acid, glutamic acid, alanine, and leucine. Essential amino acids comprised 46% of the total amino acids (Kim et al., 2015). The green stage has a carbohydrate content of around 15-17% (M. M. R. Shah et al., 2016). When *H. pluvialis* faces stressful conditions such as nutritional deficiency, high acidity, temperature, or light stress, accumulation of larger amounts of carbohydrates occurs in the red stage. It is expected that within the first day of exposure to stress, the increase in carbohydrate accumulation could be as high as 63% (Recht et al., 2012). In prolonged stressful situations, cells of *H. pluvialis* consumed carbohydrates in the form of starch (Mularczyk et al., 2020). During the green stage, the overall lipid content fluctuates between 20

to 25%. Approximately 10% of these lipids are present in the chloroplasts and are primarily made up of polyunsaturated fatty acids (PUFAs) (Mularczyk et al., 2020). Red stage cells have the ability to produce a significant quantity of secondary metabolites, particularly astaxanthin, which can make up to 4% of their content and contribute up to 40% of their overall weight. The complete fatty acid profile of *H. pluvialis*, which comprises palmitic, linoleic, and linolenic acids, may vary depending on the strain (M. M. R. Shah et al., 2016).

The major carotenoids found in green vegetative cells are Lutein (75-80%) and ß-carotene (10-20%). Other compounds that contribute to the carotenoid component include primary carotenoids, chlorophyll a and b, canthaxanthin, zeaxanthin, violaxanthin, echinenone, lactucaxanthin and neoxanthin (Chekanov et al., 2014). Astaxanthin, which is a type of carotenoid and is considered a secondary one, becomes the primary replacement for the main carotenoids during the shift from the green stage to the red stage. As a result, the total concentration of carotenoids significantly increases during the red stage (Oslan et al., 2021a). Two carotenoids that are widely recognised for their antioxidant properties include astaxanthin and lutein. One of the most effective carotenoid molecules available is astaxanthin. Due to their potent anti-inflammatory, antiproliferative, antioxidant, and perhaps anti-aging characteristics, carotenoids have drawn the attention of researchers in recent years. They may be utilised to prevent illnesses brought on by chronic inflammation and oxidative stress (Sztretye et al., 2019). Astaxanthin has a significantly greater ability to inhibit free radical chain reactions compared to ß-carotene, as it has a 38 times higher capacity. Additionally, it has 500 times

more antioxidant activity than vitamin E (Oslan et al., 2021b). Furthermore, astaxanthin possesses anti-inflammatory properties and provides medicinal advantages for various human illnesses such as cancer, liver health, inflammation, damage caused by UV-light, cardiovascular issues, joint problems, skin health, aging, and reproductive well-being (Davinelli et al., 2018; Mehariya et al., 2020).

2.4 Metallic Nanoparticles (MNPs)

Metallic particles that measure between 1 and 100 nanometers in length, width, and thickness are categorized as metallic nanoparticles. Faraday was the first to look at the possibility of Metallic nanoparticles (MNPs) in solution back in 1857. These tiny materials can now be produced and modified with various chemical groups, allowing them to interact with drugs, ligands, and antibodies. Metallic nanoparticles have a wide range of uses in medicine, biotechnology, and drug transport. The qualities, benefits, and drawbacks of MNPs are outlined in this paper (Venkatesh, 2018a). MNPs are tiny entities, smaller than one micron in size, composed of various pure metals (such as silver, gold, zinc, titanium, and copper) or their compounds, including oxides, hydroxides, sulfides, chlorides, and fluorides (Mahana et al., 2021). The antimicrobial, optical characteristics and biocompatibility properties of MNPs made them to be widely used in biomedicine. The small size of MNPs allows them to interact with biomolecules present on the surfaces and inside the cells of microalgae in various ways. These interactions can be interpreted and associated with distinct biochemical and physiochemical features of the cells

(Mody et al., 2010). TiO_2 NPs are frequently employed in sunscreens, iron oxide is utilized in magnetic resonance imaging (MRI), silica is used as a vaccine adjuvant, and cerium dioxide (CeO_2) is used in catalysts and the automobile industry (Sengul and Asmatulu, 2020).

Depending on the method used, MNPs can be obtained in the shape of nanoparticles, nanospheres, or nano capsules. A variety of substances, including proteins, polysaccharides, and synthetic polymers, may be used to create MNPs. The desired NP size, surface properties, amount of biodegradability, biocompatibility, toxicity, and antigenicity of the end product will all have an impact on the choice of matrix materials (Mohanraj and Chen, 2007). The top three methods commonly used to generate NPs are the coacervation or ionic gelation of hydrophilic polymers, the polymerization of monomers, and the dispersion of pre-existing polymers. (Mohanraj and Chen, 2007). Additional techniques for producing MNPs include the utilization of supercritical fluid technology and particle replication in the non-wetting templates (PRINT) approach. These methods have been reported to provide complete management over particle composition, size, and structure (Rolland et al., 2005). Besides chemical synthesis, MNP can also be synthesized using living organisms like bacteria, fungi, and plants (Li et al., 2012).

MNPs have a range of advantages and disadvantages. On the positive side, they can enhance Rayleigh scattering, surface-enhanced Raman scattering,

strong plasma absorption, and provide information about chemical properties on metallic nanoscale substrates (Li et al., 2007). One of the disadvantages of MNPs is particle instability. MNPs are capable of transformation because they are located in a zone of energetic local minima and are thermodynamically unstable. This causes the quality to decline, and the corrosion resistance to be poor, and the primary problem is that maintaining the structure of MNPs becomes challenging. The chance of impurity in MNPs can also be high as NPs are highly reactive. NPs are synthesized in the form of encapsulation in solution form, where this becomes a challenge to overcome impurities in NPs. Additionally, it has been claimed that MNPs are poisonous, cancer-causing, and irritable since they become transparent to the cell dermis (Granqvist and Buhrman, 1976; Venkatesh, 2018a).

MNPs can be characterized using multiple approaches to obtain information on the organic layers surrounding the MNPs and to comprehend MNPs' surface structure. A transmission electron microscope (TEM) may be used to examine the NPs' size, shape, crystallinity, and interparticle interactions. The interaction of the incident electron beam with the specimen in a scanning electron microscope (SEM) results in secondary electrons, which can be used to determine the purity of MNPs samples. A practical and often-used method for figuring out the crystalline structure of MNPs is X-ray diffractometry (XRD). The Debye-Scherrer method can also be employed with the XRD line to determine the particle size. Besides, Fourier transform infrared (FTIR) spectroscopy is commonly used as compared to IR spectroscopy to determine the functional groups attached to the surface of MNPs. The oxidation state of

the surface of MNPs can be detected using X-ray photoelectron spectroscopy (XPS) (Kumar and Dixit, 2017; Venkatesh, 2018a).

MNPs are generally used in different functions such as optimal, thermal, electrical, and others. Imaging sensors, displays, solar cells, photocatalysts, biomedical devices, optical detectors, and lasers are a few examples of MNPs employed in optical functions. These devices heavily depend on the size, shape, surface area, doping, and interactions of MNPs with the environment. Polymers filled with nanotubes lead to improvement in mechanical functions and highly depend on the filter type and how the nanotubes are conducted. MNPs can be used to make electronic wiring as they have a lower boiling point where the MNPs particle size of less than 10 nm has a lower melting point than bulk materials. MNPs also can be used to make high-temperature superconductivity materials. By combining NPs with metals or ceramics, the mechanical properties of MNPs can be increased. Some MNPs such as platinum (Pt) and gold (Au) NPs can have magnetic properties in nanosize but not in bulk size, providing chances to adjust the physical characteristics of NPs (Venkatesh, 2018b).

In short, MNPs are highly demanded in this 21st century as they can be synthesized in various methods and the process of MNPs synthesis is important as it can affect the properties of the MNPs being synthesized. Although further study is required, noble MNPs may be useful in therapeutic and diagnostic agents because they exhibit novel features at the atomic and

nanoscale. MNPs can play a significant role in personalised medicine. It is undeniable that the demand for MNPs used in healthcare, industry, and cosmetics is rising, but safety precautions must also be taken to safeguard both human health and the environment.

2.5 Titanium Dioxide Nanoparticles (TiO_2 NPs)

TiO_2 NPs are highly useful in many different applications such as pharmaceuticals, coatings, inks, polymers, food, cosmetics, and textiles due to their high refractive index (n = 2.4). These nanoparticles also have the added benefit of helping to clean the environment. Various methods are utilized to produce TiO_2 NPs including sol-gel, flame hydrolysis, co-precipitation, impregnation, and chemical vapour deposition. Researchers are particularly interested in the biosynthesis of TiO_2 NPs due to their cost-effectiveness, eco-friendliness, and ability to be repeated consistently (Shi et al., 2013). Because of their brightness, high refractive index, and ability to resist discolouration, TiO_2 NPs are commonly used in large quantities as pigments. Each year, millions of tons of TiO_2 NPs are produced worldwide for various purposes. While TiO_2 NPs are primarily used as a pigment in paints, which make up more than 70% of its production, it is also used in a range of other products, including glazes, enamels, plastics, paper, textiles, foods, medications, cosmetics, and toothpaste (Weir et al., 2012a). TiO_2 NPs have been used for various purposes such as their ability to prevent microbial growth, their use as a catalyst for filtering air and water, their medicinal properties, and their

potential for energy storage. Recently, TiO_2 as a nanomaterial has gained more attention.

TiO_2 nanoparticles are perfect for treating wastewater due to their cheap cost, corrosion resistance, and general stability. When heavy metals need to be preconcentrated and extracted from water for surface water remediation, they may be employed as solid-phase extraction (SPE) packing material. Groundwater contains the organophosphate pesticide diazinon, which is regarded as a moderately dangerous toxin (Class II by the World Health Organization). The elimination efficiency of diazinon was 98.58% when combined with UV light and iron-doped TiO_2 NPs. Furthermore, xenobiotic compounds including pesticides, dyes, and dangerous substances may be removed from wastewater using TiO_2 NPs (Kiser et al., 2009).

Recent years have seen a variety of new uses for TiO_2 NPs in the medical field. Due to their toxic nature, traditional chemotherapy cancer treatments may have disastrous consequences on cells. As a consequence, attention has turned to the potential applications of nanotechnology in the detection and treatment of cancer. At the moment, minimising the negative effects of medicine delivery methods made possible by nanotechnology is the biggest obstacle to be surmounted. Controlling the number of pharmaceuticals delivered to the cell or selecting certain cells to administer treatment to them are some ways that have shown promise (Ziental et al., 2020).

In 2005, the global production of TiO_2 NPs was estimated to be 2000 tonnes, costing around 70 million; out of which 1300 tonnes were utilised in personal care products (PCPs) ranging from topical sunscreens to cosmetics. The production had significantly increased by two fold, and it is projected to elevate until the year 2025, hugely depending on nanomaterials. As a consequence, several sources of TiO_2 NPs might be exposed to people, hence increasing their accumulation in the environment (air, water, or soil compartments) (Landsiedel et al., 2010).

When TiO_2 NPs are used in meals, consumer goods, and home items, they may leak out as urine or faeces, wash off surfaces, or be dumped into sewage that goes to wastewater treatment facilities (WWTPs). Although the bulk of nanoscale and larger-sized TiO_2 NPs from influent sewage may be removed by WWTPs, TiO_2 NPs between 4 and 30 nm were still discovered in the treated effluent (Weir et al., 2012b). Following their discharge, these nanomaterials may interact with biological things in surface waters. The greatest concentrations of TiO_2 NPs in river water, according to one research monitoring them, were found to be just downstream of a WWTP (Neal et al., 2011). Although the qualitative release of TiO_2 NPs to the environment has been shown, quantifying the amount released is challenging. Since it is hard to identify all sources or quantify the quantity of emitted TiO_2 NPs, emissions are often modelled to improve predictions of the environmental effects of TiO_2 nanomaterials (Semmler-Behnke et al., 2008).

2.6 MNPs in the Aquatic Ecosystem

The anthropogenic revolution began with the agricultural revolution 10,000 years ago and continued with the industrial revolution in the 1700s and the information revolution that followed after is consistent with the technological development of each revolution and era. These revolutions were able to and now can meet the demands of the world's expanding population, with a cost associated with pollution and global warming (Al-Homaidan et al., 2014; Anastopoulos and Kyzas, 2015). This has a negative and irreversible impact on the environment, as well as on the health, economy, and society (Al-Homaidan et al., 2014). However, regardless of the difficulties that have yet to discover a long-term solution to the pollution, microalgae are the front-runners in tackling this situation (Anastopoulos and Kyzas, 2015). Metal and MNP pollution of the soil and aquatic environment is being brought on by the rising usage of metals and MNPs in the commercial sector (Lohse et al., 2017; Lone et al., 2013a). Algae are the most vulnerable aquatic species to NPs as they are toxicant-sensitive and would have impacts on those higher organisms through the intake of NPs contaminated biomass (Banerjee and Roychoudhury, 2019).

Microalgae has the ability to withstand a high level of nanoparticles despite the increasing toxicity level of concentrations through its bioaccumulation process (Govindaraju et al., 2008; Li et al., 2017). This is due to its ability to create resistance towards such incidence, which enables such a high level of concentration of chemicals to be accumulated (Govindaraju et al., 2008). Even

though a moderate dosage of metals and MNPs might encourage the development of microalgae, a large amount can be hazardous (Liang et al., 2020). Numerous studies have shown that metals and MNPs are toxic to microalgae, which negatively impacts the nutritional value of such organisms. Although metals and MNPs generally show negative effects on microalgae, however, some research also observed stimulatory outcomes during the cultivation of microalgae, depending on the metals or MNPs used and also the species used in the study.

In a study conducted by (Gaiser et al., 2011) regarding *Daphnia magna*, it was found that after being exposed to silver nanoparticles (Ag NPs) for 96 hours, all *D. magna* perished at a concentration of 1 mg/mL, while 43.3% of them died at 0.1 mg/mL. Multiple studies have demonstrated that the capacity of algal cells to perform photosynthesis is negatively affected by the toxicity of Ag NPs. In 2012, Dewez and Oukarroum conducted a study where they investigated how toxic Ag NPs is to a type of freshwater green algae called *Chlamydomonas reinhardtii*. They exposed the algae cells to different concentrations of Ag NPs (1, 5, and 10 mol/L) for 6 hours, both in the presence and absence of light. They found that when the algae were exposed to light, the photosynthetic system's electron transport activity was more strongly inhibited due to a failure of protective mechanisms against excess light absorption. In another experiment, on the fifteenth day of exposing *S. platensis* to TiO_2 NPs at a concentration of 100 mg/L, the biomass decreased by 74.1% (Comotto et al., 2014a). With a substantial decrease in growth (EC_{50}) at 42 mg/L in *Pseudokirchneriella subcapitata* and 4.6 mg/L in *Thalassiosa*

pseudonana, ZnO NPs showed the greatest degree of toxicity among other metal and metal oxide NPs (Wong et al., 2010). Research by Navarro et al., (2008) found that Ag NPs were more harmful to *C. reinhardtii's* photosynthetic response than Ag+ (Ag NO_3) by the assessment of chlorophyll fluorescence emission. When Ag NPs were used on *Chlorella vulgaris* and *D. tertiolecta*, two different types of microalgae in freshwater and marine environments, a temperature rise had a more significant effect on changing the way electrons are transported during photosynthesis. This took place at two distinct temperatures, specifically at 25°C and 31°C (Oukarroum et al., 2012). According to a study by Lone et al., (2013), *S. platensis* lost 93.5% of its chlorophyll-a and 50% of its carotenoids after being treated with ZnO NPs on day 10 (Mary Leema et al., 2010) found that subjecting *S. platensis* to salt stress after being treated with sea water caused the plant to lose 53.1% of its chlorophyll-a, 37.5% of its carotenoids, and (Gupta et al., 2014a) reported a concentration- and time-dependent decline in *S. platensis'* chlorophyll-a, with a substantial maximum drop of 63.9% at 10 mg/L of chromium (Cr) on day 9. Nickel oxide nanoparticles (NiO NPs) were observed to have an EC_{50} value of 32.28 mg/L after 72 hours of exposure to *C. vulgaris*. Plasmolysis, cell membrane disintegration, and disarray were brought on by the toxicity of NiO NPs in *C. vulgaris'* thylakoid structures. Additionally, it was claimed that creatures in the upper food chain that consume algae polluted with NiO NPs were vulnerable to those substances' hazardous effects (Gong et al., 2011). (Zinicovscaia et al., 2017a) found that treatment with Se (100 mg/L) reduced the pigment phycocyanin in *S. platensis* by 90% on day 3 and that treatment

with copper (0.5 mg/L) on day 7 resulted in a 50% reduction in algal biomass (Deniz et al., 2011).

2.7 Effects of MNPs on Microalgae

2.7.1 Growth rate

The percentage change in the biomass concentration of microalgae during a given period is known as the growth rate of microalgae. The growth rate of microalgae is influenced by several factors, including temperature, light intensity, carbon dioxide, pH, and the composition of the culture media (Papapolymerou et al., 2019). The ideal temperature and the need for light for various species of microalgae are the two key environmental parameters influencing the pace of growth and biomass concentration of microalgae (Li and Lenhart, 2012). Microalgae that are cultivated under stressful conditions such as inadequate nutrients in culture medium, and excessively low or high light intensities and temperatures can cause the decreased production of microalgae biomass and growth rate (Wijffels et al., 2010). As only a few of these metals and MNPs are required by microalgae for growth, they do not harm the cellular processes of microalgae and are therefore considered non-toxic (Aravantinou et al., 2015). Certain components play the role of foundational units for vitamins, centres that oxidize water during photosynthesis, and proteins involved in the transport of electrons during photosynthesis (Liang et al., 2020). They may also function as cofactors for enzymes involved in N_2 assimilation, nitrate reduction, DNA transcription,

and phosphorus acquisition (Liang et al., 2020; Moroney et al., 2001). However, toxic levels of metal and MNPs make microalgae sick (Aravantinou et al., 2015; Monteiro et al., 2012). The growth rate of microalgae was often inhibited or negatively affected by metals, however, other studies also noted stimulatory effects while microalgae were being grown. Multiple research studies have indicated that certain types of nanoparticles, including TiO_2, ZnO, Ag, and Pt NPs, can prevent the growth of various microalgae species or strains. The majority of these studies suggest that the inhibitory mechanism involves either physical damage caused by the nanoparticles or the formation of reactive oxygen species (ROS). This information comes from research conducted by Castro-Bugallo et al., (2014); Suman et al., (2015); Xia et al., (2015a). Furthermore, as per various research (Aravantinou et al., 2015; Lee and An, 2013; Suman et al., 2015), multiple factors such as the discharge of metal ions from MNPs, shading caused by light, interaction with the cultivation substrate, and the combined influence of numerous variables have an impact on the growth of microalgae (Manzo et al., 2013). Moreover, studies have demonstrated that the discharge of metallic particles from MNPs has a positive effect on the growth of microalgae (Pádrová et al., 2015). The duration of contact between metals and MNPs has varying effects on the inhibition percentage of microalgae. If the exposure time is longer, and the MNP concentration is constant, there will be a higher growth inhibition rate. This is because high concentrations of metals and MNPs can damage the cell membrane, which can lead to uncontrolled release or absorption of electrolytes. Additionally, this damage can impact the photosynthesis system and the

production of biological macromolecules such as proteins and carbohydrates, which may explain the inhibitory activity of microalgae (Liang et al., 2020).

2.7.2 Macromolecules

The macromolecules or macronutrient composition of microalgae is proteins, carbohydrates, and lipids. Environmental and cultural factors, including temperature, light intensity, pH, and the nutritional composition of the culture medium, have a significant impact on the formation of these macromolecules (Metsoviti et al., 2019; Zhu et al., 2015). Increased light intensity led to greater lipid content and decreased protein and carbohydrate content in certain algae species, such as *Botryococcus braunii* (Ruangsomboon, 2012), while, in some other species like *Nannochloropsis* sp. (Sukenik et al., 1989) and *Ankistrodesmus falcatus* (George et al., 2014), low light intensity resulted in high lipid content. The toxicity of ions produced in large concentrations, which results in the oxidation of biological macromolecules is frequently linked to the breakdown and destruction of biological macromolecules. When the conditions are unfavorable for microalgae growth, the essential cellular functions within the cell cannot be supported, which leads to the degradation of macromolecules (Zinicovscaia et al., 2017a). One can utilize the protein, carbohydrate, and lipid levels present in microalgae to comprehend the influence of MNPs on primary cellular metabolism (Romero et al., 2020). In order to protect their vital metabolic processes from harmful substances during times of stress, microalgae may alter their biochemical composition and adjust their cellular metabolism to increase their storage of larger molecules like

proteins, carbohydrates, and lipids (Pham, 2019). The techniques commonly used to determine the overall protein levels in microalgae usually rely on identifying peptide bonds, and a reduction in protein levels indicates that the biomass has been broken down (Zinicovscaia et al., 2017a). Microalgae produce carbohydrates through photosynthesis, and these compounds are stored in the form of starch particles in the chloroplast (Huang et al., 2016). Microalgae may have a protective mechanism that increases the concentration of carbohydrates when they are under stress, possibly due to the production of specific ROS scavengers. However, when present in higher concentrations, carbohydrates can also function as ROS scavengers themselves. Glucose and sucrose are important for ROS signaling (Bolouri-Moghaddam et al., 2010). Alternatively, the decrease in overall carbohydrate levels observed during MNPs exposure could potentially be attributed to the disturbance of the cell membrane, which subsequently resulted in unregulated electrolyte release and uptake (Liang et al., 2020). Microalgae have the ability to survive in toxic environments where the concentration of toxins is usually lower. As lipids are the main components of their cell membranes, their lipid composition can be modified to adapt to changes in the microalgae's physiological condition (Zinicovscaia et al., 2017a).

2.7.3 Pigments

Primary photosynthetic pigments called chlorophylls are made up of tetra pyrrole macrocycle rings and come in a variety of shapes in different types of microalgae (Miazek et al., 2015). The amount of chlorophyll in microalgae is

usually used to gauge how quickly cells divide or how quickly photosynthesis occurs (Pham, 2019). Microalgae need low metal concentrations to develop, however, excessive metal concentrations may affect the rate of growth and the capacity of microalgae to synthesize chlorophyll. This is due to the possibility that too many metals will inhibit chlorophyll's ability to function (El-Sheekh et al., 2003; Puspitasari et al., 2018). According to Djearamane et al., (2018a); El-Sheekh et al., (2003); Puspitasari et al., (2018), it has been found that low levels of magnetic and MNPs can improve the production of chlorophyll to a small extent, but high levels can significantly reduce the amount of chlorophyll. Microalgae cells require cobalt and copper for their metabolism and respiration, and the substitution of zinc with cobalt (El-Sheekh et al., 2003) and magnesium with copper (Puspitasari et al., 2018) may contribute to the slight enhancement of chlorophyll synthesis at low concentrations of nanoparticles. Chlorophyll concentration falls because the donour center's electron transport chain is inhibited, whereas chlorophyll content increases due to an inhibition in the acceptor center (Sendra et al., 2018). The auxiliary photosynthetic pigments known as carotenoids are fat-soluble tetraterpenoids that can be divided into oxygen-containing xanthophyll (lutein, astaxanthin, and zeaxanthin) and no-oxygen-containing carotenoids (β-carotene) (Miazek et al., 2015). Phycobiliproteins are a type of protein that is soluble in water, and they function as additional pigments in blue-green or red microalgae. These pigments give the microalgae cells a blue or red colour, which allows them to absorb light energy and transfer it to chlorophyll a. There are two types of blue pigments, namely allophycocyanin, and c-phycocyanin, while

there are two types of red pigments, namely b-phycoerythrin, and c-phycoerythrin, according to Miazek et al., (2015).

2.7.4 Phenolic Compounds

A wide group of secondary metabolites known as phenolic compounds has polyphenol structures with two or more six-carbon aromatic rings (Tibbetts et al., 2015). According to Aliakbarian et al., (2009a); Ben Hamissa et al., (2012); Comotto et al., (2014a); Palmieri et al., (2012), phenolic compounds are one of the most significant families of natural antioxidants that may reduce or avoid the consequences of oxidative stress by donating an electron or a hydrogen atom to create stable radical intermediates (Hajimahmoodi et al., 2010). The total phenolic compound of microalgae varies in different species and strains, which can be influenced by environmental factors (Machu et al., 2015) and cultivation conditions like temperature, light intensity, and the availability of nutrients (Metsoviti et al., 2019). When the microalgae cells are subjected to environmental stress, antioxidant enzymes are produced to protect the algal cells from free radical damage (Li et al., 2006a). The strong ability of TiO_2 NPs to catalyze reactions under light exposure boosts the production of phenolic compounds in reaction to stress. However, once these phenolic compounds are released into the surrounding environment, they are vulnerable to damage from free radicals. This suggests that the level of phenolic compounds outside of cells decreases when exposed to nanoparticles (Comotto et al., 2014a).

2.8 Toxicity of TiO_2 NPs

One of the most widely utilised manmade nanomaterials (MNMs), TiO_2 NPs are used in a wide range of consumer goods, including creams, perfumes, paintings, and protective coatings, as well as in the environmental decontamination of air, soil, and water. Their greater discharge into the environment as a result of these extensive uses is inevitable (Zhu et al., 2011). Direct evidence has been recorded showing the release of synthetic TiO_2 NPs from urban sources into waterways. Water that came into contact with painted surfaces had a significant concentration of TiO_2 NPs (3.5 x 10^8 particles/L). Due to their closeness to modern humans, industry, and industrial effluent, freshwater, and coastal settings raise the possibility that TiO_2 NPs exposure poses a danger to these ecosystems (Zhu et al., 2011).

Although no negative effects were observed in experiments conducted on *D. magna*, Hund-Rinke and Simon, (2006) discovered that the toxicity of TiO_2 NPs on green algae (*Des modesmus subspicatus*) was dependent on the amount administered, with an EC_{50} of 44 mg/L. A more recent study revealed that at a concentration of 20 g/L, both bulk TiO_2 and TiO_2 NPs did not result in any immediate toxicity to bacteria (*Vibrio fischeri*), crustaceans (*D. magna* and *Thamnocephalus platyurus*), fish (*Danio rerio*), or fish eggs (Zhu et al., 2011). On the contrary, it was found that extended exposure (over 8 days) to TiO_2 NPs at concentrations ranging from 0.1 to 20 mg/L had a notable adverse effect on the survival and reproductive capacity of *D. magna* (Adams et al., 2006; Wiench et al., 2009; Zhu et al., 2010). Furthermore, prolonged

exposure (over 14 days) to TiO_2 NPs at concentrations lower than 1.0 mg/L can cause respiratory toxicity and interfere with the metabolism of certain trace elements, such as Zn and Cu, in rainbow trout (*Oncorhynchus mykiss*) (Federici et al., 2007). These findings suggest that the species and exposure duration may affect TiO_2 NPs' ecotoxicity.

When TiO_2 NPs are released into the aquatic environment, it harms the ecology as a whole (Aitken et al., 2009). TiO_2 is nanoscale in size has a strong oxidising capacity and may generate free radicals. Since nanoparticles are mainly absorbed through the skin and respiratory system, TiO_2 NPs exposed to sunlight can cause damage to DNA both inside and outside of a living organism (Srivastava et al., 2015). The exposure of TiO_2 nanoparticles has been observed to affect microglial cells in the brain of mice, generating superoxide radicals that result in significant DNA damage, indicating potential environmental hazards (Long et al., 2006). In addition, research has demonstrated that continual inhalation of TiO_2 NPs can lead to harmful consequences for the lungs in rats (Aitken et al., 2009).

The harmful effects of TiO_2 NPs on aquatic creatures have been shown in some research that reported that when planktonic and biofilm bacteria were exposed to 5.3 mg/L of TiO_2 NPs for 24 hours, it caused harm to the cell membrane. Dabrunz et al., (2011) found that at 72 hours, the concentration of TiO_2 NPs that resulted in 50% cytotoxicity and immobilization of *D. magna* was 3.8 mg/L, and at 96 hours, the concentration was 0.73 mg/L. Another

research on *D. magna* by (Zhu et al., 2011) found that exposure to TiO_2 NPs had a modest toxic effect after 48 hours with an EC_{50} > 100 mg/L, but that substantial toxicity was seen after 72 hours. Furthermore, zebrafish died after prolonged exposure for 21 days due to growth retardation, reproductive abnormalities, and the buildup of substantial amounts of nanoparticles. As a consequence, the findings suggested that long-term exposure to TiO_2 NPs might have an impact on aquatic creatures' ability to develop, suggesting a potential danger to aquatic ecosystems. Additionally, several researchers have looked at how TiO_2 NPs affect aquatic animals. Chen et al., (2011) discovered that even small amounts of TiO_2 NPs (0.1-1 mg/L) on the tenth day of exposure led to a significant decrease in the swimming speed of zebrafish embryo larvae. Similarly, Federici et al., (2007) found that after 14 days of treatment with TiO_2 NPs, rainbow trout experienced mild lipidosis and apoptotic bodies in liver cells, as well as a reduction in the activity of Na+/K+-ATPase in the brain, gills, and gut. Additionally, the findings indicated that the fish's intestinal epithelium had eroded, probably as a consequence of ingesting water polluted with TiO_2 NPs. Hao et al., (2009) conducted research to investigate how TiO_2 NPs affects *Cyprinus carpio*, which is a type of freshwater fish. To do this, they examined the levels of antioxidant enzymes and lipid peroxidation in the fish's brain cells, liver, and gill. They also conducted pathological examinations after exposing the fish to TiO_2 NPs (100-200 mg/L) for 20 days, which revealed edema, thickening of gill lamellae and filaments, necrosis, and apoptosis of liver cells. Later, it was shown that *H. pluvialis* was sensitive to TiO_2 NPs (100 mg/L), which resulted in a drop in

biomass on day 9 and a significant rise in extracellular phenolic chemicals as a defence mechanism.

As microalgae *H. pluvialis* is one the of most popular algae used for diet and supplements, and also TiO_2 NPs are among the most commonly manufactured nanoparticles, the effect of how TiO_2 NPs will affect the nutritional properties of *H. pluvialis* is not widely reported. Multiple studies have reported that *H. pluvialis* has the capacity to effectively accumulate metals and MNPs in their biomass. However, the accumulative capacity of *H. pluvialis* for TiO_2 NPs and the corresponding detrimental effects of TiO_2 NPs on the nutritional values of *H. pluvialis* has not been reported yet. Hence the current investigation aimed to address this research gap and provide evidence on the detrimental effects of TiO_2 NPs on *H. pluvialis*.

2.8 Mechanism of TiO_2 NPs on microalgae

Algae, including *Phaeodactylum tricornutum*, can be negatively affected by the toxicity of metal nanoparticles, such as TiO_2 NPs. Studies have suggested that the toxicity of TiO_2 NPs on algae may be attributed to direct physical effects, such as damage to the cell wall caused by the entrapment of algae by the nanoparticles (Hou et al., 2019). To assess TiO_2 NP toxicity in microalgae, researchers commonly use parameters like cell growth inhibition, as well as membrane and DNA damage bioassays. When large aggregates of TiO_2 NPs entrap algal cells, it reduces the amount of light available to those cells,

inhibiting their growth. Furthermore, particle adhesion and entrapment can disrupt the cell membrane and interrupt energy transduction processes (Wang et al., 2016).

TiO_2 NPs have been found to cause membrane damage and potentially genotoxic damage in various coastal marine microalgae species. For instance, TiO_2 NP-induced growth inhibition in *Karenia brevis* was attributed to oxidative stress caused by the production of reactive oxygen species (ROS). The chloroplast, where ROS is produced and accumulates, is particularly affected in *K. brevis* cells. Similar physiological effects of TiO_2 NPs, including changes in chlorophyll-a content, soluble sugar content, malondialdehyde content, and enzyme activities, have been observed in the diatom *P. tricornutum*, and these effects were also attributed to ROS generation (Li et al., 2015).

TiO_2 NPs have been shown to increase tocochromanol content in Arabidopsis thaliana under light exposure, potentially due to TiO_2 NP photo-activation and the enhancement of ROS production. ROS and free radicals can directly damage chlorophyll molecules, cause lipid peroxidation in cell membranes, increase malondialdehyde content, reduce chlorophyll-a content, photosynthetic efficiency, and superoxide dismutase (SOD) activity, ultimately leading to membrane lipid damage (Wang et al., 2016).

Additionally, ROS can attack specific amino acid residues in proteins, such as Tyr, Phe, Trp, Met, and Cys, resulting in the formation of carbonyl derivatives. Hydrogen peroxide (H_2O_2) can generate more highly reactive hydroxyl radicals (OH-) through the Haber-Weiss reaction, which can further contribute to membrane lipid peroxidation, DNA strand breaks, protein damage, and base mutation (Hou et al., 2019).

CHAPTER 3

MATERIALS AND METHODS

3.1 Overview of Methodology

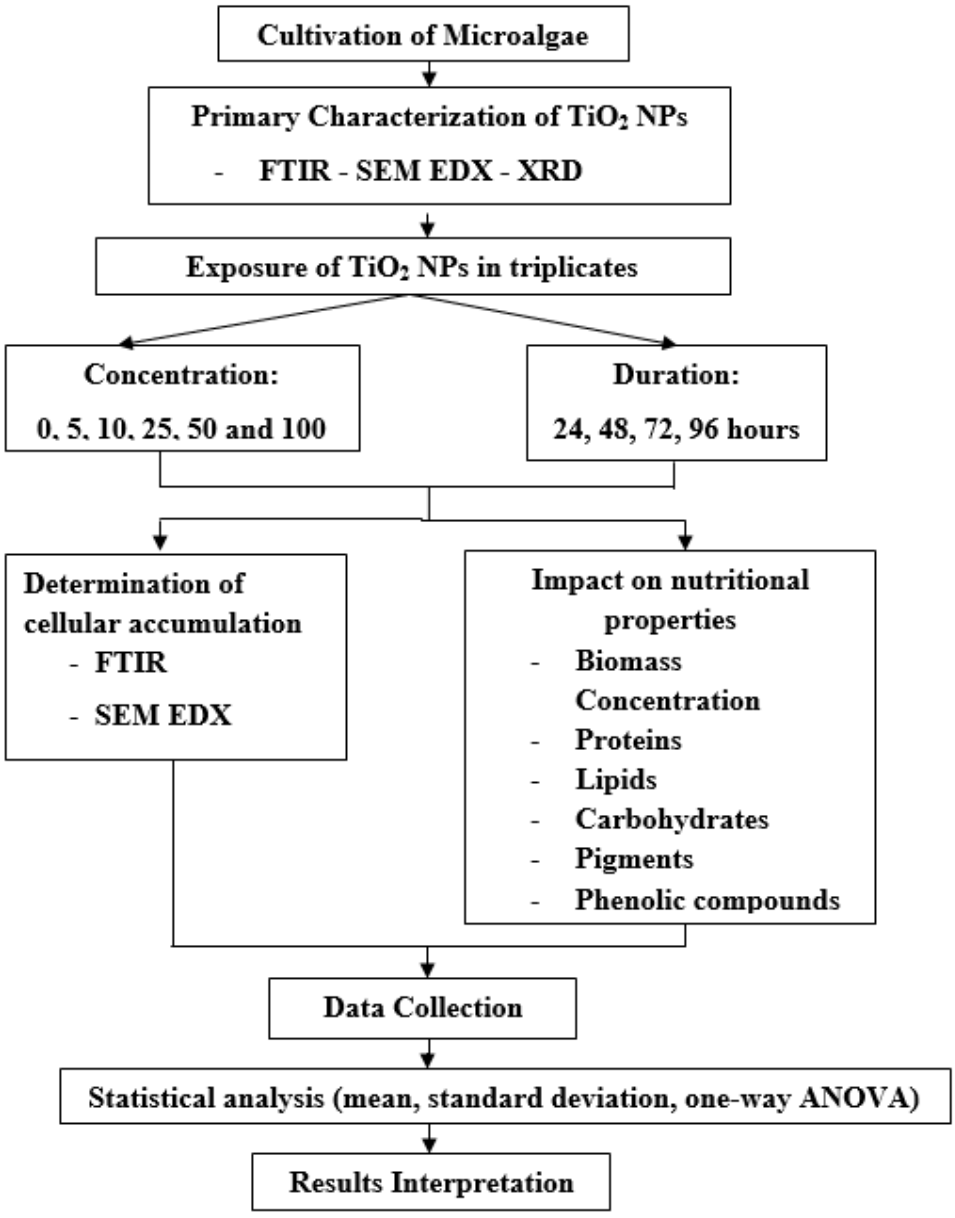

3.3 Characterization of TiO_2 NPs

The TiO_2 NPs powder, which had a particle size of 100 nm, was studied using various techniques. SEM was used to measure the particle size, with an acceleration voltage of 4.0 kV and a working distance of 6.0 mm. Energy dispersive X-ray (EDX) analysis, with an acceleration voltage of 10kV, was used to confirm the chemical composition of TiO_2 NPs. XRD was used to examine the crystalline nature of TiO_2 NPs, with Cu radiation and a scan range of 2=20-80, operated at a voltage of 40 kV and a current of 30 mA. FTIR spectroscopy, using Nicoler IS 10 instrument, was used to identify the functional groups present in the TiO_2 NPs powder, with a line frequency of 50, and operating at 120 V and 15 A. All the instruments used were from various manufacturers in Japan and the United States.

3.4 Cultivation of Microalgae

The University of Texas Culture Collection in Austin, Texas provided the original stock culture of *H. pluvialis*, a type of microalgae that lives in freshwater. The *H. pluvialis* were cultivated in Erlenmeyer flasks at room temperature (21-23 °C), under cool white fluorescent lamps that provided 1200 lux of light for 16 hours a day, followed by 8 hours of darkness. The algal cultures were sustained using BBM.

3.5 Exposure of Microalgae to TiO_2 NPs

A solution containing TiO_2 NPs at a concentration of 200 µg/mL was made and used to create five different concentrations of TiO_2 NPs (5, 10, 25, 50, and 100 µg/mL) by diluting the solution with BBM. *H. pluvialis* cells in the exponential growth phase (Day 8) with an initial OD680 of 0.4 were exposed to the five different concentrations of TiO_2 NPs for 24, 48, 72, and 96 hours in 1 L Erlenmeyer flasks. A control group of *H. pluvialis* cells was cultured in a medium without TiO_2 NPs to serve as a negative control.

3.6 TiO_2 NPs-Treated Algal Biomass Morphological Examination

After each contact session, 10 µL of the algal suspension was transferred to a glass slide and covered with a cover glass. The slide was then looked through a pair of microscopes (Leica DM500; Germany's Wetzlar).

3.7 Cellular Interaction and Cellular Accumulation of TiO_2 NPs on Algal Cells

3.7.1 Fourier Transformed Infrared Spectroscopy (FTIR)

FTIR spectroscopy was carried out to confirm the functional groups from the microalgal cell wall involved in the attachment of TiO_2 NPs on the cell surface of microalgal cells. A 25 mL of algal suspension was treated with different concentrations of TiO_2 NPs at different incubation periods and was centrifuged (Velocity 14R, Dynamica Scientific Ltd., Australia) at 5,000 rpm

for 10 min. The isolated pellet was then washed twice with 1x PBS and distilled water. The washed cells were freeze-dried to remove moisture and subjected to FTIR (Spectrum Two, Perkin-Elmer, United States of America) analysis over the range of 4000 to 400 cm^{-1} using the reflection technique.

3.7.2 SEM-EDX Analysis

To determine if TiO_2 NPs were present in *H. pluvialis* biomass, SEM-EDX analysis was conducted. The purpose was also to evaluate how TiO_2 NPs affected cell morphology. The algal cells were pelleted, washed twice with 0.1X PBS and distilled water, and freeze-dried after being exposed to TiO_2 NPs. Subsequently, the freeze-dried algal cells were examined using SEM-EDX (JSM-6701F, Joel, Japan).

3.8 Effects of TiO_2 NPs on Growth Pattern and Biomass

The concentration of algal biomass was determined by using a spectrophotometer (Gynesys 10S UV-Vis, Thermo Scientific, USA) to measure the optical density at 680 nm, along with a control. To eliminate any interference from TiO_2 NPs, an additional control was recorded and subtracted from the test reading for each concentration (Equation 1). The blank for both the tests and controls was the BBM, which is used for algal growth. To assess the effect of different concentrations of TiO_2 NPs on algal growth at various

time intervals, the percentage change in the test compared to the control was calculated (Equation 2).

OD of the culture at 680 nm = $OD_1 – OD_0$ (Eq. 1)

OD_0 = OD of the medium with TiO_2 NPs only

OD_1 = OD of cell culture with TiO_2 NPs

% change in biomass = (OD_{680} of negative control – OD_{680} of cell culture x 100) / (OD_{680} of negative control) (Eq.2)

3.9 Effects of TiO_2 NPs on Proteins, Carbohydrates and Lipids

3.9.1 Proteins

The alkali technique was used to obtain proteins from microalgae. The treated and untreated algal cultures were centrifuged, resulting in a supernatant volume of 10 mL after 10 minutes at 5,000 rpm. The pellet was then mixed with 4.5 mL of 0.5 N sodium NaOH, and incubated in an 80°C water bath (FCE20 Serials, Sastec, Malaysia) for 10 minutes to extract the protein. The mixture was then centrifuged again and the Lowry method was used to determine the protein content in the supernatant (Anusha et al., 2017a). The clear liquid layer above a solid residue and a solution called "Supernatant" was mixed with a solution called "Lowry reagent" which consists of three components in a ratio of 48:1:1. The mixture was left to incubate at room temperature for 10 minutes. After 30 minutes in the dark, 0.2 mL of a chemical called "Folin-Ciocalteau phenol reagent" was added to the mixture

and mixed by shaking. The absorbance of the mixture was measured at 600 nm using a microplate reader called "FLUOstar Omega" made by "BMG labtech" in Germany (Tan et al., 2020). To determine the amount of protein in the supernatant, a standard curve was established using BSA. The variation between the tests and the control was measured as a percentage using Equation 3.

% change in protein content = $(P_0 – P_1)$ x 100 % / P_0 (Eq. 3)

P_0 = Proteins in untreated cells

P_1 = Protein in treated cells

3.9.2 Carbohydrates

The process of HCl extraction was employed to isolate carbohydrates from microalgae. After spinning 10 mL of algal samples at 5,000 rpm for 10 minutes, the liquid portion above the sediment was discarded. Next, 5 mL of 2.5 N HCl was mixed with the remaining solid material, which was then heated in a water bath at 90 °C for three hours. After that, it was allowed to cool to room temperature (Sharma et al., 2019). In each of the test tubes, sodium carbonate was added until the effervescence stopped and the substance was neutralized. After diluting the sample with 50 mL of distilled water, it was centrifuged at 5,000 rpm for 10 minutes to separate the solid particles (Agrawal et al., 2015). The phenol-sulfuric acid method was used to determine the amount of carbohydrates in the sample. A new tube was filled with 1 mL of the sample's supernatant, 1 mL of distilled water, and 50 µL of 80% phenol,

then mixed by vortexing. The resulting mixture was combined with 5 mL of concentrated sulfuric acid (96% H_2SO_4), then vortexed again. After allowing the mixture to stand for 10 minutes, it was cooled in a water bath at room temperature for an additional 10 minutes. The mixture was vortexed again, and the absorbance at 490 nm was measured using a microplate reader (FLUOstar Omega, BMG labtech, Germany) (Nielsen, 2010). A typical graph made using glucose was used to assess the sample's carbohydrate content. Equation 4 was used to analyse the percentage difference between the test and control groups.

% change in carbohydrate content = $(C_0 – C_1)$ x 100 % / C_0 (Eq. 4)

C_0 = Carbohydrates in untreated cells

C_1 = Carbohydrates in treated cells

3.9.3 Lipids

A revised version of the Bligh and Dyer method was utilized to extract the overall lipids from the samples. After the algae sample was centrifuged at 5,000 rpm for 10 minutes, the pellet was resuspended with 7.6 mL of a mixture of chloroform, methanol, and water (1/2/0.8, v/v/v). The combination was then vortexed for 30 seconds and sonicated for 1 minute at 200 W and 45 kHz. To obtain a final ratio of chloroform, methanol, and water of 1/1/0.9 (v/v/v), roughly 2 mL of chloroform and water were added to the mixture. To split the mixture into three layers, the solution was agitated again for 30 seconds using a vortex, and then spun at a speed of 5,000 revolutions per

minute for five minutes using a centrifuge. The lower layer that contained lipids, which was the chloroform layer, was moved into a new tube that had been weighed beforehand, after removing the top layer of methanol. The middle layer that was left underwent a different extraction method. The chloroform layers were collected and combined into a single tube, then dried in an oven at a temperature of 80 °C for 24 hours (Rizwan et al., 2017). The weight of the resultant lipid was assessed and noted concerning the control (Eq. 5).

% change in the lipid content = $(L_0 – L_1)$ x 100 % / L_0 (Eq. 5)

L_0 = Lipids in untreated cells

L_1 = Lipid in treated cells

3.10 Effects of TiO_2 NPs on Pigments

3.10.1 Chlorophyll-*a* and Carotenoids

Chlorophyll-a and carotenoids were extracted using 90% methanol and then examined through spectrophotometry. To do this, a 5 mL algal sample was centrifuged at 5,000 rpm for 10 minutes, and the remaining liquid was discarded. The solid material obtained was mixed with 5 mL of 90% methanol and then agitated using a vortex. The resulting mixture was then kept in a 60 °C water bath for 10 minutes. After the mixture was left to incubate, it was subjected to centrifugation at a speed of 5,000 revolutions per minute (rpm) for 5 minutes to isolate the solid particles. To determine the absorbance of the liquid portion (supernatant), microplate readers were utilized to measure its

optical density at wavelengths 470, 652, and 665 nm (Kondzior and Butarewicz, 2018). Equations 6, 7, and 8 were applied to determine the levels of carotenoids and chlorophyll-a. Algal samples were examined for the percentage difference in carotenoids and chlorophyll-a relative to the control after being treated with various concentrations and duration intervals.

Chlorophyll-a (C_a) = 16.82A665 – 9.28A652 (mg/mL) (Eq. 6)

Chlorophyll-b (C_b) = 36.92A652 – 16.54A665 (mg/mL) (Eq. 7)

Carotenoid (C_t) = (1000A470 – 1.91Ca – 95.15Cb)/225 (mg/mL) (Eq. 8)

3.10.2 Astaxanthin

Extracting and analyzing the astaxanthin from 5 mL of nanoparticle-treated cell cultures was done by centrifuging them at 5000 rpm for 10 mins at 4 ^{o}C. Then, the supernatant was removed and the cell pellet was boiled for 2 mins at 70 ^{o}C with 3mL of 4M HCl in a centrifuge tube. The sample was then chilled before being centrifuged for 5 mins at 4 °C at 5000 rpm. After being treated with HCl, samples were resuspended in 3 mL of acetone for an hour, and their astaxanthin content was then determined using a UV spectrophotometer (Biochrom, U.K.). The astaxanthin concentrations (mg/L) were calculated using Equation 9 (Cheng et al., 2018). The percentage change relative to the control in the treated samples was calculated and analysed.

$$\text{Astaxanthin (mg/L)} = \text{OD480 x 4.5mg/L x Va/Vb} \quad \text{(Eq. 9)}$$

V_a = Volume of acetone

V_b = Volume of microalgae sample

3.11 Effects of TiO_2 NPs on Total Phenolic Compounds

The phenolic compounds present in the algal samples were extracted using distilled water. A 5 mL sample of algae was centrifuged for 10 minutes at 5,000 rpm, and the resulting supernatant was removed. The remaining pellet was mixed with 5 mL of distilled water and then incubated in an 80 °C water bath for 10 minutes. After cooling down to room temperature for 5 minutes, the mixture was centrifuged at 5,000 rpm to separate any solid particles. The total phenolic content of the resulting supernatant was determined using the Folin-Ciocalteau method (Machu et al., 2015). After transferring approximately 1 mL of supernatant to a new tube, a mixture was created by adding 1 mL of Folin-Ciocalteau reagent (FCR) and 5 mL of distilled water. The mixture was then vortexed and left at room temperature for five minutes in the absence of light. The resulting solution was further diluted with distilled water to a final volume of 10 mL, followed by the addition of 1 mL of 20% Na_2CO_3. After another round of vortexing, the solution was left at room temperature for 1 hour in the absence of light. Finally, the solution's absorbance was measured at 765 nm using a microplate reader (Casazza et al., 2015a). Gallic acid was utilized to construct a standard curve for quantifying the total phenolic content of the algal samples. To assess the findings, Equation 10 was utilized to determine the percentage difference between the tests and the control and to analyze the results.

% change in total phenolic compounds = $(P_0 – P_1)$ x 100 % / P_0 (Eq. 10)

P_0 = Phenolic compounds in untreated cells

P_1 = Phenolic compounds in treated cells

3.12 Statistical analysis

In order to examine the dispersion caused by TiO_2 NPs on algal cells, statistical analysis was done. All challenge tests were performed in triplicate (n = 3) and data are conferred as mean ± standard error. Data were tested for normality using the Shapiro-Wilk test. One-way analysis of variance (ANOVA) was used for all analyses with significant values ($p<0.05$), followed by the Tukey's post hoc test for multiple comparisons (SPSS version 22).

CHAPTER 4

RESULTS

4.1 Characterization of TiO_2 NPs

TiO_2 NPs was observed using an SEM and showed agglomerates and NPs in a variety of shapes and sizes. The TiO_2 NPs were analyzed, and it was found that the particles had an average size of 35.8 nm, ranging from 23.2 to 35.8.4 nm as shown in Figure 4.1A. Additionally, the EDX spectra displayed peaks that matched those of titanium and oxygen molecules, proving that the TiO_2 NPs were elemental, as seen in Figure 4.1B. The nanopowder's XRD spectrum (Fig 4.1C) also showed the strongest diffraction peaks. The XRD peaks of the sample were intense, denoting that the TiO_2 NPs are crystalline and are very small that is shown by the diffraction peaks. The average crystallite size of TiO_2 NPs was confirmed using Debye-Scherrer's equation and was estimated to be 18.52 nm. The chemical composition of TiO_2 NPs was investigated further using FTIR (Fig 4.1D). The existence of unresolved Ti-O-Ti stretching vibrations might be classified as a broad band in the 400–900 cm^{-1} range (Fig 4.1D). Furthermore, two bands at 1634 and 3431 cm^{-1} were linked to O-H group bending and stretching vibrations (Gohari et al., 2020).

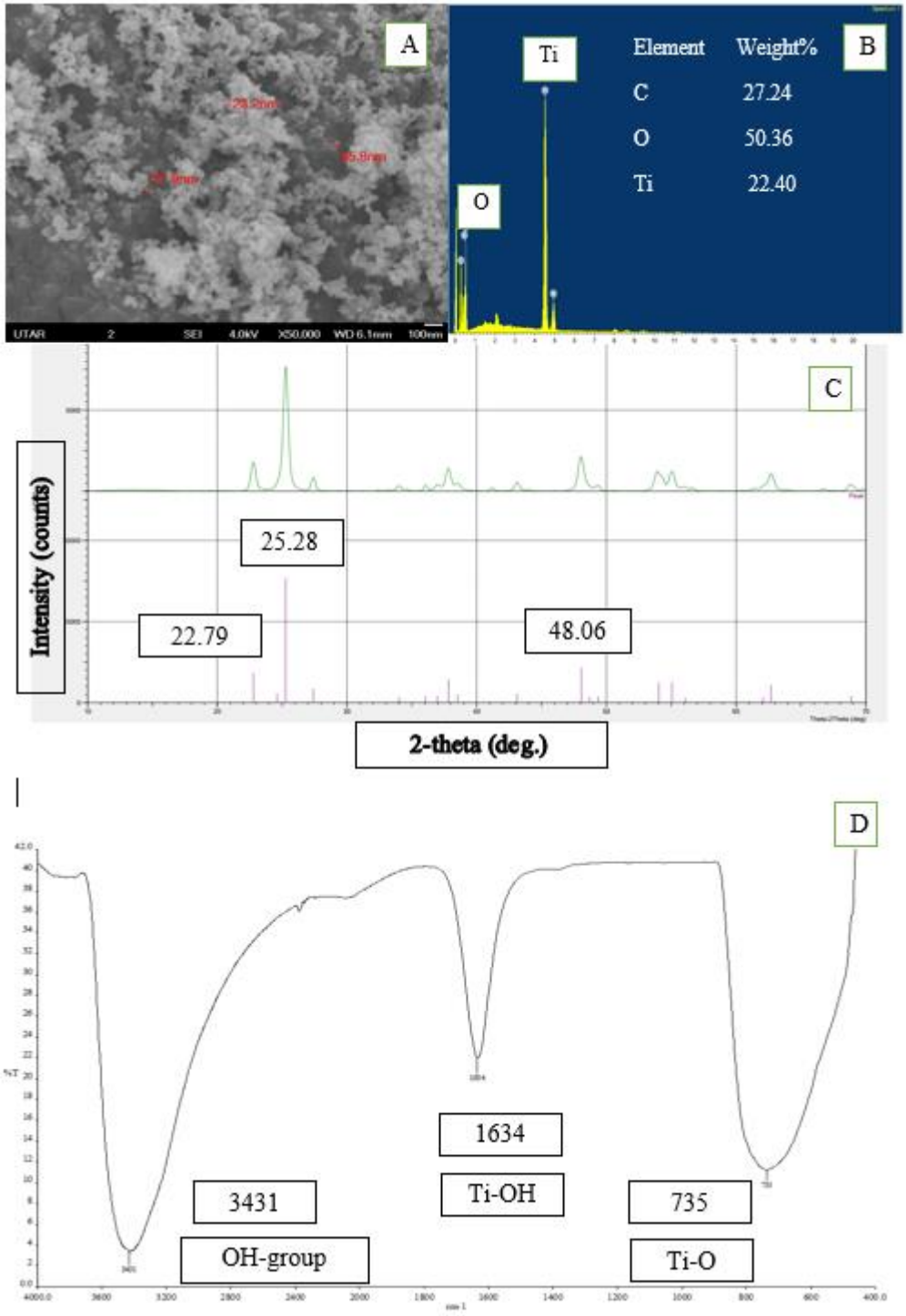

Figure 4.1: TiO_2 NPs Characterization under SEM image (A), EDX spectrum (B), XRD spectrum (C) and (D) FTIR spectroscopy of TiO_2 NPs.

4.2 Morphological examination of TiO_2 NPs treated algal cells

Figure 4.2 illustrates the differences between control *H. pluvialis* cells and those treated with 100 μg/mL TiO_2 NPs, as seen through light microscopy. In Figure 4.2 (A and B), the algal cells are shown to have intact membranes, and many of them are motile, indicating that they have not been treated with TiO_2 NPs. However, in the case of the TiO_2 NPs treated cells, the images reveal the presence of the nanoparticles attached to the cell surface, as well as the formation of clusters of deformed cells, ghost cells, and algal cell aggregation.

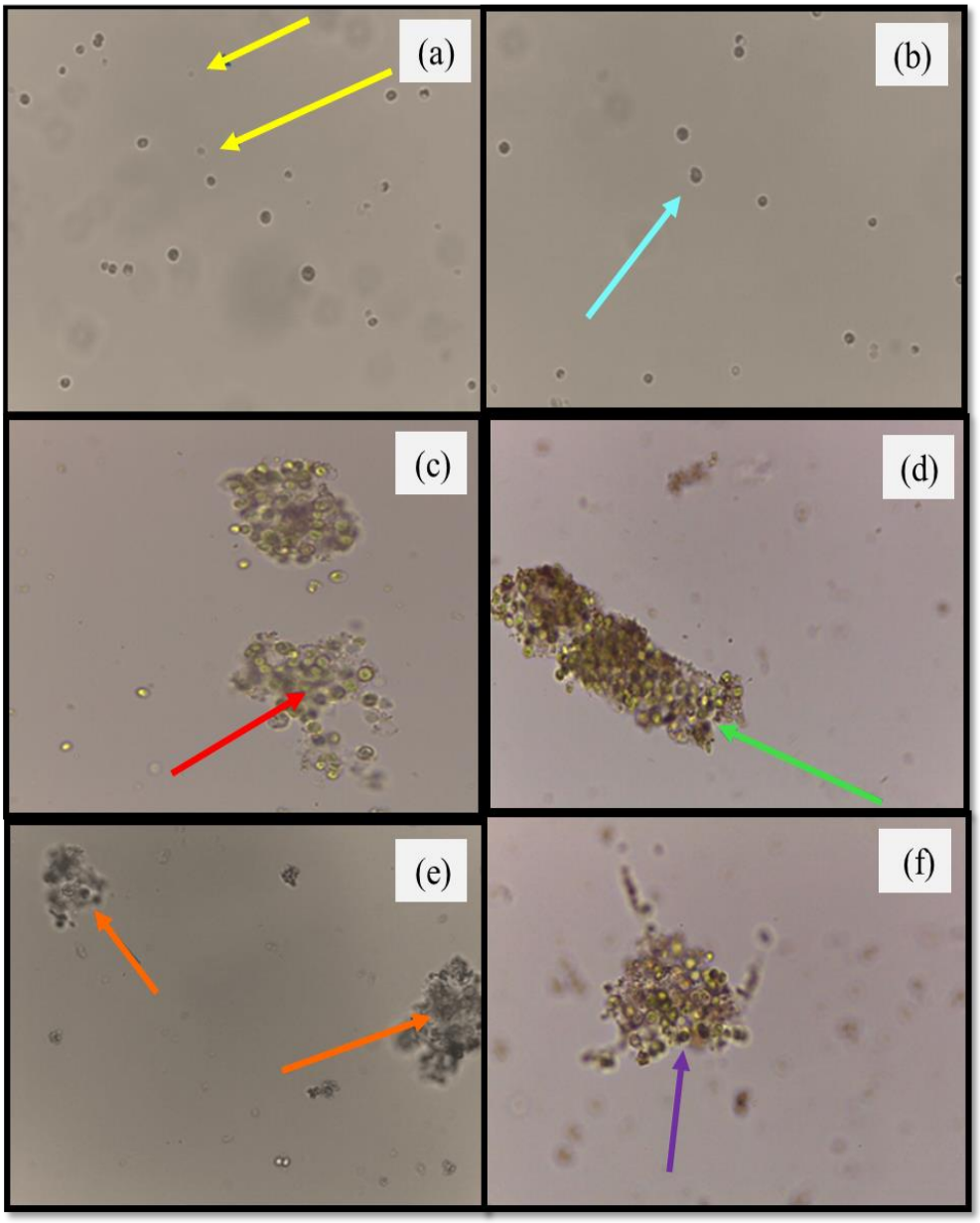

Figure 4.2: Light microscopy images of control and 100 µg/mL TiO_2 NPs treated *H. pluvialis* at 96 h. (A and B) control at 40X magnification and (C, D, E and F) 100 µg/mL TiO_2 NPs treated *H. pluvialis* at 40X magnification. Motile *H. pluvialis* cells can be seen (yellow arrow), cell membrane of the control cells is visible (blue arrow), algal cells wrapped around the NP agglomerates (red arrow), aggregated *H. pluvialis* cells (green arrow), aggregated with bleached ghost cells (orange arrow) and aggregated with deformed cells (purple arrow) of *H. pluvialis* can be seen clearly.

4.3 Cellular Interaction and Cellular Accumulation of TiO_2 NPs on Algal Cells

4.3.1 FTIR Spectroscopy

FTIR spectroscopy was used to confirm which functional groups in the algal cell wall were responsible for binding and taking in TiO_2 NPs. Figure 4.3 shows the results of this analysis. By comparing the shifted peaks in algal samples treated with 100 μg/mL TiO_2 NPs to the control group at 96 hours, possible functional groups involved in the process were identified and analyzed. These functional groups are listed in Table 4.1.

Table 4.1: Potential participation of various functional groups found in the cell wall of *H. pluvialis* in the attachment of TiO_2 NPs to the surface of the algal cells.

Absorption (cm^{-1})	Functional Groups	Component
3435 - 3401	-OH, -NH	Hydroxyl, amine (protein)
2918 - 2917	$-CH_2$	Methyl (lipid fraction)
1654	C=O	Amide I (protein)
1544	N-H, C-N	Amide II (protein)
1249	P=O	Phosphodiesters (nucleic acid, phospholipids
1077 - 1076	C-C, C-O, C-OH	Carboxyl, Hydroxyl
528 - 525	-PO, -CH	Phosphate

Figure 4.3: FTIR spectrum of *H. pluvialis* biomass without the treatment of TiO_2 NPs (control) at 96 h.

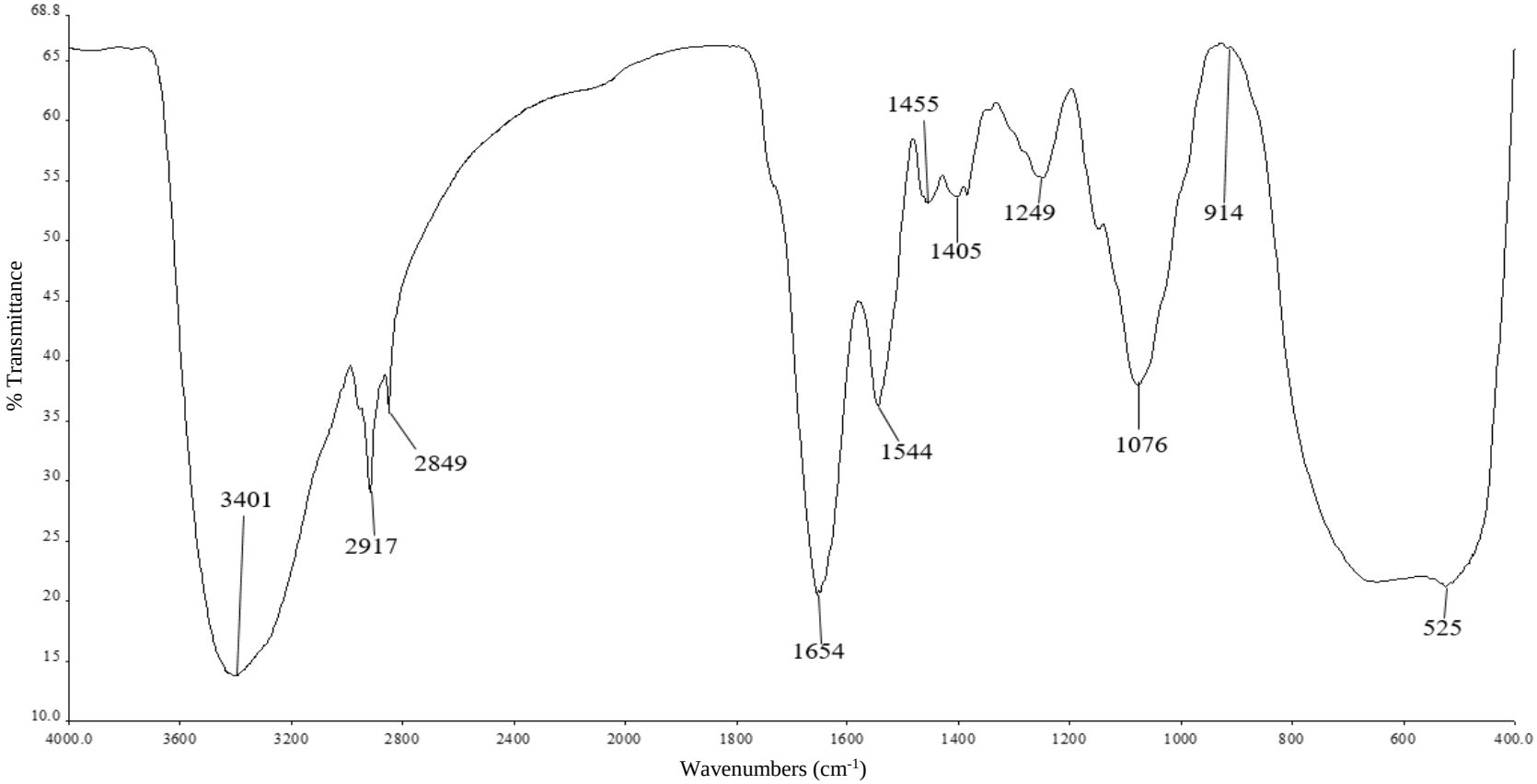

Figure 4.4: FTIR spectrum of *H. pluvialis* biomass treated with of TiO_2 NPs at 96 h.

4.3.2 SEM-EDX Analysis

Figure 4.5 illustrates SEM images of *H. pluvialis* cells treated with 100 μg/mL TiO_2 NPs and untreated control cells. The images demonstrate that cells in Figure 4.5 (A and B) appear as smooth cylindrical structures with undamaged cell membranes when they were not treated with TiO_2 NPs. While, the cells treated with TiO_2 NPs show cell entrapment with NP clusters, aggregation of algal cells, and rupture of the cell membrane, which led to cell rupture, as well as wrinkled cells of *H. pluvialis cells*. The presence of titanium was detected in the EDX spectrum of cells treated with TiO_2 NPs (Figure 4.6), but not in the control cells. This confirms that TiO_2 NPs have accumulated on *H. pluvialis*. The carbon and oxygen element signals may be due to the X-ray emission from *H. pluvialis* cell wall. The cell wall of *H. pluvialis* primarily consists of polysaccharides, such as cellulose and pectin. These components contain carbon and oxygen atoms, which can be detected through SEM-EDX analysis (Zinicovscaia et al., 2017a).

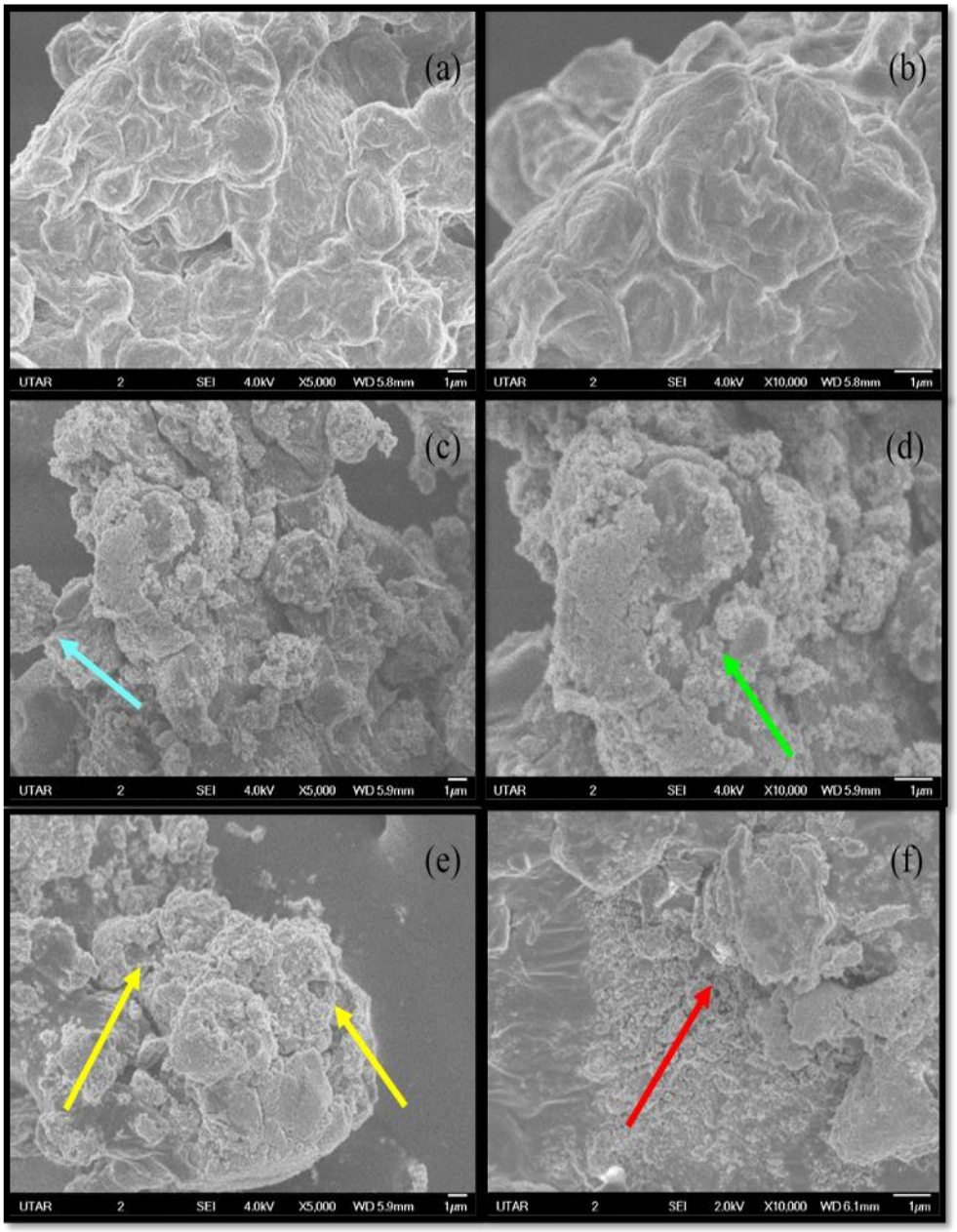

Figure 4.5: SEM images of control and 100 µg/mL TiO_2 NPs treated *H. pluvialis* at 96 h. (A) control at 5000X magnification; (B) control at 10000X magnification; (C, E) 100 µg/mL TiO_2 NPs treated *H. pluvialis* at 5000X magnification; (D, F) 100 µg/mL TiO_2 NPs treated *H. pluvialis* at 10000X magnification. Aggregates of distorted cells (blue arrow), Adsorption of TiO_2 NPs agglomerates on the *H. pluvialis cells* (green arrow), Cell and cell membrane rupture (yellow arrow), and Wrinkling of *H. pluvialis cells* (red arrow) can be clearly seen.

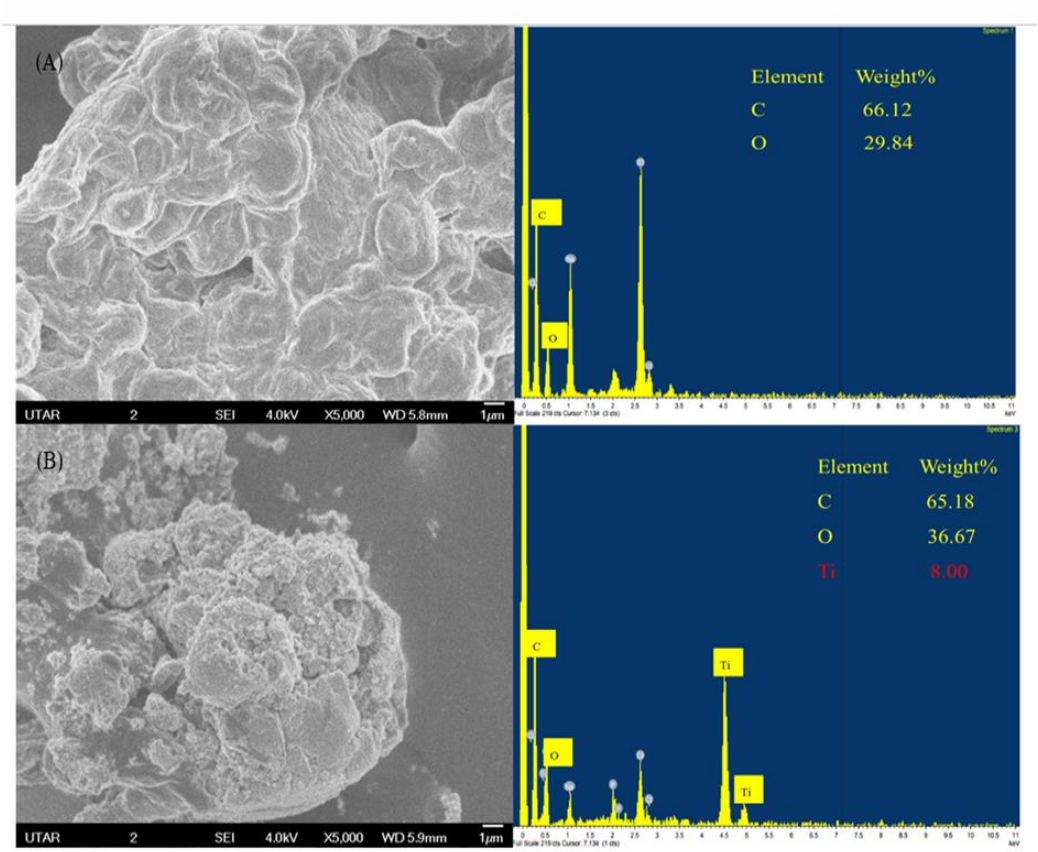

Figure 4.6: EDX image and spectrum of control (A) and 100 µg/mL TiO_2 NPs treated *H. pluvialis* at 96 h (B).

4.4 Effects of TiO_2 NPs on Growth Pattern and Biomass

Figure 4.7 and Figure 4.8 display the growth patterns and cultures of *H. pluvialis* treated with varying concentrations of TiO_2 NPs at different time intervals. The amount of biomass in *H. pluvialis* decreased with an increase in the concentration of TiO_2 NPs and the duration of exposure, as shown in Figure 4.9. This figure illustrates the percentage of biomass loss in *H. pluvialis* when treated with different concentrations of TiO_2 NPs, ranging from 5 to 100 µg/mL, for 24 to 96 hours, relative to the control. The exposure of TiO_2 NPs

resulted in a significant ($p < 0.05$) reduction in the biomass of *H. pluvialis* between 24 and 96 hours. Moreover, a significant ($p < 0.05$) loss in biomass was observed for all tested concentrations of TiO_2 NPs, ranging from 5 to 100 µg/mL, between 24 and 96 hours. The highest loss in biomass occurred at 96 hours, with values reported as 10.42 ± 3.29, 16.15 ± 3.02, 22.87 ± 2.83, 30.29 ± 2.5, and 43.29 ± 2.02% for 5, 10, 25, 50, and 100 µg/mL TiO_2 NPs, respectively.

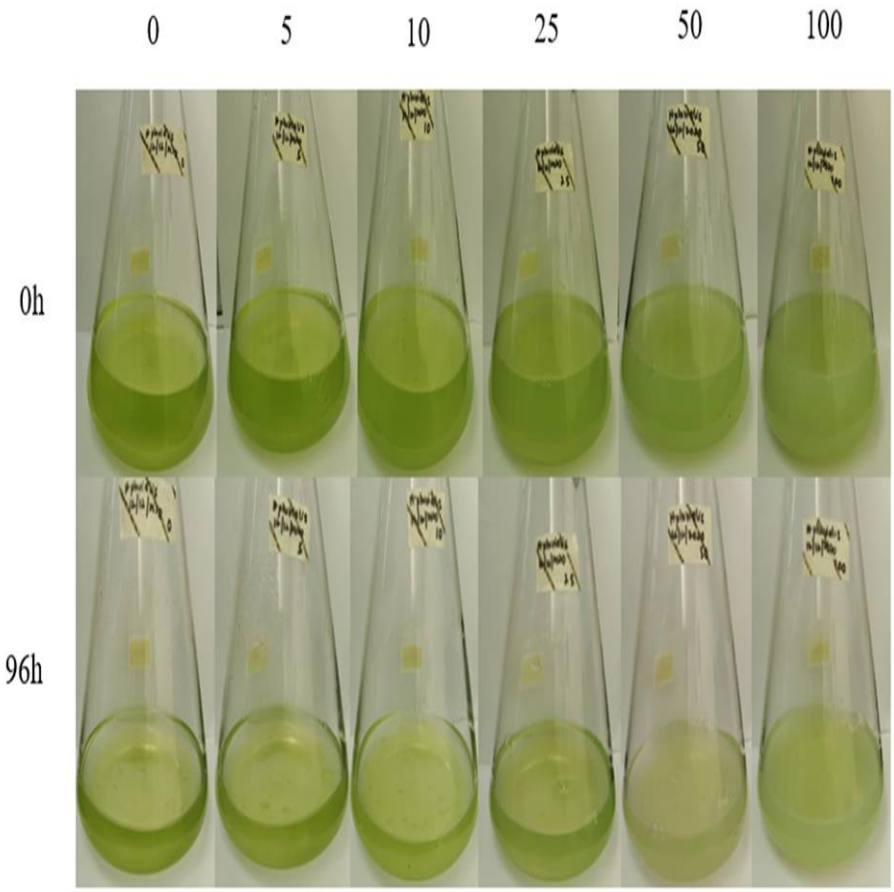

Figure 4.7: *H. pluvialis* cultures treated with different concentrations of TiO_2 NPs at 0 and 96h.

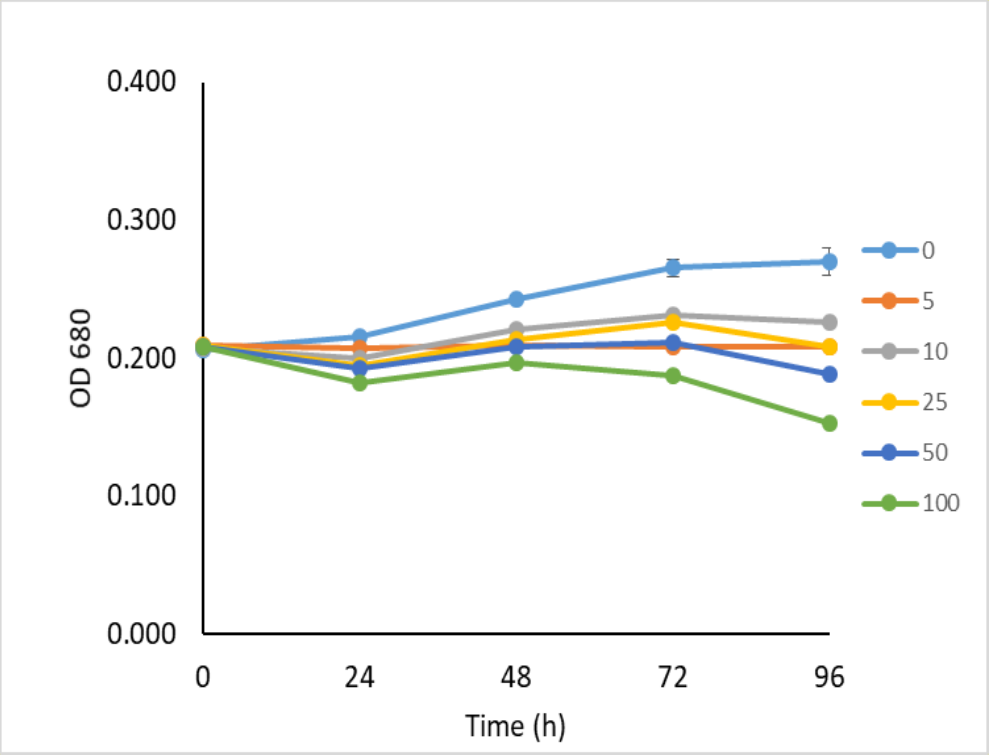

Figure 4.8: Growth pattern of *H. pluvialis* treated with different concentrations of TiO_2 NPs at each time interval

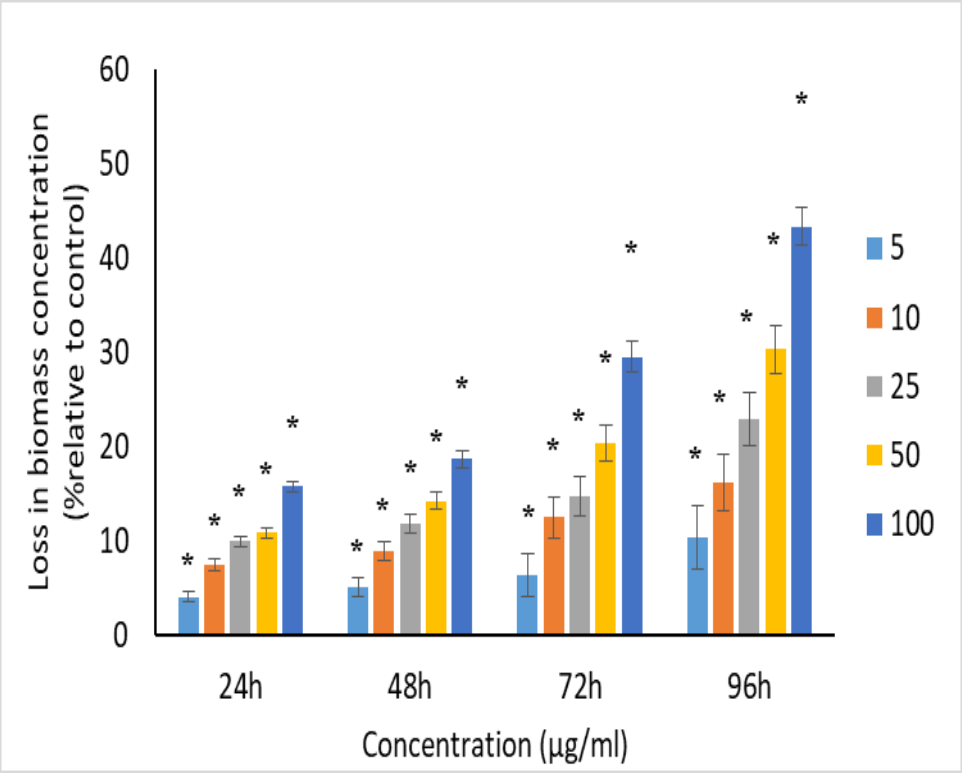

Figure 4.9: Percentage of loss in biomass concentration of *H. pluvialis* relative to control from 24 to 96 h upon treatment of TiO_2 NPs. The values plotted are in mean ± standard deviation. * indicates the significance difference at $p < 0.05$ between the control and TiO_2 NPs treated algal suspension for each time interval.

4.5 Effects of TiO_2 NPs to Proteins, Carbohydrates and Lipids

4.5.1 Proteins

In Figure 4.10, it can be seen that as the dose of TiO_2 NPs and time interval increased, there was an increase in the percentage of protein loss in *H. pluvialis*. All of the concentrations of TiO_2 NPs that were tested resulted in a significant ($p < 0.05$) reduction in the protein content of *H. pluvialis* from 24 to 96 hours. At 96 hours, the maximum decrease in protein content was observed, with values of 18.61 ± 2.76%, 33.52 ± 1.39%, 40.50 ± 4.07%, 54.12

± 1.31%, and 67.05 ± 0.99% for 5, 10, 25, 50, and 100 µg/mL of TiO_2 NPs, respectively.

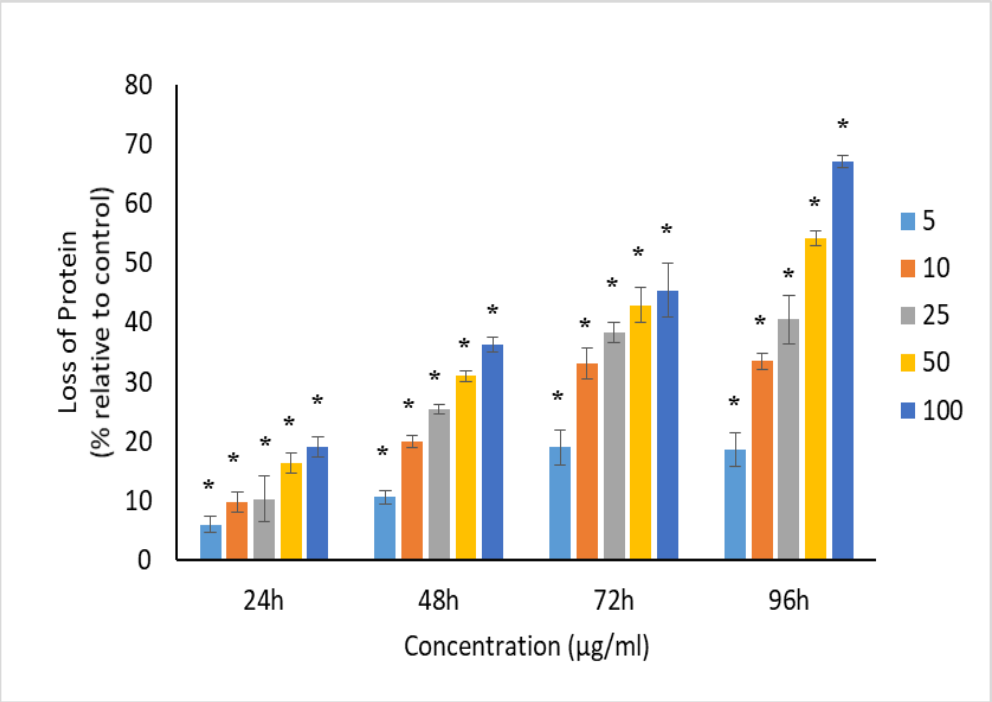

Figure 4.10: Percentage of loss in proteins of *H. pluvialis* relative to control from 24 to 96 h upon treatment of TiO_2 NPs. The values plotted are in mean ± standard deviation. * indicates the significance difference at $p < 0.05$ between the control and TiO_2 NPs treated algal suspension for each time interval.

4.5.2 Carbohydrates

The graph in Figure 4.11 illustrates the percentage of carbohydrate loss in *H. pluvialis* compared to a control group when exposed to TiO_2 NPs. The results indicate that exposure to TiO_2 NPs resulted in a significant increase in carbohydrate content for concentrations of 5 µg/mL or greater after 24 hours. However, a significant loss in carbohydrate content was observed for

concentrations ranging from 10 to 100 µg/mL after 24 hours. Furthermore, all tested concentrations of TiO_2 NPs showed a significant decrease in carbohydrate content from 48 to 96 hours. The maximum reduction in carbohydrate content was observed after 96 hours, with values of 7.51 ± 0.24%, 19.16 ± 0.22%, 28.82 ± 0.25%, 39.36 ± 0.22%, and 48.67 ± 0.18% for TiO_2 NPs concentrations of 5, 10, 25, 50, and 100 µg/mL, respectively.

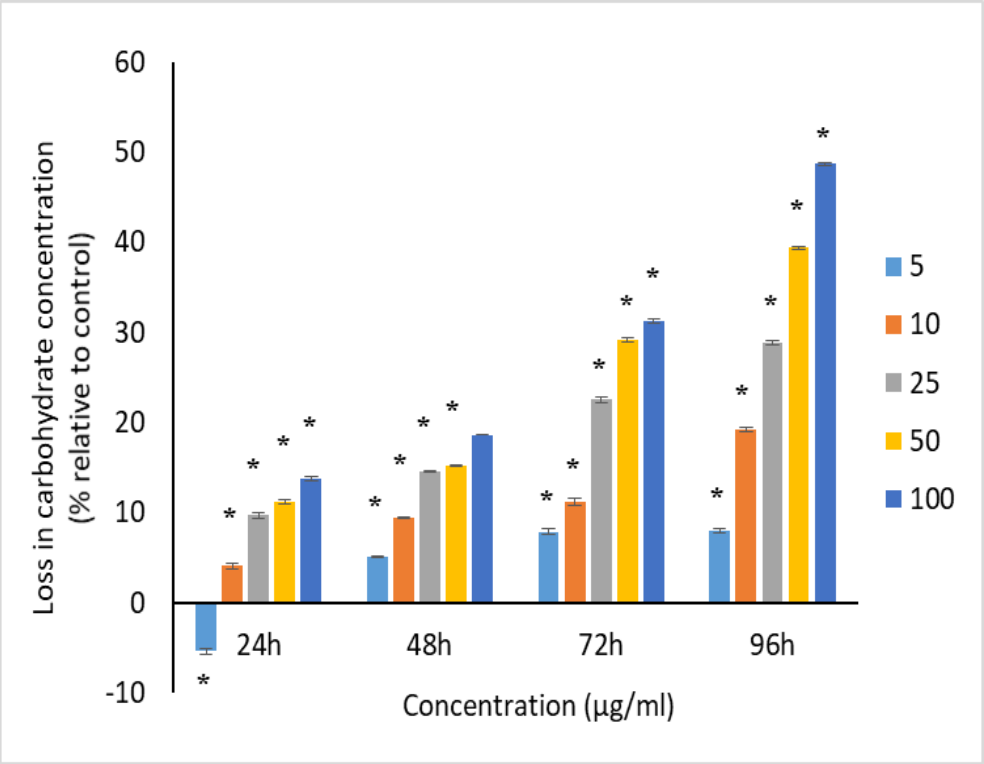

Figure 4.11: Percentage of loss in carbohydrates of *H. pluvialis* relative to control from 24 to 96 h upon treatment of TiO_2 NPs. The values plotted are in mean ± standard deviation. * indicates the significance difference at $p < 0.05$ between the control and TiO_2 NPs treated algal suspension for each time interval.

4.5.3 Lipids

The figure depicted in Figure 4.12 illustrates the increase in the percentage of lipid loss in *H. pluvialis* as the concentration of TiO_2 NPs and the duration of exposure increased. All concentrations of TiO_2 NPs that were tested caused a significant reduction in lipid content in *H. pluvialis* from 24 to 96 hours, with the maximum reduction occurring at 96 hours. The resulting values for lipid reduction were 8.84 ± 0.22%, 18.08 ± 0.54%, 22.55 ± 0.12%, 31.11 ± 0.36%, and 44.22 ± 0.49% for TiO_2 NP concentrations of 5, 10, 25, 50, and 100 µg/mL, respectively.

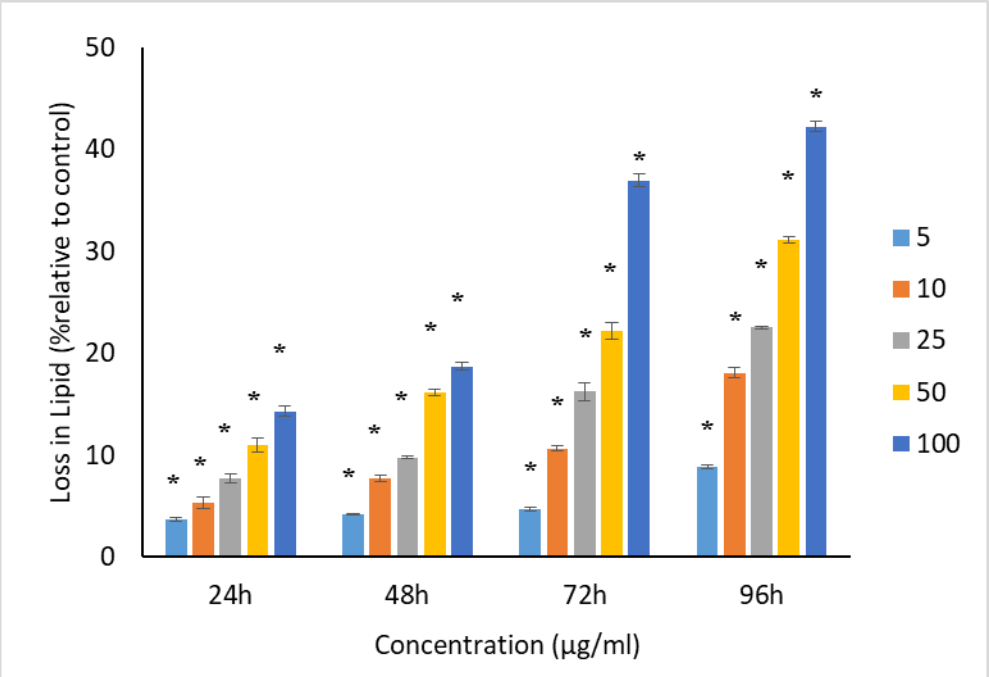

Figure 4.12: Percentage of loss in lipids of *H. pluvialis* relative to control from 24 to 96 h upon treatment of TiO_2 NPs. The values plotted are in mean ± standard deviation. * indicates the significance difference at $p < 0.05$ between the control and TiO_2 NPs treated algal suspension for each time interval.

4.6 Effects of TiO_2 NPs on Chlorophyll-*a*, Carotenoids and Astaxanthin

4.6.1 Chlorophyll-*a*

In Figure 4.13, the decrease in chlorophyll-a levels in *H. pluvialis* can be seen. As the dose of TiO_2 NPs and exposure time increased, the percentage of chlorophyll-a loss also increased. The exposure to TiO_2 NPs resulted in a significant ($p < 0.05$) reduction in chlorophyll-a levels in *H. pluvialis* across all tested concentrations of TiO_2 NPs from 24 to 96 hours. The largest reduction in chlorophyll-a content was observed after 96 hours, with values of 15.52 ± 0.87, 24.50 ± 0.94, 26.41 ± 1.05, 32.21 ± 2.46, and 39.31 ± 2.54% for 5, 10, 25, 50, and 100 μg/mL of TiO_2 NPs, respectively.

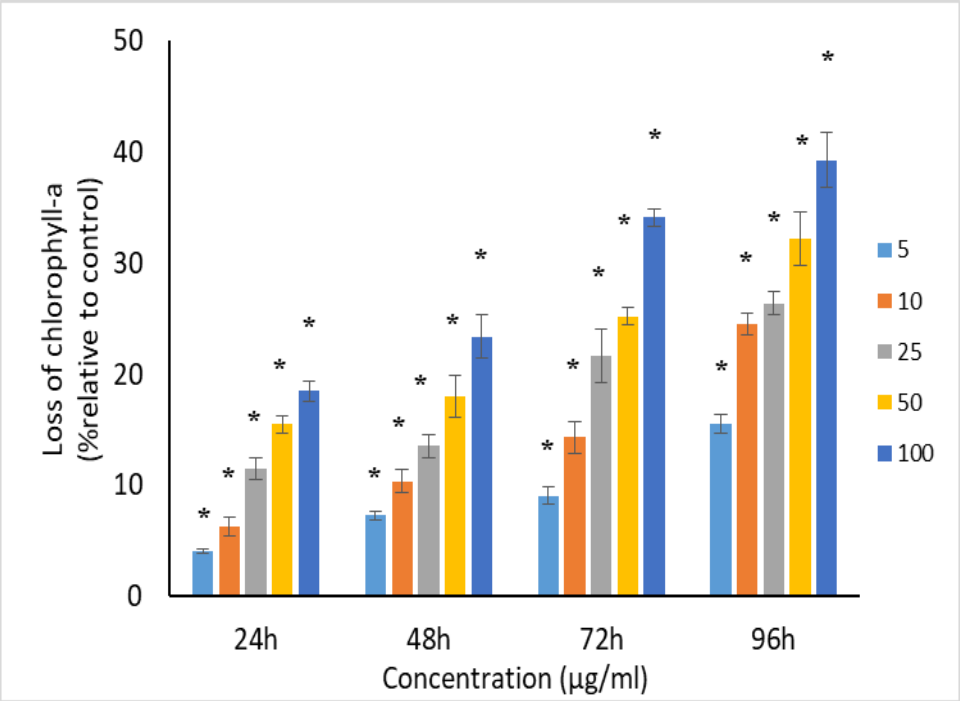

Figure 4.13: Percentage of loss in chlorophyll-a of *H. pluvialis* relative to control from 24 to 96 h upon treatment of TiO_2 NPs. The values plotted are in mean ± standard deviation. * indicates the significance difference at $p < 0.05$ between the control and TiO_2 NPs treated algal suspension for each time interval.

4.6.2 Carotenoids

In Figure 4.14, the increase in the concentration of TiO_2 NPs and time interval led to a higher percentage of carotenoid loss in *H. pluvialis*. All concentrations of TiO_2 NPs that were tested resulted in a significant ($p < 0.05$) decrease in carotenoid levels in *H. pluvialis* between 24 and 96 hours. The greatest decrease in carotenoid content was seen at 96 hours, with the resulting values of 13.39 ± 0.55, 20.43 ± 0.21, 22.19 ± 0.70, 26.22 ± 1.76, and 34.92 ± 0.84% for TiO_2 NPs at 5, 10, 25, 50, and 100 µg/mL concentrations, respectively.

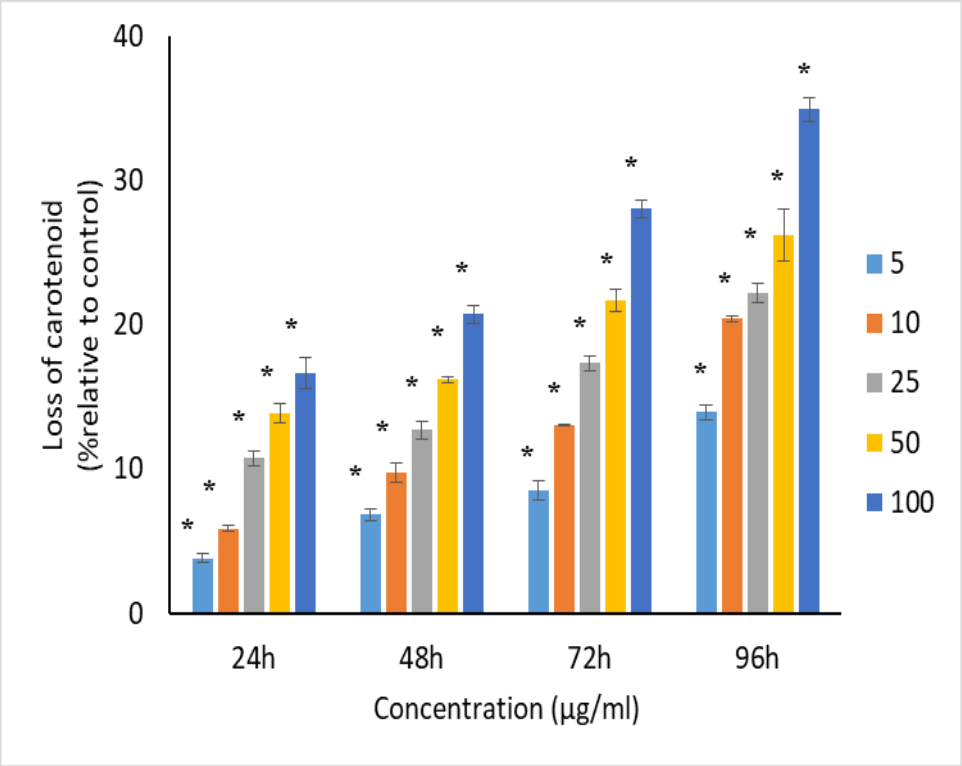

Figure 4.14: Percentage of loss in carotenoids of *H. pluvialis* relative to control from 24 to 96 h upon treatment of TiO_2 NPs. The values plotted are in mean ± standard deviation. * indicates the significance difference at $p < 0.05$ between the control and TiO_2 NPs treated algal suspension for each time interval.

4.6.3 Astaxanthin

In Figure 4.15, it can be observed that as the concentration of TiO_2 NPs and the time interval increased, there was an increase in the percentage of loss of astaxanthin in *H. pluvialis*. All concentrations of TiO_2 NPs that were tested resulted in a significant ($p < 0.05$) decrease in astaxanthin content in *H. pluvialis* from 24 to 96 hours. At 96 hours, the maximum reduction in astaxanthin content was observed, with values of 12.14 ± 0.48, 17.73 ± 0.46, 20.05 ± 0.43, 26.35 ± 0.40, and 34.24 ± 0.36% for 5, 10, 25, 50, and 100 µg/mL of TiO_2 NPs, respectively.

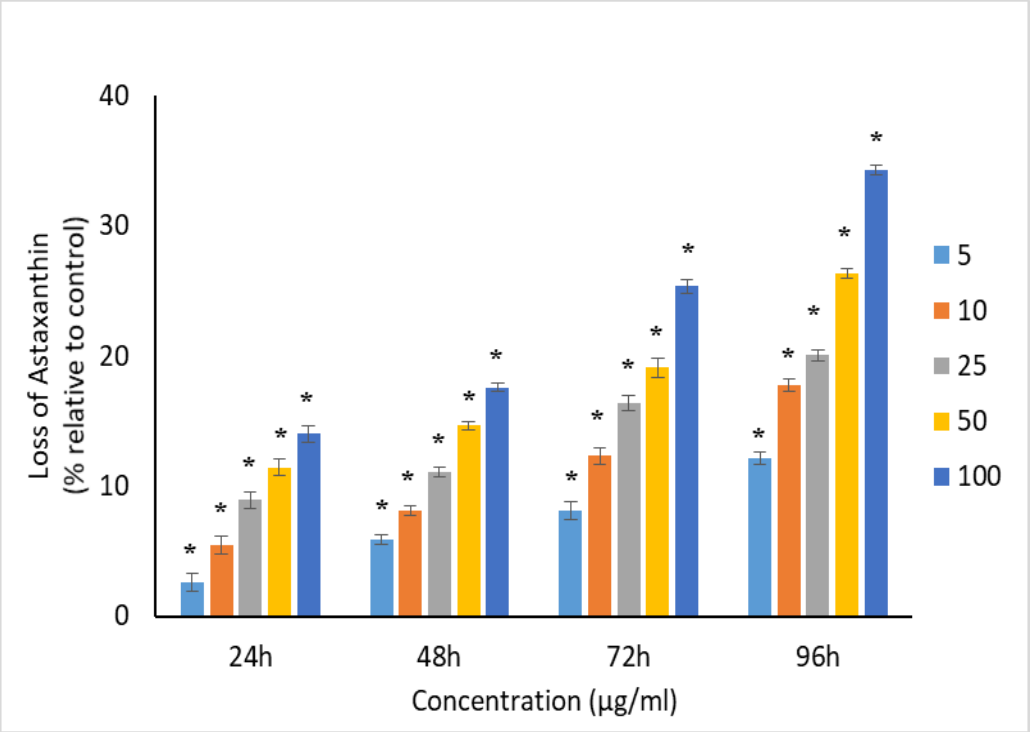

Figure 4.15: Percentage of loss in astaxanthin of *H. pluvialis* relative to control from 24 to 96 h upon treatment of TiO_2 NPs. The values plotted are in mean ± standard deviation. * indicates the significance difference at $p < 0.05$ between the control and TiO_2 NPs treated algal suspension for each time interval.

4.7 Effects of TiO_2 NPs on Total Phenolic Compounds

Figure 4.16 shows the impact of different concentrations of TiO_2 NPs on the total phenolic content of *H. pluvialis* over a period of time. At 24 hours, all tested concentrations of TiO_2 NPs showed a significant increase in total phenolic content, while at 48 hours, only 5 and 10 µg/mL of TiO_2 NPs had a significant effect. However, after 48 hours, the overall phenolic content of *H. pluvialis* treated with TiO_2 NPs at concentrations between 25 and 100 µg/mL began to decline, and a significant loss was observed at 48 hours. From 72 to 96 hours, all tested concentrations of TiO_2 NPs caused a significant loss in

total phenolic compound of *H. pluvialis*. The maximum reduction in phenolic content was observed at 96 hours, with percentage reductions of 9.11 ± 1.34%, 14.41 ± 1.37%, 18.24 ± 1.30%, 27.22 ± 1.51%, and 42.66 ± 0.94% for 5, 10, 25, 50, and 100 µg/mL of TiO_2 NPs, respectively.

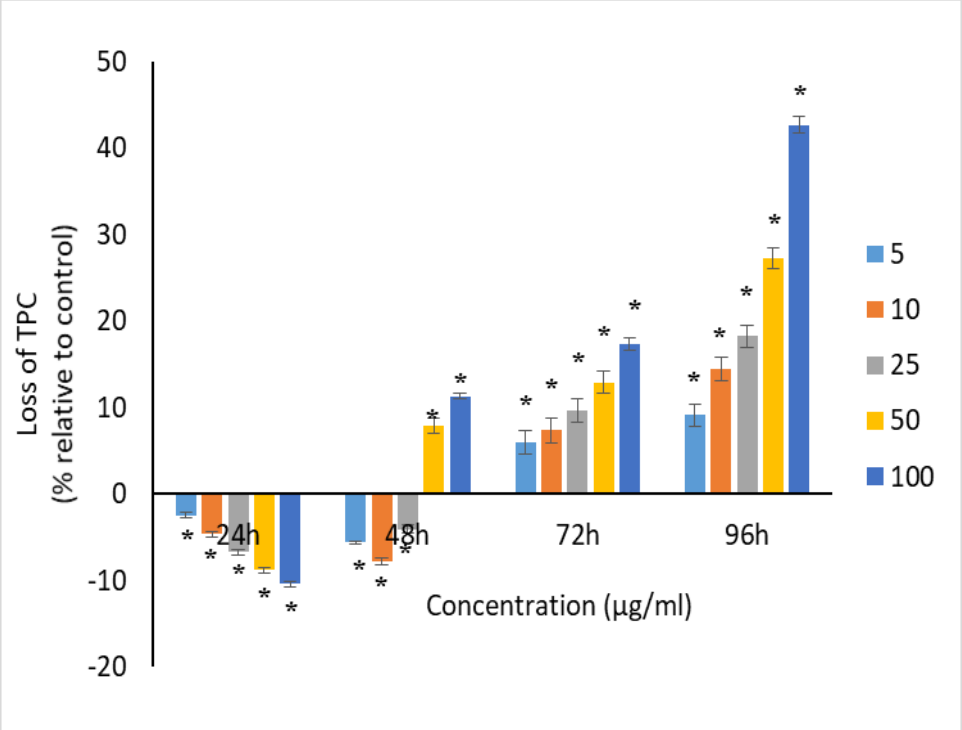

Figure 4.16: Percentage of loss in total phenolic compounds of *H. pluvialis* relative to control from 24 to 96 h upon treatment of TiO_2 NPs. The values plotted are in mean ± standard deviation. * indicates the significance difference at p < 0.05 between the control and TiO_2 NPs treated algal suspension for each time interval.

CHAPTER 5

DISCUSSION

5.1 Morphological examination of TiO_2 NPs treated algal cells

Images captured using a light microscope of *H. pluvialis* cells exposed to TiO_2 NPs revealed a decline in the ability of cells to move, the occurrence of ghost cells (as illustrated in Figure 4.2), clusters of NPs that were attached to algal cells, the formation of groups of cells, and modifications in the structure, such as uneven surfaces, breakage of cell membranes, and cell bursting. According to our findings, (M. M. R. Shah et al., 2016) showed that *H. pluvialis* has both non-motile resting vegetative cells with loosing flagella and expanded cell size under favourable growth conditions as well as motile flagellated vegetative cells under unfavourable environmental or culture conditions like nutrient deficiency, salt stress, and high light illumination. (Comotto et al., 2014a) found that when TiO_2 NPs were exposed to cells of *C. vulgaris*, *H. pluvialis*, and *S. platensis*, they observed the aggregation of cells and degradation of the cell wall. Meanwhile, Dong et al., (2014) observed heavily wrinkled and damaged cell walls in *H. pluvialis* cells that had been treated with hydrochloric acid-acetone (HCl-ACE). (Harker et al., 1996) found that ghost cells of *H. pluvialis* that had been completely bleached did not contain chlorophyll or carotenoids when they were subjected to high levels of salt and

strong light. When the algal cells were subjected to progressively unfavourable environmental circumstances, it was discovered that the number of ghost cells significantly increased. According to theory, such cell bleaching results from metabolic imbalance brought on by environmental stress and may also be produced by cytoplasmic leaking of cells as a result of cell membrane rupture.

5.2 Cellular Interaction and Cellular Accumulation of TiO_2 NPs on Algal Cells

5.2.1 FTIR Spectroscopy

The attachment of TiO_2 NPs to the microalgae was studied using FTIR to identify potential functional groups that may be involved. The TiO_2 NPs may interact with *H. pluvialis* by utilizing some of its functional groups such as hydroxyl, amine, methyl, amide I, amide II, carboxyl, carbonyl, and phosphate groups. When the hydroxyl and amide functional groups from water and protein are symmetrically stretched, it creates a range between 3435 and 3401 cm^{-1}, which has been observed in previous studies (Ansari et al., 2019; Dotto et al., 2012; Zinicovscaia et al., 2020). It was observed that there is an asymmetric stretching vibration of the methyl group in the long methylenic chains of lipidic fractions between the range of 2918 to 2917 cm^{-1} (Ansari et al., 2019; Ferreira et al., 2011). While the symmetric deformation of N-H bend and C-N stretching of protein amide II may be detected between 1544 cm^{-1} and 1654 cm^{-1}, the peaks at 1654 cm^{-1} were the symmetric C=O stretching of protein amide I (Ansari et al., 2019; Bataller and Capareda, 2018). Peaks

observed at 1249 cm^{-1} were found to be associated with the asymmetric stretching of the P=O bond in the phosphodiester of phospholipids and nucleic acids (Ansari et al., 2019; Fang et al., 2011). Compared to the control cell, in the cell treated with TiO_2 NPs, there was a shift in the peak at 1077 cm-^{1} that represents the CO stretching of the alcoholic group (Sheng et al., 2004), and it formed a new band at 1076 cm^{-1}, indicating stretching of C-O, C-C, and C-OH of the carboxyl and hydroxyl groups. Additionally, the peaks at 528 and 525 cm^{-1} that represents the aromatic -CH stretching of phosphate were observed (Zinicovscaia et al., 2020).

The results presented in Figures 4.3 and 4.4 demonstrate that the presence of TiO_2 NPs in treated cells leads to a reduction in the relative intensities of both the OH and NH bands, indicating an interaction between ions and NH groups through the electron lone pairs of the nitrogen atom (Ferreira et al., 2011). The adsorption of NPs did not appear to have a substantial impact on the positions of the phosphate and carbohydrate functional groups (Ferreira et al., 2011). Similar results were obtained when Ag NPs exposed to *S. platensis* for 96 hr with a concentration of 100 µg/ml (Liang et al., 2022a).

5.2.2 SEM-EDX Analysis

SEM-EDX analysis was conducted on *H. pluvialis* cells exposed to TiO_2 NPs to determine the accumulation of the particles in the biomass and any resulting changes in cell morphology. Two pathways for metal ion uptake into algal cells were reported (Gupta et al., 2014b). The initial step involves the

adherence of metal ions onto the surface of the algae, after which the ions are taken up by cytoplasmic organelles and transported through the cell membranes. The current investigation used SEM-EDX to determine the build-up of TiO_2 NPs in the algal biomass, according to the mechanisms outlined in Gupta et al., (2014b), Similar findings were published by (Djearamane et al., 2018b; Dmytryk et al., 2014; Zinicovscaia et al., 2017b), who used EDX analysis to show how ZnO NPs, zinc, and Se were accumulating within cells of *S. platensis'* algal biomass.

Multiple layers of NPs adhering to and building up on the cell surface might interfere with food uptake and put photosynthetic bacteria under physical stress (Metzler et al., 2011). Based on the findings that the pore diameter in the cell walls of microalgae, which range from 5 to 20 nm (Navarro et al., 2008), is larger than the size of the TiO_2 NP_S used in this study, it is assumed that the majority of TiO_2 nanoparticles were attached to the surface of *H. pluvialis*. It has been noted that the physical barrier created by the NPs' surface attachment to the cells prevents the development of microorganisms that use sunlight for photosynthesis. (Hazeem et al., 2016) suggested that when NPs adhere to the surface of cells and cluster together, it could lead to physical harm and changes in the cellular metabolic processes. These changes may restrict growth, lower the concentration of biomass, and affect the production of photosynthetic pigments (Metzler et al., 2011).

5.3 Effects of TiO_2 NPs on Growth Pattern and Biomass

To investigate the impacts of TiO_2 NPs on the growth pattern and biomass of *H. pluvialis*, the changes in *H. pluvialis* biomass as a result of exposure to TiO_2 NPs over 96 hours were evaluated using spectrophotometric techniques. The presence of TiO_2 nanoparticles resulted in a decrease in the concentration of *H. pluvialis* biomass, and this reduction was found to be dependent on the concentration and duration of exposure. Contradicting our results, recent research (Comotto et al., 2014b) discovered that the biomass of *H. pluvialis* decreased by 18.1% on day 9 after treatment with 100 µg/mL TiO_2 NPs. This could be due to the nanoparticles' small size. The toxicity of nanoparticles increases as their size decreases. According to a study, TiO_2 NPs and bulk particles both limit *N. closterium's* growth (Xia et al., 2015b). According to the calculated EC_{50} values, which were 88.78 ± 6.43 and 118.80 ± 12.78 mg/L for 21 and 60 nm TiO_2 NPs, respectively, the 21 nm TiO_2 NPs were more dangerous than the 60 nm TiO_2 NPs and TiO_2 BPs after 96 hours. The cytotoxicity of TiO_2 NPs may also be influenced by their size, which is a factor in the study. When *C. reinhardtii* was exposed to Ag NPs of 4.5 and 16.7 nm size at a concentration of 10 g/L, more than half of the growth was inhibited after 72 hours, with an EC_{50} value of 10 µg/L for these particles. In contrast, larger Ag NPs of 46.7 nm size had an EC_{50} value of > 300 µg/L, indicating lower toxicity. The results suggest that smaller Ag NPs were more effective in inhibiting the growth of *C. reinhardtii* (Sendra et al., 2017). The most recent research demonstrates that the ZnO NPs' suppression of *H. pluvialis* growth is represented in the reduction in cell viability and algal

biomass. After conducting experiments, it was discovered that all tested amounts of ZnO NPs (ranging from 10-200 μg/mL) had a significant ($p < 0.05$) negative effect on the viability and growth of *H. pluvialis* after 72 hours. The most significant decrease in growth occurred at 96 hours when 200 μg/mL of ZnO NPs resulted in a 49.35 ±3.69% reduction in algal biomass and a 52.78 ±5.12% decline in cell viability compared to the control group. Furthermore, after 15 days of exposure, a concentration of 100 μg/mL of 14 nm TiO_2 NPs reduced the biomass of *S. platensis* by 74%.

The form, shape, concentration, surface charge, and surface properties of photosynthetic microorganisms exposed to TiO_2 NPs may have an impact on how quickly they grow (Cepoi et al., 2020). Several studies have put forward the hypothesis that either the creation of ROS or the mechanical harm inflicted on cells by NPs is responsible for the inhibition of cell growth, as suggested by (Castro-Bugallo et al., 2014; Djearamane et al., 2018a; Suman et al., 2015; Xia et al., 2015a). There are indications that the growth of cells can be impacted by various factors such as the light shading effect (Sadiq et al., 2011), the discharge of metal ions (Aravantinou et al., 2015; Lee and An, 2013; Suman et al., 2015), interaction with the medium used for cell culture (Manier et al., 2013), and the combined effect of these factors (Manzo et al., 2013). One of the causes of growth inhibition is the degradation of cell membrane caused by exposure to NPs, which results in the unregulated release and absorption of electrolytes and consequently affects the photosynthetic system as well as the synthesis of macronutrients (Anusha et al., 2017b). The

rate of growth could be impacted by the manner in which metal ions interact with the functional groups present on the cell surface (Balaji et al., 2014).

5.4 Effects of TiO_2 NPs on Proteins, Carbohydrates and Lipids

The total proteins, carbohydrates, and lipids of *H. pluvialis* were tested to determine the effect of the treatment of TiO_2 NPs to the production of macronutrients of *H. pluvialis*. This research indicates that the decrease in protein, carbohydrate, and fat content observed in a dose and time-dependent manner may be attributed to the stress caused by TiO_2 NPs present in the culture media (Holan and Volesky, 1994). Study shows that when *C. vulgaris* was exposed to 50 µg/mL copper nanoparticles (Cu NPs) and 200 µg/mL magnesium nanoparticles (Mg NPs) the protein content was reduced by 50% and 36% respectively after 8 days (G et al., 2017). The results were comparable when *S. platensis* was subjected to 10 µg/mL ZnO NPs and 100 µg/mL Se. When exposed to these substances for 10 days and 24, 48, and 72 hours, respectively, reductions of 79%, 32%, 64%, and 69% in protein content were observed (Lone et al., 2013b; Zinicovscaia et al., 2017b). According to (Anusha et al., 2017b), protein content was reduced by 40% and 50% when *Microcystis* sp. *and Oscillatoria* sp. were exposed to 5 mg/L of cobalt nanoparticles (Co NPs) for 5 days. As stated in the research conducted by Balaji et al., (2014), *S. platensis* experienced the most significant reduction in protein content when it was subjected to 42 mg/L of nickel (Ni) and 48 mg/L of Zn for 18 days.

In this study, we observed that the carbohydrates in *H. pluvialis* reduced in correlation with both the dosage and duration of the experiment, just like the proteins. Changes in carbohydrate content in *H. pluvialis* biomass following interaction with TiO_2 NPs demonstrate a rapid increase in carbohydrate content for 5 µg/mL after 24 hours. This could be related to a defensive mechanism activated in reaction to stress. Carbohydrates' anti-oxidant effects are mainly related to signaling which triggers the creation of certain ROS scavengers. Carbohydrates too can behave as direct ROS scavengers at greater concentrations. In ROS signaling, glucose and sucrose are crucial (Bolouri-Moghaddam et al., 2010). The carbohydrate content falls as the concentration of TiO_2 NPs and time rise. When algal cells were exposed to nanoparticles at high metal concentrations, the cell membrane was disrupted, resulting in uncontrolled electrolyte release and intake. According to, (Zinicovscaia et al., 2017b) Se uptake by the *S. platensis* biomass resulted in a rapid reduction in carbohydrate content. The content of the polysaccharide in the biomass was reduced by 75.6 percent after 72 hours of interaction with the Se ions, to 3.7 percent in comparison to the initial content of 15% in the biomass. During the first 24 hours of contact, the polysaccharide breakdown was rapid. The lysing of the polysaccharide becomes a somewhat gradual process during the next 48 hours, with a 15% drop observed every 24 hours on average.

According to the report, the lipid production in *S. platensis* on the fifth day was decreased by 44%, 53%, and 66% when they were exposed to 100 µg/mL, 250 µg/mL, and 500 µg/mL of TiO_2 NPs, respectively (Casazza et al., 2015b). According to Zinicovscaia et al., (2017b) findings, when exposed to 100

μg/mL of Se metal for 24, 48, and 72 hours, *S. platensis* underwent a decrease in its lipid content by 23%, 50%, and 80%, respectively. In contrast, a study conducted by Pham, (2019) found that when *Thalassiosira sp* was exposed to concentrations of 5 to 200 μg/mL of Ag NPs, its lipid production increased by 11 to 17% after 72 hours. On the other hand, when *Scenedesmus* sp was exposed to concentrations of 5 and 20 μg/mL of Ag NPs, its lipid content increased by 8.1 and 7.6% respectively but decreased at higher concentrations of 100 and 200 μg/mL. This indicates that the toxicity of different MNPS varies depending on the specific area of research.

The oxidation of functional groups and structural elements in microalgae is caused by the production of ROS and the release of metals during NPs treatment. This leads to the breakdown of proteins, lipids, and carbohydrates into smaller molecules like monomers, tiny inorganic compounds, and water, ultimately resulting in the breakdown of biomass (Khalifeh et al., 2022; Zinicovscaia et al., 2017b). In addition, ROS can cause lipid peroxidation, which may disrupt the normal functioning of the cells (Wang et al., 2019). Microalgae tend to alter their cellular metabolism when exposed to NPs by decreasing the production of metabolites under stressful conditions (Khalifeh et al., 2022; Pham, 2019).

The presence of heavy metals or NPs in the growth media can cause oxidative stress, which may result in a reduction of biological macromolecules in microalgae. In research, it was shown that stressed-out cells had lessened

capability for protein production (Zeng and Vonshak, 1998). The cell membrane was harmed when cells were exposed to high quantities of NPs. Due to the decreased production of carbs, electrolytes were released and consumed in an unregulated manner (Anusha et al., 2017b). Microalgae cells contain lipids such as triacylglycerol (TAGs), fatty acids, phytosterols, and sphingolipids, which could be used as biofuels, nutraceuticals, or food additives. The nutrient deficit, such as nitrogen deficiency, is said to cause oxidative stress and fat buildup in microalgal cells (Miazek et al., 2015). Because lipids are the elementary components of cell membranes, their composition changes as a reaction to the conditions and the cells' alterations in the physiological state (Zinicovscaia et al., 2017b). Microalgae can tolerate lower toxicant concentrations in most cases. When microalgae are stressed, they change their cellular metabolism and accumulate bigger molecules like lipids and proteins (Pham, 2019).

The researchers have also described the molecular mechanism underlying the loss of macronutrients. The bulk of the proteins was strongly altered, although only at the transcriptome level rather than the proteome level, according to research that looked at the gene expression of *C. reinhardtii* in response to Ag. This finding may explain why the protein synthesis in microalgae was reduced (Pillai et al., 2014). *Chlorella pyrenoidosa's* material and energy metabolism were also reported to be disrupted by the treatment with TiO_2 NPs. The expression of genes involved in cell division, lipid synthesis, and carbohydrate synthesis at the molecular level was shown to be downregulated (Middepogu et al., 2018). This resulted in the inhibition of *C. pyrenoidosa's* cell division

and lipid and carbohydrate biosynthesis. To put it another way, when NPs attach to a cell membrane, the cell membrane is disrupted, which significantly reduces the amount of proteins, carbohydrates, and lipids that the photosynthetic microorganisms produce.

5.5 Effects of TiO_2 NPs on Chlorophyll-*a*, Carotenoids and Astaxanthin

In addition to examining the impact of macronutrients, researchers also investigated the effects of TiO_2 NPs on the pigments of *H. pluvialis*, specifically chlorophyll-a, carotenoids, and astaxanthin. Their findings indicated that exposure to TiO_2 NPs caused a reduction in the chlorophyll-a content of *H. pluvialis*, which was dependent on both the concentration and dosage of the stressor (Holan and Volesky, 1994). According to research conducted by (Djearamane et al., 2018a), the presence of ZnO nanoparticles in concentrations of 10, 50, 100, 150, and 200 g/mL resulted in a decrease in chlorophyll-a levels of *H. pluvialis* after 96 hours. (Sadiq et al., 2011) found that *Chlorella* sp. and *Scenedesmus* sp. microalgae experienced a reduction in chlorophyll after being exposed to alumina nanoparticles for 72 hours, which was dependent on both the dosage and duration of exposure. Similarly, (Oukarroum et al., 2012) demonstrated that when *C. vulgaris* and *D. tertiolecta* were exposed to Ag NPs for 24 hours, the chlorophyll levels of both species decreased proportionally to the concentration of nanoparticles present.

Similar to chlorophyll-a, *H. pluvialis* cells treated to TiO_2 NPs showed a drop in carotenoids and astaxanthin that was concentration- and time-dependent. According to the current findings, (Djearamane et al., 2018b) found that after 96 hours after exposure to 200 μg/mL of ZnO NPs, there was a maximum decline of 43.4% in carotenoids and 47.9% in astaxanthin. A research found that after 96 hours of exposure to 200 μg/mL of ZnO NPs, carotenoids had reduced by a maximum of 76.2% (Djearamane et al., 2018b). According to (Fazelian et al., 2019), when *Nannochloropsis oculata* was exposed to 200 mg/L of CuO NPs for a period of 3 days, there was a decrease of 46% in the carotenoid content. After 20 days of being exposed, the astaxanthin content was reduced the most when there were 200 mg/L of CuO NPs present in the medium (Ling Shing et al., 2019).

Prior research has demonstrated that *H. pluvialis* experiences a reduction in pigment under various forms of stress. In a specific experiment, when exposed to ferrous sulfate and intense light for a period of 48 hours, the photosynthetic activity of *H. pluvialis* was found to decline. (Li et al., 2008). After being subjected to 0.8% NaCl for a period of 11 days, *H. pluvialis* cyst cells experienced a reduction of 25.9%, 5.27%, and 19.0% in their levels of chlorophyll, carotenoids, and astaxanthin, respectively (Cifuentes et al., 2003). The levels of astaxanthin and carotenoids increased in the vegetative cells of *H. pluvialis* after being exposed to increasing amounts of NaCl (0.25 to 2% w/v) for a period of 4 days. However, on days 6 and 9, these pigments were observed to decrease at concentrations of 1.0% and 2.0% NaCl. The research also showed that on day 9, when *H. pluvialis* was exposed to 17.1 mM of

NaCl, there was a significant decrease of 90% and 56.68% in its chlorophyll and astaxanthin levels, respectively, and a 54.68% decrease in its total carotenoids (Vidhyavathi et al., 2008).

Algae cells that come into contact with TiO_2 NPs form clumps of the particles on their surfaces. This, in turn, hinders the absorption of sufficient light energy necessary for the completion of the photosynthesis process. Consequently, the quantity of photosynthetic pigments decreases and the growth of the algae is restricted (Iswarya et al., 2015). The functionality of the photosynthetic system can deteriorate due to two processes that hinder development: oxidative stress and lipid peroxidation. Excessive production of ROS during oxidative stress can lead to a reduction in photosynthetic pigments (Tang et al., 2013). Moreover, unfavorable environmental conditions for microalgae growth, such as exposure to salt, intense light, chemicals, metals, and metal nanoparticles, resulting in a reduction in the concentration of chlorophyll in the microalgae. Chlorophyll is crucial for photosynthesis (Gupta et al., 2014b). When metals are applied to microalgae, the thylakoids are destroyed. This reduces the amount of photosynthetic pigments, which harms photosynthetic activity and stunts growth or kills cells (Arunakumara et al., 2008). The presence of TiO_2 NPs on the cell surface can obstruct the cells and act as a hindrance to the process of photosynthesis. As a consequence, biomass may decrease, resulting in a reduction of macronutrients (Huang et al., 2016).

5.6 Effects of TiO_2 NPs on Total Phenolic Compounds

The total phenolic compounds of *H. pluvialis* after the exposure of TiO_2 NPs were estimated to determine the intracellular phenolic compound production which may be linked to the antioxidant activity of microalgae. The total phenolic compound increases in the first 24 hours for all concentrations tested, and in the first 48 hours for 5-10 µg/mL. This could be because of the antioxidant enzymes present, which are created when the cells are stressed in order to defend themselves from free radical damage (Li et al., 2006b). Algae have many enzymatic and nonenzymatic antioxidant defence mechanisms to keep the level of ROS where it needs to be for cell protection. Glutathione reductase, catalase, superoxide dismutase, ascorbate peroxidase, and other scavenging enzymes make up the main antioxidant defence system (Anusha et al., 2017b). Antioxidants such as phenolic compounds can help to reverse or prevent the effects of oxidative stress (Aliakbarian et al., 2009b). The total phenolic compound decreased from 25-100 µg/mL from 48 hr to 96 hr, according to the data. (Casazza et al., 2015b) found that *S. platensis* treated with TiO_2 NPs at concentrations of 100, 250, and 500 µg/mL experienced reductions in intracellular phenolic content of 34.9%, 27.9%, and 24.5%, respectively, on Day 5. Liang et al., (2022a) reported that the total phenolic compounds of *A. platensis* were significantly ($p < 0.05$) reduced by treatment with Ag NPs. The maximum decrease in phenolic content was observed after 96 hours, with values of 63.4% and respectively for 100 µg/mL of Ag NPs.

Photosynthetic microbes will release phenolic compounds during stressful situations which can cleanse the environment and function as an antioxidant (Liang et al., 2022a). Under optimal conditions, phenolic compounds are secondary plant metabolites produced by the phenylpropanoid metabolism and the shikimic acid pathway in microalgae. However, the cells' exposure to various environmental stresses might alter the quantity of phenolic content (Vogt, 2010). When under stress, cells are pushed to produce more phenolic compounds, which are then discharged into the culture medium with an increase in extracellular phenolic content and a reduction in intracellular phenolic compound concentration (Liang et al., 2020). Under heavy metal exposure, photosynthetic bacteria may produce fewer total phenolic compounds because photosynthesis is inhibited, which lowers the amount of new phenolic compounds produced (Connan and Stengel, 2011). The reduced antioxidant activity caused by reduced total phenolic compound synthesis may result in a drop in biomass (Bello-Bello et al., 2017; Fazelian et al., 2019).

5.7 Toxicity Mechanism of NPs

In order to be absorbed by algae, NPs need to overcome two obstacles, namely the cell walls and plasma membranes. The tough and robust cell walls of algae are commonly considered the first line of defence against NP internalization. Although the cell walls of algae have pores that are porous and semipermeable, they are still capable of obstructing NPs due to their strength. The diameter of these pores typically ranges from 5 to 20 nm (Wang et al., 2019). The main constituent of the cell wall in algae is cellulose, but it usually

contains other substances such as glycoproteins and polysaccharides (Navarro et al., 2008). These elements may serve as binding sites to encourage algae to absorb NPs. The plasma membrane serves as the second barrier that must be overcome once the NPs have passed the cell wall (Nambara et al., 2016). Passive diffusion and endocytosis are thought to be the primary mechanisms by which NPs travel through the bilayer lipid membrane (Wang et al., 2019). When NPs enter algal cells, they can harm both the cell wall and cell membrane, and accumulate in the periplasmic space. This can lead to significant damage or changes to the structure and function of various cellular organelles including chloroplasts, vacuoles, endoplasmic reticulum, Golgi apparatus, and mitochondria if the NPs manage to penetrate the cytoplasm and interact with them (Bhuvaneshwari et al., 2015; Zhao et al., 2016). Figure 5.1 depicts the probable distribution and harmful effects of NPs in algal cells.

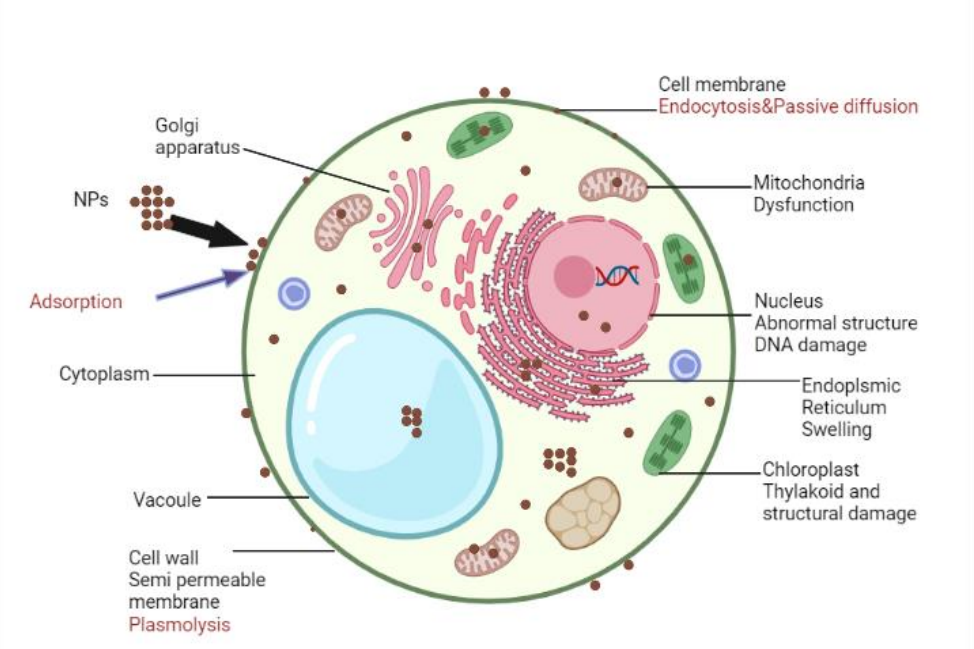

Figure 5.1: The possible distribution and potential toxic outcomes of NPs in algal cells adapted from (Wang et al., 2019).

The majority of research claimed that oxidative stress and physical restrictions are what cause NPs to be hazardous to microalgae. Large NPs aggregates trapping algal cells not only limit the amount of light accessible for photosynthesis but also hinder the intake of nutrients (Li et al., 2015, 2018). Exposure to NPs leads to the over-accumulation of ROS inside cells, resulting in the occurrence of oxidative stress (Costa et al., 2016; Hazeem et al., 2016). According to a meta-analysis conducted by Chen et al., (2019), the presence of NPs caused a significant 90% increase in ROS. This result indicates that there is an excessive build-up of ROS within the cells of microalgae, which can lead to oxidative stress in the future. The ROS accumulation in microalgae induced by NPs is not remarkably influenced by NPs surface modification, however, is strongly related to the type of NPs and the microalgae species, and the dose of NPs used. As the exposure to NPs caused the formation of ROS, the defense

mechanism of microalgae will be triggered, where the antioxidative enzymes superoxide dismutase (SOD) and peroxidase (POD) were synthesized to scavenge ROS. When the capacity of antioxidant enzymes was unable to remove the excessively generated ROS, the cell membrane of microalgae cells would be damaged by the excessive ROS, where membrane lipid peroxidation occurs. Lipid peroxidation may lead to an increase in cell membrane permeability, which results in the loss of membrane selectivity, fluidity, and integrity (Lei et al., 2016). The most common indicators of NP toxicity in microalgae are changes to the cell membrane and disruption of photosynthetic function (Sendra et al., 2018). An elevation in ROS levels within the chloroplast could potentially decrease the amount of chlorophyll present in microalgae cells. This could be achieved by modifying the ratio of lipids to proteins within the pigment-protein complexes (Du et al., 2011; Huang et al., 2016; Li et al., 2015). The decrease in chlorophyll caused by NPs hinders the energy transfer during light responses. This, in turn, leads to a decline in cell density and a postponement in the growth of algae (Chen et al., 2019). Figure 5.2 portrays the toxicity mechanism of NPs to the algal cell membrane and organelles.

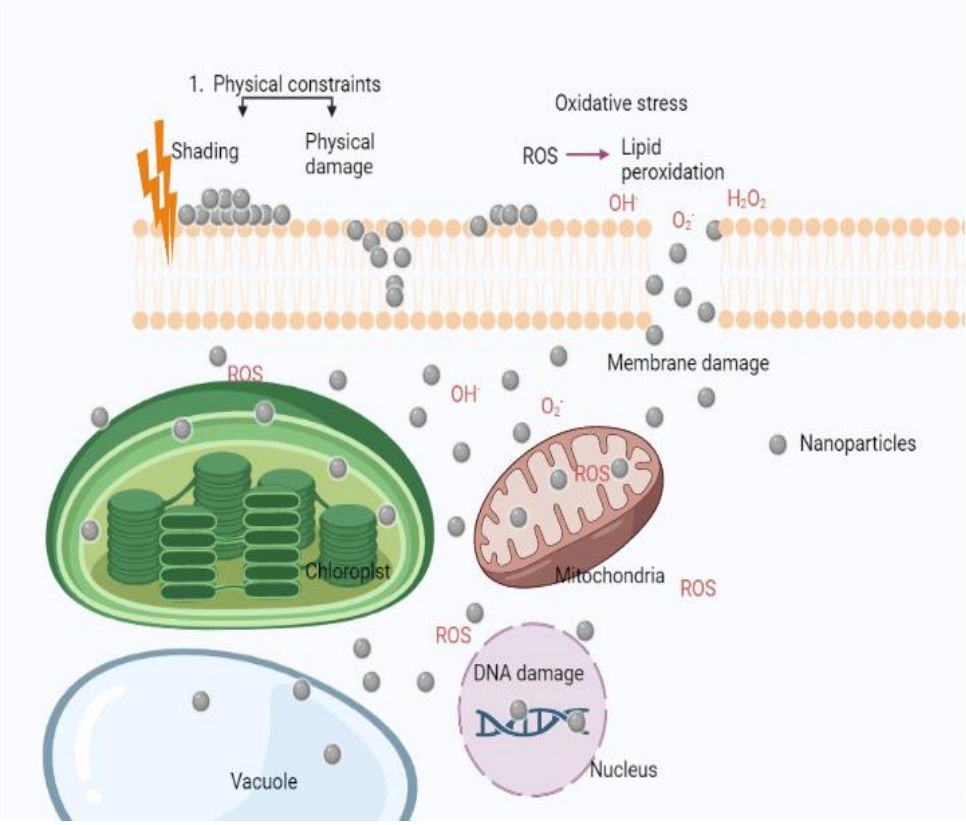

Figure 5.2: The proposed toxicity mechanism of NPs to the algal cell membrane and organelles adapted from (Chen et al., 2019).

CHAPTER 6

CONCLUSION AND RECOMMENDATION

6.1 CONCLUSION

The treatment of TiO_2 NPs on *H. pluvialis* resulted in a considerable accumulation of TiO_2 NPs in algal cells. The TiO_2 NPs attached to and accumulated on the cell of *H. pluvialis* through functional groups such as hydroxyl, amine, amides, carbonyl, phosphodiesters, and phosphates in the cell wall. The presence of TiO_2 NPs had an impact on *H. pluvialis*, resulting in a reduction of various parameters such as biomass, proteins, carbohydrates, lipids, chlorophyll-a, carotenoids, astaxanthin, and phenolic compounds. The effects were dependent on the concentration and time of exposure to TiO_2 NPs, and even a low concentration of 5 µg/mL for 24 hours produced significant results. The greatest impact was seen at a concentration of 100 µg/mL for all the parameters tested. This interaction formed a physical barrier, which inhibited photosynthesis activity, and the transfer of nutrients, and caused stress to the cells, leading to growth inhibition and a reduction in biomass, macromolecules, pigments, and phenolic compounds. These findings could be useful in detecting contamination of TiO_2 NPs in *H. pluvialis* and ensuring that consumers receive high-quality nutritional supplements without any contamination. Otherwise, consuming TiO_2 NPs contaminated *H. pluvialis*

supplements may not provide the intended nutritional benefits and could even pose health risks.

6.2 LIMITATION AND RECOMMENDATION

The study has some limitations. Firstly, the equipment used for inductively coupled plasma-optical emission spectroscopy (ICP-OES) was not functioning properly, hence hampering the investigation of the cellular accumulation of TiO_2 NPs in *H. pluvialis*. Therefore, in future studies, it is recommended that ICP-OES be used to determine the amount of TiO_2 NPs absorbed by *H. pluvialis*. Additionally, this study was unable to confirm the internalization of TiO_2 NPs in *H. pluvialis* cells through TEM analysis because TEM is not available at UTAR, and outsourcing the samples would have been too expensive. Also, the study did not test the toxicity of Ti ions on *H. pluvialis*. In the future, research can be conducted to determine the minimum concentration of TiO_2 NPs that can cause toxicity effects on human cells. Furthermore, genomic studies can be carried out to analyze the impact of NPs on the synthesis of macromolecules and pigments.

REFERENCES

Adams, L.K., Lyon, D.Y., Alvarez, P.J.J., 2006. Comparative eco-toxicity of nanoscale TiO_2, SiO_2, and ZnO water suspensions. *Water Res*. 40, 3527–3532. https://doi.org/10.1016/j.watres.2006.08.004

Agrawal, N., Minj, D.K., Rani, K., 2015. Estimation of Total Carbohydrate Present in Dryfruits 1, 4.

Aitken, R., Hankin, S., Ross, B., Tran, L., Stone, V., Fernandes, T., Donaldson, K., Duffin, R., Chaudhry, Q., Wilkins, T., SA, W., Levy, L., SA, R., Maynard, A., 2009. EMERGNANO: A review of completed and near completed environment, health and safety research on nanomaterials and nanotechnology. Report TM/09/01.

Al-Homaidan, A.A., Al-Houri, H.J., Al-Hazzani, A.A., Elgaaly, G., Moubayed, N.M.S., 2014. Biosorption of copper ions from aqueous solutions by *Spirulina platensis* biomass. *Arab. J. Chem.* 7, 57–62. https://doi.org/10.1016/j.arabjc.2013.05.022

Aliakbarian, B., Dehghani, F., Perego, P., 2009a. The effect of citric acid on the phenolic contents of olive oil. *Food Chem.* 116, 617–623. https://doi.org/10.1016/j.foodchem.2009.02.077

Aliakbarian, B., Dehghani, F., Perego, P., 2009b. The effect of citric acid on the phenolic contents of olive oil. *Food Chem.* 116, 617–623. https://doi.org/10.1016/j.foodchem.2009.02.077

Anastopoulos, I., Kyzas, G.Z., 2015. Progress in batch biosorption of heavy metals onto algae. *J. Mol. Liq.* 209, 77–86. https://doi.org/10.1016/j.molliq.2015.05.023

Ansari, F.A., Ravindran, B., Gupta, S.K., Nasr, M., Rawat, I., Bux, F., 2019. Techno-economic estimation of wastewater phycoremediation and environmental benefits using *Scenedesmus obliquus* microalgae. *J. Environ. Manage.* 240, 293–302. https://doi.org/10.1016/j.jenvman.2019.03.123

Aravantinou, A.F., Tsarpali, V., Dailianis, S., Manariotis, I.D., 2015. Effect of cultivation media on the toxicity of ZnO nanoparticles to freshwater and marine microalgae. *Ecotoxicol. Environ. Saf.* 114, 109–116. https://doi.org/10.1016/j.ecoenv.2015.01.016

Arunakumara, K.K.I.U., Zhang, X., Song, X., 2008. Bioaccumulation of Pb2+ and its effects on growth, morphology and pigment contents of *Spirulina (Arthrospira) platensis. J. Ocean Univ.* China 7, 397–403. https://doi.org/10.1007/s11802-008-0397-2

Balaji, S., Kalaivani, T., Rajasekaran, C., 2014. Biosorption of Zinc and Nickel and Its Effect on Growth of Different *Spirulina* Strains: Biosorption Potentials of *Spirulina* Strains. *CLEAN - Soil Air Water* 42, 507–512. https://doi.org/10.1002/clen.201200340

Banerjee, A., Roychoudhury, A., 2019. Nanoparticle-Induced Ecotoxicological Risks in Aquatic Environments, in: Nanomaterials in Plants, Algae and Microorganisms. *Elsevier*, pp. 129–141. https://doi.org/10.1016/B978-0-12-811488-9.00007-X

Bataller, B.G., Capareda, S.C., 2018. A rapid and non-destructive method for quantifying biomolecules in Spirulina platensis via Fourier transform infrared – Attenuated total reflectance spectroscopy. *Algal Res*. 32, 341–352. https://doi.org/10.1016/j.algal.2018.04.023

Battin, T.J., Kammer, F. v.d., Weilhartner, A., Ottofuelling, S., Hofmann, T., 2009. Nanostructured TiO_2: Transport Behavior and Effects on Aquatic Microbial Communities under Environmental Conditions. *Environ. Sci. Technol.* 43, 8098–8104. https://doi.org/10.1021/es9017046

Bello-Bello, J.J., Chavez-Santoscoy, R.A., Lecona-Guzmán, C.A., Bogdanchikova, N., Salinas-Ruíz, J., Gómez-Merino, F.C., Pestryakov, A., 2017. Hormetic Response by Silver Nanoparticles on In Vitro Multiplication of Sugarcane (*Saccharum* spp. Cv. Mex 69-290) Using a Temporary Immersion System. *Dose-Response Publ. Int. Hormesis Soc.* 15, 1559325817744945. https://doi.org/10.1177/1559325817744945

Ben Hamissa, A.M., Seffen, M., Aliakbarian, B., Casazza, A.A., Perego, P., Converti, A., 2012. Phenolics extraction from Agave americana (L.) leaves using high-temperature, high-pressure reactor. Food Bioprod. Process. 90, 17–21. https://doi.org/10.1016/j.fbp.2010.11.008

Bhuvaneshwari, M., Iswarya, V., Archanaa, S., Madhu, G.M., Kumar, G.K.S., Nagarajan, R., Chandrasekaran, N., Mukherjee, A., 2015. Cytotoxicity of ZnO NPs towards fresh water algae Scenedesmus obliquus at low exposure concentrations in UV-C, visible and dark conditions. *Aquat. Toxicol.* 162, 29–38. https://doi.org/10.1016/j.aquatox.2015.03.004

Bolouri-Moghaddam, M.R., Le Roy, K., Xiang, L., Rolland, F., Van den Ende, W., 2010. Sugar signalling and antioxidant network connections in plant cells: Sugar signalling and antioxidant networks in plants. *FEBS J*. 277, 2022–2037. https://doi.org/10.1111/j.1742-4658.2010.07633.x

Botelho, M.C., Costa, C., Silva, S., Costa, S., Dhawan, A., Oliveira, P.A., Teixeira, J.P., 2014. Effects of titanium dioxide nanoparticles in human gastric epithelial cells in vitro. *Biomed. Pharmacother*. 68, 59–64. https://doi.org/10.1016/j.biopha.2013.08.006

Burchardt, A.D., Carvalho, R.N., Valente, A., Nativo, P., Gilliland, D., Garcìa, C.P., Passarella, R., Pedroni, V., Rossi, F., Lettieri, T., 2012. Effects of Silver Nanoparticles in Diatom *Thalassiosira pseudonana* and Cyanobacterium *Synechococcus sp. Environ. Sci. Technol.* 46, 11336–11344. https://doi.org/10.1021/es300989e

Burchardt, L., Balcerkiewicz, S., Kokociński, M., Samardakiewicz, S., Adamski, Z., n.d. Occurrence of *Haematococcus pluvialis* Flotow emend. Wille in a small artificial pool on the university campus of the Collegium Biologicum in Poznań (Poland). *Biodivers. Res. Conserv.* 2006, 163–166.

Casazza, A.A., Ferrari, P.F., Aliakbarian, B., Converti, A., Perego, P., 2015a. Effect of UV radiation or titanium dioxide on polyphenol and lipid contents of *Arthrospira (Spirulina) platensis. Algal Res*. 12, 308–315. https://doi.org/10.1016/j.algal.2015.09.012

Casazza, A.A., Ferrari, P.F., Aliakbarian, B., Converti, A., Perego, P., 2015b. Effect of UV radiation or titanium dioxide on polyphenol and lipid contents of *Arthrospira (Spirulina) platensis*. Algal Res. 12, 308–315. https://doi.org/10.1016/j.algal.2015.09.012

Castro-Bugallo, A., González-Fernández, Á., Guisande, C., Barreiro, A., 2014. Comparative Responses to Metal Oxide Nanoparticles in Marine

Phytoplankton. *Arch. Environ. Contam. Toxicol.* 67, 483–493. https://doi.org/10.1007/s00244-014-0044-4

Cepoi, L., Zinicovscaia, I., Rudi, L., Chiriac, T., Rotari, I., Turchenko, V., Djur, S., 2020. Effects of PEG-Coated Silver and Gold Nanoparticles on *Spirulina platensis* Biomass during Its Growth in a Closed System. Coatings 10, 717. https://doi.org/10.3390/coatings10080717

Chekanov, K., Lobakova, E., Selyakh, I., Semenova, L., Sidorov, R., Solovchenko, A., 2014. Accumulation of Astaxanthin by a New *Haematococcus pluvialis* Strain BM1 from the White Sea Coastal Rocks (Russia). Mar. Drugs 12, 4504–4520. https://doi.org/10.3390/md12084504

Chen, F., Xiao, Z., Yue, L., Wang, J., Feng, Y., Zhu, X., Wang, Z., Xing, B., 2019. Algae response to engineered nanoparticles: current understanding, mechanisms and implications. *Environ. Sci. Nano* 6, 1026–1042. https://doi.org/10.1039/C8EN01368C

Chen, T.-H., Lin, C.-Y., Tseng, M.-C., 2011. Behavioral effects of titanium dioxide nanoparticles on larval zebrafish (*Danio rerio*). *Mar. Pollut. Bull.* 63, 303–308. https://doi.org/10.1016/j.marpolbul.2011.04.017

Cheng, H., Ling Shing, W., Zhen, H.Y., Man, T.Y., Aris, A.Z., 2018. The effect of argentum and cadmium towards astaxanthin content in green algae, *Haematococcus pluvialis. Asian J. Microbiol. Biotechnol. Environ. Sci.* 20, 43–47.

Cifuentes, A.S., González, M.A., Vargas, S., Hoeneisen, M., González, N., 2003. Optimization of biomass, total carotenoids and astaxanthin production in *Haematococcus pluvialis* Flotow strain Steptoe (Nevada, USA) under laboratory conditions. *Biol. Res.* 36, 343–357. https://doi.org/10.4067/s0716-97602003000300006

Comotto, M., Casazza, A.A., Aliakbarian, B., Caratto, V., Ferretti, M., Perego, P., 2014a. Influence of TiO_2 Nanoparticles on Growth and Phenolic Compounds Production in Photosynthetic Microorganisms. *Sci. World J.* 2014, 1–9. https://doi.org/10.1155/2014/961437

Comotto, M., Casazza, A.A., Aliakbarian, B., Caratto, V., Ferretti, M., Perego, P., 2014b. Influence of TiO_2 Nanoparticles on Growth and Phenolic

Compounds Production in Photosynthetic Microorganisms. *Sci. World J.* 2014, 1–9. https://doi.org/10.1155/2014/961437

Connan, S., Stengel, D.B., 2011. Impacts of ambient salinity and copper on brown algae: 2. Interactive effects on phenolic pool and assessment of metal binding capacity of phlorotannin. *Aquat. Toxicol.* 104, 1–13. https://doi.org/10.1016/j.aquatox.2011.03.016

Costa, C.H. da, Perreault, F., Oukarroum, A., Melegari, S.P., Popovic, R., Matias, W.G., 2016. Effect of chromium oxide (III) nanoparticles on the production of reactive oxygen species and photosystem II activity in the green alga *Chlamydomonas reinhardtii*. *Sci. Total Environ.* 565, 951–960. https://doi.org/10.1016/j.scitotenv.2016.01.028

Croteau, M.-N., Misra, S.K., Luoma, S.N., Valsami-Jones, E., 2011. Silver Bioaccumulation Dynamics in a Freshwater Invertebrate after Aqueous and Dietary Exposures to Nanosized and Ionic Ag. *Environ. Sci. Technol.* 45, 6600–6607. https://doi.org/10.1021/es200880c

Dabrunz, A., Duester, L., Prasse, C., Seitz, F., Rosenfeldt, R., Schilde, C., Schaumann, G.E., Schulz, R., 2011. Biological Surface Coating and Molting Inhibition as Mechanisms of TiO_2 Nanoparticle Toxicity in *Daphnia magna*. *PLoS ONE* 6, e20112. https://doi.org/10.1371/journal.pone.0020112

Das, P., Aziz, S.S., Obbard, J.P., 2011. Two phase microalgae growth in the open system for enhanced lipid productivity. Renew. Energy 36, 2524–2528. https://doi.org/10.1016/j.renene.2011.02.002

Davinelli, S., Nielsen, M.E., Scapagnini, G., 2018. Astaxanthin in Skin Health, Repair, and Disease: A Comprehensive Review. *Nutrients* 10, 522. https://doi.org/10.3390/nu10040522

Deniz, F., Saygideger, S.D., Karaman, S., 2011. Response to Copper and Sodium Chloride Excess in Spirulina sp. (Cyanobacteria). *Bull. Environ. Contam. Toxicol.* 87, 11–15. https://doi.org/10.1007/s00128-011-0300-5

Devi, K.U., Swapna, G., Suneetha, S., 2014. Microalgae in Bioremediation, in: Microbial Biodegradation and Bioremediation. *Elsevier*, pp. 433–454. https://doi.org/10.1016/B978-0-12-800021-2.00019-4

Djearamane, S., Lim, Y.M., Wong, L.S., Lee, P.F., 2018a. Cytotoxic effects of zinc oxide nanoparticles on cyanobacterium *Spirulina (Arthrospira) platensis*. *PeerJ* 6, e4682. https://doi.org/10.7717/peerj.4682

Djearamane, S., Lim, Y.M., Wong, L.S., Lee, P.F., 2018b. Cytotoxic effects of zinc oxide nanoparticles on cyanobacterium *Spirulina (Arthrospira) platensis*. *PeerJ* 6, e4682. https://doi.org/10.7717/peerj.4682

Dmytryk, A., Saeid, A., Chojnacka, K., 2014. Biosorption of Microelements by *Spirulina* : Towards Technology of Mineral Feed Supplements. *Sci. World J.* 2014, 1–15. https://doi.org/10.1155/2014/356328

Dong, S., Huang, Y., Zhang, R., Wang, S., Liu, Y., 2014. Four Different Methods Comparison for Extraction of Astaxanthin from Green Alga *Haematococcus pluvialis*. *Sci. World J.* 2014, 1–7. https://doi.org/10.1155/2014/694305

Dotto, G.L., Cadaval, T.R.S., Pinto, L.A.A., 2012. Use of *Spirulina platensis* micro and nanoparticles for the removal synthetic dyes from aqueous solutions by biosorption. *Process Biochem.* 47, 1335–1343. https://doi.org/10.1016/j.procbio.2012.04.029

Du, W., Sun, Y., Ji, R., Zhu, J., Wu, J., Guo, H., 2011. TiO_2 and ZnO nanoparticles negatively affect wheat growth and soil enzyme activities in agricultural soil. *J. Environ.* Monit. 13, 822. https://doi.org/10.1039/c0em00611d

El-Sheekh, M.M., El-Naggar, A.H., Osman, M.E.H., El-Mazaly, E., 2003. Effect of cobalt on growth, pigments and the photosynthetic electron transport in *Monoraphidium minutum* and *Nitzchia perminuta. Braz. J. Plant Physiol.* 15, 159–166. https://doi.org/10.1590/S1677-04202003000300005

Fang, L., Zhou, C., Cai, P., Chen, W., Rong, X., Dai, K., Liang, W., Gu, J.-D., Huang, Q., 2011. Binding characteristics of copper and cadmium by cyanobacterium *Spirulina platensis*. J. Hazard. Mater. 190, 810–815. https://doi.org/10.1016/j.jhazmat.2011.03.122

Fazelian, N., Movafeghi, A., Yousefzadi, M., Rahimzadeh, M., 2019. Cytotoxic impacts of CuO nanoparticles on the marine microalga *Nannochloropsis oculata. Environ. Sci. Pollut. Res.* 26, 17499–17511. https://doi.org/10.1007/s11356-019-05130-0

Federici, G., Shaw, B., Handy, R., 2007. Toxicity of titanium dioxide nanoparticles to rainbow trout (*Oncorhynchus mykiss*): Gill injury, oxidative stress, and other physiological effects. *Aquat. Toxicol.* 84, 415–430. https://doi.org/10.1016/j.aquatox.2007.07.009

Ferreira, L.S., Rodrigues, M.S., de Carvalho, J.C.M., Lodi, A., Finocchio, E., Perego, P., Converti, A., 2011. Adsorption of Ni^{2+}, Zn^{2+} and Pb^{2+} onto dry biomass of *Arthrospira (Spirulina) platensis and Chlorella vulgaris.* I. Single metal systems. *Chem. Eng. J.* 173, 326–333. https://doi.org/10.1016/j.cej.2011.07.039

G, S., Kumar, D.A., Gopal, T., Harinath, K., S, B., S, C., 2017. Metal Nanoparticle Triggered Growth and Lipid Production in *Chlorella Vulgaris. Int. J. Sci. Res. Environ. Sci. Toxicol*. 2.

Gaiser, B.K., Biswas, A., Rosenkranz, P., Jepson, M.A., Lead, J.R., Stone, V., Tyler, C.R., Fernandes, T.F., 2011. Effects of silver and cerium dioxide micro- and nano-sized particles on *Daphnia magna. J. Environ. Monit.* 13, 1227. https://doi.org/10.1039/c1em10060b

George, B., Pancha, I., Desai, C., Chokshi, K., Paliwal, C., Ghosh, T., Mishra, S., 2014. Effects of different media composition, light intensity and photoperiod on morphology and physiology of freshwater microalgae *Ankistrodesmus falcatus* – A potential strain for bio-fuel production. *Bioresour. Technol.* 171, 367–374. https://doi.org/10.1016/j.biortech.2014.08.086

Gohari, G., Mohammadi, A., Akbari, A., Panahirad, S., Dadpour, M.R., Fotopoulos, V., Kimura, S., 2020. Titanium dioxide nanoparticles (TiO_2 NPs) promote growth and ameliorate salinity stress effects on essential oil profile and biochemical attributes of *Dracocephalum moldavica. Sci. Rep.* 10, 912. https://doi.org/10.1038/s41598-020-57794-1

Gong, N., Shao, K., Feng, W., Lin, Z., Liang, C., Sun, Y., 2011. Biotoxicity of nickel oxide nanoparticles and bio-remediation by microalgae *Chlorella vulgaris. Chemosphere* 83, 510–516. https://doi.org/10.1016/j.chemosphere.2010.12.059

Govindaraju, K., Basha, S.K., Kumar, V.G., Singaravelu, G., 2008. Silver, gold and bimetallic nanoparticles production using single-cell protein

(*Spirulina platensis*) Geitler. *J. Mater. Sci.* 43, 5115–5122. https://doi.org/10.1007/s10853-008-2745-4

Granqvist, C.G., Buhrman, R.A., 1976. Ultrafine metal particles. *J. Appl. Phys*. 47, 2200–2219. https://doi.org/10.1063/1.322870

Gupta, S., Sharma, S., Singh, S., 2014a. Hexavalent Chromium Toxicity to Cyanobacterium *Spirulina platensis. Int. Res. J. Pharm.* 5, 910–914. https://doi.org/10.7897/2230-8407.0512184

Gupta, S., Sharma, S., Singh, S., 2014b. Hexavalent Chromium Toxicity to Cyanobacterium *Spirulina platensis. Int. Res. J. Pharm.* 5, 910–914. https://doi.org/10.7897/2230-8407.0512184

Hajimahmoodi, M., Faramarzi, M.A., Mohammadi, N., Soltani, N., Oveisi, M.R., Nafissi-Varcheh, N., 2010. Evaluation of antioxidant properties and total phenolic contents of some strains of microalgae. *J. Appl. Phycol.* 22, 43–50. https://doi.org/10.1007/s10811-009-9424-y

Han, D., Li, Y., Hu, Q., 2013. Astaxanthin in microalgae: pathways, functions and biotechnological implications. *ALGAE* 28, 131–147. https://doi.org/10.4490/algae.2013.28.2.131

Hao, L., Wang, Z., Xing, B., 2009. Effect of sub-acute exposure to TiO2 nanoparticles on oxidative stress and histopathological changes in Juvenile Carp (*Cyprinus carpio). J. Environ. Sci.* 21, 1459–1466. https://doi.org/10.1016/S1001-0742(08)62440-7

Harker, M., Tsavalos, A.J., Young, A.J., 1996. Factors responsible for astaxanthin formation in the Chlorophyte *Haematococcus pluvialis. Bioresour. Technol.* 55, 207–214. https://doi.org/10.1016/0960-8524(95)00002-X

Hazeem, L.J., Bououdina, M., Rashdan, S., Brunet, L., Slomianny, C., Boukherroub, R., 2016. Cumulative effect of zinc oxide and titanium oxide nanoparticles on growth and chlorophyll a content of *Picochlorum* sp. *Environ. Sci. Pollut. Res. Int.* 23, 2821–2830. https://doi.org/10.1007/s11356-015-5493-4

Holan, Z.R., Volesky, B., 1994. Biosorption of lead and nickel by biomass of marine algae. Biotechnol. *Bioeng*. 43, 1001–1009. https://doi.org/10.1002/bit.260431102

Hong, M.-E., Choi, Y.Y., Sim, S.J., 2016. Effect of red cyst cell inoculation and iron(II) supplementation on autotrophic astaxanthin production by *Haematococcus pluvialis* under outdoor summer conditions. *J. Biotechnol.* 218, 25–33. https://doi.org/10.1016/j.jbiotec.2015.11.019

Huang, J., Cheng, J., Yi, J., 2016. Impact of silver nanoparticles on marine diatom *Skeletonema costatum*: Silver nanoparticles are phototoxic to marine diatom. *J. Appl. Toxicol.* 36, 1343–1354. https://doi.org/10.1002/jat.3325

Hund-Rinke, K., Simon, M., 2006. Ecotoxic Effect of Photocatalytic Active Nanoparticles (TiO_2) on Algae and Daphnids (8 pp). *Environ. Sci. Pollut. Res. - Int.* 13, 225–232. https://doi.org/10.1065/espr2006.06.311

Iswarya, V., Bhuvaneshwari, M., Alex, S.A., Iyer, S., Chaudhuri, G., Chandrasekaran, P.T., Bhalerao, G.M., Chakravarty, S., Raichur, A.M., Chandrasekaran, N., Mukherjee, A., 2015. Combined toxicity of two crystalline phases (anatase and rutile) of Titania nanoparticles towards freshwater microalgae: *Chlorella sp. Aquat. Toxicol.* 161, 154–169. https://doi.org/10.1016/j.aquatox.2015.02.006

Janer, G., Mas del Molino, E., Fernández-Rosas, E., Fernández, A., Vázquez-Campos, S., 2014. Cell uptake and oral absorption of titanium dioxide nanoparticles. Toxicol. Lett. 228, 103–110. https://doi.org/10.1016/j.toxlet.2014.04.014

Jibri, S.M., Jakada, B.H., Umar, H.Y., Ahmad, T.A., 2016. Importance of Some Algal Species as a Source of Food and Supplement. Int. J. Curr. Microbiol. Appl. Sci. 5, 186–193. https://doi.org/10.20546/ijcmas.2016.505.020

Kahru, A., Dubourguier, H.-C., 2010. From ecotoxicology to nanoecotoxicology. Toxicology, Potential Hazard of Nanoparticles: From Properties to Biological & Environmental Effects 269, 105–119. https://doi.org/10.1016/j.tox.2009.08.016

Khalifeh, F., Salari, H., Zamani, H., 2022. Mechanism of MnO_2 nanorods toxicity in marine microalgae *Chlorella sorokiniana* during long-term exposure. Mar. Environ. Res. 179, 105669. https://doi.org/10.1016/j.marenvres.2022.105669

Khan, M.I., Shin, J.H., Kim, J.D., 2018. The promising future of microalgae: current status, challenges, and optimization of a sustainable and renewable industry for biofuels, feed, and other products. *Microb. Cell Factories* 17, 36. https://doi.org/10.1186/s12934-018-0879-x

Kim, J.H., Affan, A., Jang, J., Kang, M.-H., Ko, A.-R., Jeon, S.-M., Oh, C., Heo, S.-J., Lee, Y.-H., Ju, S.-J., Kang, D.-H., 2015. Morphological, molecular, and biochemical characterization of astaxanthin-producing green microalga *Haematococcus* sp. KORDI03 (Haematococcaceae, Chlorophyta) isolated from Korea. *J. Microbiol. Biotechnol.* 25, 238–246. https://doi.org/10.4014/jmb.1410.10032

Kiser, M.A., Westerhoff, P., Benn, T., Wang, Y., Pérez-Rivera, J., Hristovski, K., 2009. Titanium Nanomaterial Removal and Release from Wastewater Treatment Plants. *Environ. Sci. Technol.* 43, 6757–6763. https://doi.org/10.1021/es901102n

Kondzior, P., Butarewicz, A., 2018. Effect of Heavy Metals (Cu and Zn) on the Content of Photosynthetic Pigments in the Cells of Algae *Chlorella Vulgaris. J. Ecol. Eng.* 19, 18–28. https://doi.org/10.12911/22998993/85375

Koyande, A.K., Chew, K.W., Rambabu, K., Tao, Y., Chu, D.-T., Show, P.-L., 2019. Microalgae: A potential alternative to health supplementation for humans. *Food Sci. Hum. Wellness* 8, 16–24. https://doi.org/10.1016/j.fshw.2019.03.001

Kumar, A., Dixit, C.K., 2017. 3 - Methods for characterization of nanoparticles, in: Nimesh, S., Chandra, R., Gupta, N. (Eds.), Advances in Nanomedicine for the Delivery of Therapeutic Nucleic Acids. *Woodhead Publishing*, pp. 43–58. https://doi.org/10.1016/B978-0-08-100557-6.00003-1

L, A., Devi, C.S., G, S., 2017a. Inhibition Effects of Cobalt Nano Particles Against Fresh Water Algal Blooms Caused by *Microcystis* and *Oscillatoria*. *Am. J. Appl. Sci. Res.* 3, 26. https://doi.org/10.11648/j.ajasr.20170304.12

L, A., Devi, C.S., G, S., 2017b. Inhibition Effects of Cobalt Nano Particles Against Fresh Water Algal Blooms Caused by *Microcystis* and *Oscillatoria*. *Am. J. Appl. Sci. Res.* 3, 26. https://doi.org/10.11648/j.ajasr.20170304.12

Landsiedel, R., Ma-Hock, L., Kroll, A., Hahn, D., Schnekenburger, J., Wiench, K., Wohlleben, W., 2010. Testing Metal-Oxide Nanomaterials for

Human Safety. *Adv. Mater.* 22, 2601–2627. https://doi.org/10.1002/adma.200902658

Lee, W.-M., An, Y.-J., 2013. Effects of zinc oxide and titanium dioxide nanoparticles on green algae under visible, UVA, and UVB irradiations: No evidence of enhanced algal toxicity under UV pre-irradiation. *Chemosphere* 91, 536–544. https://doi.org/10.1016/j.chemosphere.2012.12.033

Lei, C., Zhang, L., Yang, K., Zhu, L., Lin, D., 2016. Toxicity of iron-based nanoparticles to green algae: Effects of particle size, crystal phase, oxidation state and environmental aging. *Environ. Pollut.* 218, 505–512. https://doi.org/10.1016/j.envpol.2016.07.030

Li, C., Shuford, K.L., Park, Q.-H., Cai, W., Li, Y., Lee, E.J., Cho, S.O., 2007. High-Yield Synthesis of Single-Crystalline Gold Nano-octahedra. *Angew. Chem. Int. Ed*. 46, 3264–3268. https://doi.org/10.1002/anie.200604167

Li, F., Liang, Z., Zheng, X., Zhao, W., Wu, M., Wang, Z., 2015. Toxicity of nano-TiO_2 on algae and the site of reactive oxygen species production. *Aquat. Toxicol.* 158, 1–13. https://doi.org/10.1016/j.aquatox.2014.10.014

Li, M., Chen, D., Liu, Y., Chuang, C.Y., Kong, F., Harrison, P.J., Zhu, X., Jiang, Y., 2018. Exposure of engineered nanoparticles to *Alexandrium tamarense* (Dinophyceae): Healthy impacts of nanoparticles via toxin-producing dinoflagellate. *Sci. Total Environ.* 610–611, 356–366. https://doi.org/10.1016/j.scitotenv.2017.05.170

Li, M., Hu, C., Zhu, Q., Chen, L., Kong, Z., Liu, Z., 2006a. Copper and zinc induction of lipid peroxidation and effects on antioxidant enzyme activities in the microalga *Pavlova viridis* (Prymnesiophyceae). *Chemosphere* 62, 565–572. https://doi.org/10.1016/j.chemosphere.2005.06.029

Li, M., Hu, C., Zhu, Q., Chen, L., Kong, Z., Liu, Z., 2006b. Copper and zinc induction of lipid peroxidation and effects on antioxidant enzyme activities in the microalga Pavlova viridis (Prymnesiophyceae). Chemosphere 62, 565–572. https://doi.org/10.1016/j.chemosphere.2005.06.029

Li, X., Chen, Y., Ye, J., Fu, F., Pokhrel, G.R., Zhang, H., Zhu, Y., Yang, G., 2017. Determination of different arsenic species in food-grade spirulina

powder by ion chromatography combined with inductively coupled plasma mass spectrometry. *J. Sep. Sci.* 40, 3655–3661. https://doi.org/10.1002/jssc.201700618

Li, X., Lenhart, J.J., 2012. Aggregation and Dissolution of Silver Nanoparticles in Natural Surface Water. *Environ. Sci. Technol.* 46, 5378–5386. https://doi.org/10.1021/es204531y

Li, Y., Sommerfeld, M., Chen, F., Hu, Q., 2008. Consumption of oxygen by astaxanthin biosynthesis: A protective mechanism against oxidative stress in *Haematococcus pluvialis* (Chlorophyceae). *J. Plant Physiol.* 165, 1783–1797. https://doi.org/10.1016/j.jplph.2007.12.007

Li, Y., Zhou, W., Hu, B., Min, M., Chen, P., Ruan, R.R., 2012. Effect of light intensity on algal biomass accumulation and biodiesel production for mixotrophic strains *Chlorella kessleri* and *Chlorella protothecoide* cultivated in highly concentrated municipal wastewater. *Biotechnol. Bioeng.* 109, 2222–2229. https://doi.org/10.1002/bit.24491

Liang, S.X.T., Djearamane, S., Dhanapal, A.C.T.A., Wong, L.S., 2022a. Impact of silver nanoparticles on the nutritional properties of *Arthrospira platensis*. *PeerJ* 10, e13972. https://doi.org/10.7717/peerj.13972

Liang, S.X.T., Djearamane, S., Tanislaus Antony Dhanapal, A.C., Wong, L.S., 2022b. Impact of silver nanoparticles on the nutritional properties of *Arthrospira platensis*. *PeerJ* 10, e13972. https://doi.org/10.7717/peerj.13972

Liang, S.X.T., Wong, L.S., Dhanapal, A.C.T.A., Djearamane, S., 2020. Toxicity of Metals and Metallic Nanoparticles on Nutritional Properties of Microalgae. *Water. Air. Soil Pollut.* 231, 52. https://doi.org/10.1007/s11270-020-4413-5

Ling Shing, W., Batumalai, T., Cheng, H., Ong, H., 2019. The Effect of Copper Nanoparticle to Astaxanthin Content in Microalgae 6, 81–85.

Lohse, S.E., Abadeer, N.S., Zoloty, M., White, J.C., Newman, L.A., Murphy, C.J., 2017. Nanomaterial Probes in the Environment: Gold Nanoparticle Soil Retention and Environmental Stability as a Function of Surface Chemistry. *ACS Sustain. Chem. Eng.* 5, 11451–11458. https://doi.org/10.1021/acssuschemeng.7b02622

Lone, J.A., Kumar, A., Kundu, S., Lone, F.A., Suseela, M.R., 2013a. Characterization of Tolerance Limit in *Spirulina platensis* in Relation to Nanoparticles. *Water. Air. Soil Pollut.* 224, 1670. https://doi.org/10.1007/s11270-013-1670-6

Lone, J.A., Kumar, A., Kundu, S., Lone, F.A., Suseela, M.R., 2013b. Characterization of Tolerance Limit in *Spirulina platensis* in Relation to Nanoparticles. *Water. Air. Soil Pollut.* 224, 1670. https://doi.org/10.1007/s11270-013-1670-6

Machu, L., Misurcova, L., Vavra Ambrozova, J., Orsavova, J., Mlcek, J., Sochor, J., Jurikova, T., 2015. Phenolic Content and Antioxidant Capacity in Algal Food Products. *Molecules* 20, 1118–1133. https://doi.org/10.3390/molecules20011118

Mahana, A., Guliy, O.I., Mehta, S.K., 2021. Accumulation and cellular toxicity of engineered metallic nanoparticle in freshwater microalgae: Current status and future challenges. *Ecotoxicol. Environ. Saf.* 208, 111662. https://doi.org/10.1016/j.ecoenv.2020.111662

Manier, N., Bado-Nilles, A., Delalain, P., Aguerre-Chariol, O., Pandard, P., 2013. Ecotoxicity of non-aged and aged CeO_2 nanomaterials towards freshwater microalgae. *Environ. Pollut.* 180, 63–70. https://doi.org/10.1016/j.envpol.2013.04.040

Manzo, S., Miglietta, M.L., Rametta, G., Buono, S., Di Francia, G., 2013. Toxic effects of ZnO nanoparticles towards marine algae *Dunaliella tertiolecta. Sci. Total Environ.* 445–446, 371–376. https://doi.org/10.1016/j.scitotenv.2012.12.051

Mary Leema, J.T., Kirubagaran, R., Vinithkumar, N.V., Dheenan, P.S., Karthikayulu, S., 2010. High value pigment production from *Arthrospira (Spirulina) platensis* cultured in seawater. *Bioresour. Technol.* 101, 9221–9227. https://doi.org/10.1016/j.biortech.2010.06.120

Matos, J., Cardoso, C., Bandarra, N.M., Afonso, C., 2017. Microalgae as healthy ingredients for functional food: a review. *Food Funct.* 8, 2672–2685. https://doi.org/10.1039/C7FO00409E

Mehariya, S., Sharma, N., Iovine, A., Casella, P., Marino, T., Larocca, V., Molino, A., Musmarra, D., 2020. An Integrated Strategy for Nutraceuticals

from Haematoccus pluvialis: From Cultivation to Extraction. *Antioxid. Basel Switz.* 9, 825. https://doi.org/10.3390/antiox9090825

Menezes, R.S., Soares, A.T., Marques Júnior, J.G., Lopes, R.G., da Arantes, R.F., Derner, R.B., Filho, N.R.A., 2016. Culture medium influence on growth, fatty acid, and pigment composition of *Choricystis minor* var. minor: a suitable microalga for biodiesel production. *J. Appl. Phycol.* 28, 2679–2686. https://doi.org/10.1007/s10811-016-0828-1

Metsoviti, M.N., Papapolymerou, G., Karapanagiotidis, I.T., Katsoulas, N., 2019. Comparison of Growth Rate and Nutrient Content of Five Microalgae Species Cultivated in Greenhouses. *Plants* 8, 279. https://doi.org/10.3390/plants8080279

Metzler, D.M., Li, M., Erdem, A., Huang, C.P., 2011. Responses of algae to photocatalytic nano-TiO_2 particles with an emphasis on the effect of particle size. *Chem. Eng. J*. 170, 538–546. https://doi.org/10.1016/j.cej.2011.02.002

Miao, A.-J., Luo, Z., Chen, C.-S., Chin, W.-C., Santschi, P.H., Quigg, A., 2010. Intracellular Uptake: A Possible Mechanism for Silver Engineered Nanoparticle Toxicity to a Freshwater Alga *Ochromonas danica*. *PLOS ONE* 5, e15196. https://doi.org/10.1371/journal.pone.0015196

Miao, A.-J., Schwehr, K.A., Xu, C., Zhang, S.-J., Luo, Z., Quigg, A., Santschi, P.H., 2009. The algal toxicity of silver engineered nanoparticles and detoxification by exopolymeric substances. *Environ. Pollut.* 157, 3034–3041. https://doi.org/10.1016/j.envpol.2009.05.047

Miazek, K., Iwanek, W., Remacle, C., Richel, A., Goffin, D., 2015. Effect of Metals, Metalloids and Metallic Nanoparticles on Microalgae Growth and Industrial Product Biosynthesis: *A Review. Int. J. Mol. Sci.* 16, 23929–23969. https://doi.org/10.3390/ijms161023929

Middepogu, A., Hou, J., Gao, X., Lin, D., 2018. Effect and mechanism of TiO_2 nanoparticles on the photosynthesis of *Chlorella pyrenoidosa. Ecotoxicol. Environ. Saf.* 161, 497–506. https://doi.org/10.1016/j.ecoenv.2018.06.027

Mody, V., Siwale, R., Singh, A., Mody, H., 2010. Introduction to metallic nanoparticles. J. Pharm. Bioallied Sci. 2, 282. https://doi.org/10.4103/0975-7406.72127

Mohanraj, V.J., Chen, Y., 2007. Nanoparticles - *A review. Trop. J. Pharm. Res*. 5, 561–573. https://doi.org/10.4314/tjpr.v5i1.14634

Molino, A., Iovine, A., Casella, P., Mehariya, S., Chianese, S., Cerbone, A., Rimauro, J., Musmarra, D., 2018. Microalgae Characterization for Consolidated and New Application in Human Food, Animal Feed and Nutraceuticals. *Int. J. Environ. Res. Public. Health* 15, 2436. https://doi.org/10.3390/ijerph15112436

Monteiro, C.M., Castro, P.M.L., Malcata, F.X., 2012. Metal uptake by microalgae: Underlying mechanisms and practical applications. *Biotechnol. Prog.* 28, 299–311. https://doi.org/10.1002/btpr.1504

Moroney, J.V., Bartlett, S.G., Samuelsson, G., 2001. Carbonic anhydrases in plants and algae. *Plant Cell Environ.* 24, 141–153. https://doi.org/10.1111/j.1365-3040.2001.00669.x

Mularczyk, M., Michalak, I., Marycz, K., 2020. Astaxanthin and other Nutrients from *Haematococcus pluvialis*-Multifunctional Applications. *Mar. Drugs* 18, 459. https://doi.org/10.3390/md18090459

Nambara, K., Niikura, K., Mitomo, H., Ninomiya, T., Takeuchi, C., Wei, J., Matsuo, Y., Ijiro, K., 2016. Reverse Size Dependences of the Cellular Uptake of Triangular and Spherical Gold Nanoparticles. *Langmuir* 32, 12559–12567. https://doi.org/10.1021/acs.langmuir.6b02064

Navarro, E., Baun, A., Behra, R., Hartmann, N.B., Filser, J., Miao, A.-J., Quigg, A., Santschi, P.H., Sigg, L., 2008. Environmental behavior and ecotoxicity of engineered nanoparticles to algae, plants, and fungi. *Ecotoxicology* 17, 372–386. https://doi.org/10.1007/s10646-008-0214-0

Neal, C., Jarvie, H., Rowland, P., Lawler, A., Sleep, D., Scholefield, P., 2011. Titanium in UK rural, agricultural and urban/industrial rivers: Geogenic and anthropogenic colloidal/sub-colloidal sources and the significance of within-river retention. *Sci. Total Environ.* 409, 1843–1853. https://doi.org/10.1016/j.scitotenv.2010.12.021

Nielsen, S.S., 2010. Phenol-Sulfuric Acid Method for Total Carbohydrates, in: Nielsen, S.S. (Ed.), Food Analysis Laboratory Manual, Food Science Texts

Series. *Springer US, Boston, MA*, pp. 47–53. https://doi.org/10.1007/978-1-4419-1463-7_6

Oslan, S.N.H., Shoparwe, N.F., Yusoff, A.H., Rahim, A.A., Chang, C.S., Tan, J.S., Oslan, S.N., Arumugam, K., Ariff, A.B., Sulaiman, A.Z., Mohamed, M.S., 2021a. A Review on Haematococcus pluvialis Bioprocess Optimization of Green and Red Stage Culture Conditions for the Production of Natural Astaxanthin. *Biomolecules* 11, 256. https://doi.org/10.3390/biom11020256

Oslan, S.N.H., Tan, J.S., Oslan, S.N., Matanjun, P., Mokhtar, R.A.M., Shapawi, R., Huda, N., 2021b. *Haematococcus pluvialis* as a Potential Source of Astaxanthin with Diverse Applications in Industrial Sectors: Current Research and Future Directions. *Molecules* 26. https://doi.org/10.3390/molecules26216470

Oukarroum, A., Polchtchikov, S., Perreault, F., Popovic, R., 2012. Temperature influence on silver nanoparticles inhibitory effect on photosystem II photochemistry in two green algae, *Chlorella vulgaris* and *Dunaliella tertiolecta*. *Environ. Sci. Pollut. Res*. 19, 1755–1762. https://doi.org/10.1007/s11356-011-0689-8

Pádrová, K., Lukavský, J., Nedbalová, L., Čejková, A., Cajthaml, T., Sigler, K., Vítová, M., Řezanka, T., 2015. Trace concentrations of iron nanoparticles cause overproduction of biomass and lipids during cultivation of cyanobacteria and microalgae. *J. Appl. Phycol.* 27, 1443–1451. https://doi.org/10.1007/s10811-014-0477-1

Palmieri, D., Aliakbarian, B., Casazza, A.A., Ferrari, N., Spinella, G., Pane, B., Cafueri, G., Perego, P., Palombo, D., 2012. Effects of polyphenol extract from olive pomace on anoxia-induced endothelial dysfunction. *Microvasc. Res.* 83, 281–289. https://doi.org/10.1016/j.mvr.2012.02.010

Papapolymerou, G., Karayannis, V., Mpesios, A., Riga, A., Gougoulias, N., Spiliotis, X., 2019. Scaling-up sustainable *Chlorella vulgaris* microalgal biomass cultivation from laboratory to pilot-plant photobioreactor, towards biofuel. Glob. Nest J. 21, 37–42. https://doi.org/10.30955/gnj.002777

Pham, T.-L., 2019. Effect of Silver Nanoparticles on Tropical Freshwater and Marine Microalgae. *J. Chem.* 2019, 1–7. https://doi.org/10.1155/2019/9658386

Pillai, S., Behra, R., Nestler, H., Suter, M.J.-F., Sigg, L., Schirmer, K., 2014. Linking toxicity and adaptive responses across the transcriptome, proteome, and phenotype of *Chlamydomonas reinhardtii* exposed to silver. *Proc. Natl. Acad. Sci.* 111, 3490–3495. https://doi.org/10.1073/pnas.1319388111

Prokop, A., Bajpai, R.K., Zappi, M.E. (Eds.), 2015. Algal Biorefineries. Springer International Publishing, Cham. https://doi.org/10.1007/978-3-319-20200-6

Puspitasari, R., Suratno, Purbonegoro, T., Agustin, A.T., 2018. Cu toxicity on growth and chlorophyll-a of *Chaetoceros* sp. *IOP Conf. Ser. Earth Environ. Sci.* 118, 012061. https://doi.org/10.1088/1755-1315/118/1/012061

Recht, L., Zarka, A., Boussiba, S., 2012. Patterns of carbohydrate and fatty acid changes under nitrogen starvation in the microalgae *Haematococcus pluvialis* and *Nannochloropsis sp. Appl. Microbiol. Biotechnol.* 94, 1495–1503. https://doi.org/10.1007/s00253-012-3940-4

Rizwan, M., Mujtaba, G., Lee, K., 2017. Effects of iron sources on the growth and lipid/carbohydrate production of marine microalga *Dunaliella tertiolecta. Biotechnol. Bioprocess Eng.* 22, 68–75. https://doi.org/10.1007/s12257-016-0628-0

Rolland, J.P., Maynor, B.W., Euliss, L.E., Exner, A.E., Denison, G.M., DeSimone, J.M., 2005. Direct Fabrication and Harvesting of Monodisperse, Shape-Specific Nanobiomaterials. *J. Am. Chem. Soc.* 127, 10096–10100. https://doi.org/10.1021/ja051977c

Romero, N., Visentini, F.F., Márquez, V.E., Santiago, L.G., Castro, G.R., Gagneten, A.M., 2020. Physiological and morphological responses of green microalgae *Chlorella vulgaris* to silver nanoparticles. *Environ. Res.* 189, 109857. https://doi.org/10.1016/j.envres.2020.109857

Ruangsomboon, S., 2012. Effect of light, nutrient, cultivation time and salinity on lipid production of newly isolated strain of the green microalga, *Botryococcus braunii* KMITL 2. *Bioresour. Technol.* 109, 261–265. https://doi.org/10.1016/j.biortech.2011.07.025

Sadiq, I.M., Pakrashi, S., Chandrasekaran, N., Mukherjee, A., 2011. Studies on toxicity of aluminum oxide (Al_2O_3) nanoparticles to microalgae species: *Scenedesmus* sp. and *Chlorella* sp. *J. Nanoparticle Res.* 13, 3287–3299. https://doi.org/10.1007/s11051-011-0243-0

Sathasivam, R., Radhakrishnan, R., Hashem, A., Abd_Allah, E.F., 2019. Microalgae metabolites: A rich source for food and medicine. *Saudi J. Biol. Sci.* 26, 709–722. https://doi.org/10.1016/j.sjbs.2017.11.003

Semmler-Behnke, M., Kreyling, W.G., Lipka, J., Fertsch, S., Wenk, A., Takenaka, S., Schmid, G., Brandau, W., 2008. Biodistribution of 1.4- and 18-nm Gold Particles in Rats. *Small* 4, 2108–2111. https://doi.org/10.1002/smll.200800922

Sendra, M., Blasco, J., Araújo, C.V.M., 2018. Is the cell wall of marine phytoplankton a protective barrier or a nanoparticle interaction site? Toxicological responses of *Chlorella autotrophica* and *Dunaliella salina* to Ag and CeO_2 nanoparticles. *Ecol. Indic.* 95, 1053–1067. https://doi.org/10.1016/j.ecolind.2017.08.050

Sendra, M., Yeste, M.P., Gatica, J.M., Moreno-Garrido, I., Blasco, J., 2017. Direct and indirect effects of silver nanoparticles on freshwater and marine microalgae (*Chlamydomonas reinhardtii* and *Phaeodactylum tricornutum). Chemosphere* 179, 279–289. https://doi.org/10.1016/j.chemosphere.2017.03.123

Sengul, A.B., Asmatulu, E., 2020. Toxicity of metal and metal oxide nanoparticles: a review. *Environ. Chem. Lett.* 18, 1659–1683. https://doi.org/10.1007/s10311-020-01033-6

Shah, M., Liang, Y., Cheng, J., Daroch, M., 2016. Astaxanthin-Producing Green Microalga *Haematococcus pluvialis*: From Single Cell to High Value Commercial Products. *Front. Plant Sci.*

Shah, M.M.R., Liang, Y., Cheng, J.J., Daroch, M., 2016. Astaxanthin-Producing Green Microalga *Haematococcus pluvialis*: From Single Cell to High Value Commercial Products. *Front. Plant Sci.* 7, 531. https://doi.org/10.3389/fpls.2016.00531

Sharma, J., Kumar, S.S., Bishnoi, N.R., Pugazhendhi, A., 2019. Screening and enrichment of high lipid producing microalgal consortia. *J. Photochem. Photobiol.* B 192, 8–12. https://doi.org/10.1016/j.jphotobiol.2019.01.002

Sheng, P.X., Ting, Y.-P., Chen, J.P., Hong, L., 2004. Sorption of lead, copper, cadmium, zinc, and nickel by marine algal biomass: characterization of biosorptive capacity and investigation of mechanisms. *J. Colloid Interface Sci.* 275, 131–141. https://doi.org/10.1016/j.jcis.2004.01.036

Shi, H., Magaye, R., Castranova, V., Zhao, J., 2013. Titanium dioxide nanoparticles: a review of current toxicological data. *Part. Fibre Toxicol.* 10, 15. https://doi.org/10.1186/1743-8977-10-15

Srivastava, V., Gusain, D., Sharma, Y.C., 2015. Critical Review on the Toxicity of Some Widely Used Engineered Nanoparticles. *Ind. Eng. Chem. Res.* 54, 6209–6233. https://doi.org/10.1021/acs.iecr.5b01610

Sukenik, A., Carmeli, Y., Berner, T., 1989. Regulation of Fatty Acid Composition by Irradiance Level in the Eustigmatophyte *Nannochloropsis* sp. *J. Phycol*. 25, 686–692. https://doi.org/10.1111/j.0022-3646.1989.00686.x

Suman, T.Y., Radhika Rajasree, S.R., Kirubagaran, R., 2015. Evaluation of zinc oxide nanoparticles toxicity on marine algae *Chlorella vulgaris* through flow cytometric, cytotoxicity and oxidative stress analysis. *Ecotoxicol. Environ. Saf.* 113, 23–30. https://doi.org/10.1016/j.ecoenv.2014.11.015

Sztretye, M., Dienes, B., Gönczi, M., Czirják, T., Csernoch, L., Dux, L., Szentesi, P., Keller-Pintér, A., 2019. Astaxanthin: A Potential Mitochondrial-Targeted Antioxidant Treatment in Diseases and with Aging. *Oxid. Med. Cell. Longev.* 2019, 1–14. https://doi.org/10.1155/2019/3849692

Tang, Y., Li, S., Qiao, J., Wang, H., Li, L., 2013. Synergistic effects of nano-sized titanium dioxide and zinc on the photosynthetic capacity and survival of *Anabaena* sp. *Int. J. Mol. Sci.* 14, 14395–14407. https://doi.org/10.3390/ijms140714395

Tibbetts, S.M., Milley, J.E., Lall, S.P., 2015. Chemical composition and nutritional properties of freshwater and marine microalgal biomass cultured in photobioreactors. *J. Appl. Phycol*. 27, 1109–1119. https://doi.org/10.1007/s10811-014-0428-x

Tripathi, U., Sarada, R., Rao, S.R., Ravishankar, G.A., 1999. Production of astaxanthin in *Haematococcus pluvialis* cultured in various media. *Bioresour. Technol.* 68, 197–199. https://doi.org/10.1016/S0960-8524(98)00143-6

Vance, M.E., Marr, L.C., 2015. Exposure to airborne engineered nanoparticles in the indoor environment. *Atmos. Environ.* 106, 503–509. https://doi.org/10.1016/j.atmosenv.2014.12.056

Venkatesh, N., 2018a. Metallic Nanoparticle: A Review. *Biomed. J. Sci. Tech. Res.* 4. https://doi.org/10.26717/BJSTR.2018.04.0001011

Venkatesh, N., 2018b. Metallic Nanoparticle: A Review. *Biomed. J. Sci. Tech. Res.* 4. https://doi.org/10.26717/BJSTR.2018.04.0001011

Vidhyavathi, R., Venkatachalam, L., Sarada, R., Ravishankar, G.A., 2008. Regulation of carotenoid biosynthetic genes expression and carotenoid accumulation in the green alga *Haematococcus pluvialis* under nutrient stress conditions. *J. Exp. Bot.* 59, 1409–1418. https://doi.org/10.1093/jxb/ern048

Vogt, T., 2010. Phenylpropanoid Biosynthesis. *Mol. Plan*t 3, 2–20. https://doi.org/10.1093/mp/ssp106

Wang, Guan, Xu, Ding, Ma, Ma, Terry, 2019. Effects of Nanoparticles on Algae: Adsorption, Distribution, Ecotoxicity and Fate. *Appl. Sci.* 9, 1534. https://doi.org/10.3390/app9081534

Wang, T., Jiang, H., Wan, L., Zhao, Q., Jiang, T., Wang, B., Wang, S., 2015. Potential application of functional porous TiO_2 nanoparticles in light-controlled drug release and targeted drug delivery. *Acta Biomater*. 13, 354–363. https://doi.org/10.1016/j.actbio.2014.11.010

Wang, Y., Tibbetts, S.M., McGinn, P.J., 2021. Microalgae as Sources of High-Quality Protein for Human Food and Protein Supplements. *Foods* 10, 3002. https://doi.org/10.3390/foods10123002

Weir, A., Westerhoff, P., Fabricius, L., Hristovski, K., von Goetz, N., 2012a. Titanium Dioxide Nanoparticles in Food and Personal Care Products. *Environ. Sci. Technol.* 46, 2242–2250. https://doi.org/10.1021/es204168d

Weir, A., Westerhoff, P., Fabricius, L., Hristovski, K., von Goetz, N., 2012b. Titanium Dioxide Nanoparticles in Food and Personal Care Products. *Environ. Sci. Technol.* 46, 2242–2250. https://doi.org/10.1021/es204168d

Wiench, K., Wohlleben, W., Hisgen, V., Radke, K., Salinas, E., Zok, S., Landsiedel, R., 2009. Acute and chronic effects of nano- and non-nano-scale TiO_2 and ZnO particles on mobility and reproduction of the freshwater invertebrate *Daphnia magna*. *Chemosphere* 76, 1356–1365. https://doi.org/10.1016/j.chemosphere.2009.06.025

Wijffels, R.H., Barbosa, M.J., Eppink, M.H.M., 2010. Microalgae for the production of bulk chemicals and biofuels. *Biofuels Bioprod. Biorefining* 4, 287–295. https://doi.org/10.1002/bbb.215

Wong, S.W.Y., Leung, P.T.Y., Djurisić, A.B., Leung, K.M.Y., 2010. Toxicities of nano zinc oxide to five marine organisms: influences of aggregate size and ion solubility. *Anal. Bioanal. Chem.* 396, 609–618. https://doi.org/10.1007/s00216-009-3249-z

Xia, B., Chen, B., Sun, X., Qu, K., Ma, F., Du, M., 2015a. Interaction of TiO_2 nanoparticles with the marine microalga *Nitzschia closterium*: Growth inhibition, oxidative stress and internalization. *Sci. Total Environ.* 508, 525–533. https://doi.org/10.1016/j.scitotenv.2014.11.066

You, D.G., Deepagan, V.G., Um, W., Jeon, S., Son, S., Chang, H., Yoon, H.I., Cho, Y.W., Swierczewska, M., Lee, S., Pomper, M.G., Kwon, I.C., Kim, K., Park, J.H., 2016. ROS-generating TiO_2 nanoparticles for non-invasive sonodynamic therapy of cancer. *Sci. Rep*. 6, 23200. https://doi.org/10.1038/srep23200

Yu, L., Fang, T., Xiong, D., Zhu, W., Sima, X., 2011. Comparative toxicity of nano-ZnO and bulk ZnO suspensions to zebrafish and the effects of sedimentation, ˙OH production and particle dissolution in distilled water. *J. Environ. Monit.* 13, 1975. https://doi.org/10.1039/c1em10197h

Yuan, L., Li, Y., Zeng, T., Wang, D., Liu, X., Xu, Q., Yang, Q., Yang, F., Chen, H., 2021. Revealing how the entering nano-titanium dioxide in wastewater worsened sludge dewaterability. *Chem. Eng. J.* 411, 128465. https://doi.org/10.1016/j.cej.2021.128465

Zeng, M.-T., Vonshak, A., 1998. Adaptation of *Spirulina platensis* to salinity-stress. Comp. *Biochem. Physiol. A. Mol. Integr. Physiol.* 120, 113–118. https://doi.org/10.1016/S1095-6433(98)10018-1

Zhao, J., Cao, X., Liu, X., Wang, Z., Zhang, C., White, J.C., Xing, B., 2016. Interactions of CuO nanoparticles with the algae *Chlorella pyrenoidosa* : adhesion, uptake, and toxicity. *Nanotoxicology* 10, 1297–1305. https://doi.org/10.1080/17435390.2016.1206149

Zhu, S., Wang, Y., Shang, C., Wang, Z., Xu, J., Yuan, Z., 2015. Characterization of lipid and fatty acids composition of *Chlorella zofingiensis* in response to nitrogen starvation. *J. Biosci. Bioeng.* 120, 205–209. https://doi.org/10.1016/j.jbiosc.2014.12.018

Zhu, X., Chang, Y., Chen, Y., 2010. Toxicity and bioaccumulation of TiO_2 nanoparticle aggregates in *Daphnia magna*. *Chemosphere* 78, 209–215. https://doi.org/10.1016/j.chemosphere.2009.11.013

Zhu, X., Zhou, J., Cai, Z., 2011. The toxicity and oxidative stress of TiO_2 nanoparticles in marine abalone (*Haliotis diversicolor supertexta*). *Mar. Pollut. Bull*. 63, 334–338. https://doi.org/10.1016/j.marpolbul.2011.03.006

Ziental, D., Czarczynska-Goslinska, B., Mlynarczyk, D.T., Glowacka-Sobotta, A., Stanisz, B., Goslinski, T., Sobotta, L., 2020. Titanium Dioxide Nanoparticles: Prospects and Applications in Medicine. *Nanomaterials* 10, 387. https://doi.org/10.3390/nano10020387

Zinicovscaia, I., Chiriac, T., Cepoi, L., Rudi, L., Culicov, O., Frontasyeva, M., Rudic, V., 2017a. Selenium uptake and assessment of the biochemical changes in *Arthrospira* (*Spirulina*) *platensis* biomass during the synthesis of selenium nanoparticles. *Can. J. Microbiol*. 63, 27–34. https://doi.org/10.1139/cjm-2016-0339

Zinicovscaia, I., Yushin, N., Pantelica, A., Demcak, S., Mitu, A., Apostol, A., 2020. Lithium Biosorption by *Arthrospira (Spirulina) platensis* Biomass 27, 271–280. https://doi.org/10.2478/eces-2020-0017

LIST OF PUBLICATIONS AND CONFERENCE PRESENTATIONS

PUBLICATIONS

1. Mahendran, M.S., Wong, L.S., Dhanapal, A.C.T.A., Djearamane, S., 2023. The Effect of Titanium Dioxide Nanoparticles on *Haematococcus pluvialis* Biomass Concentration. *J. Exp. Biol. Agric. Sci*. 11, 416–422. https://doi.org/10.18006/2023.11(2).416.422.

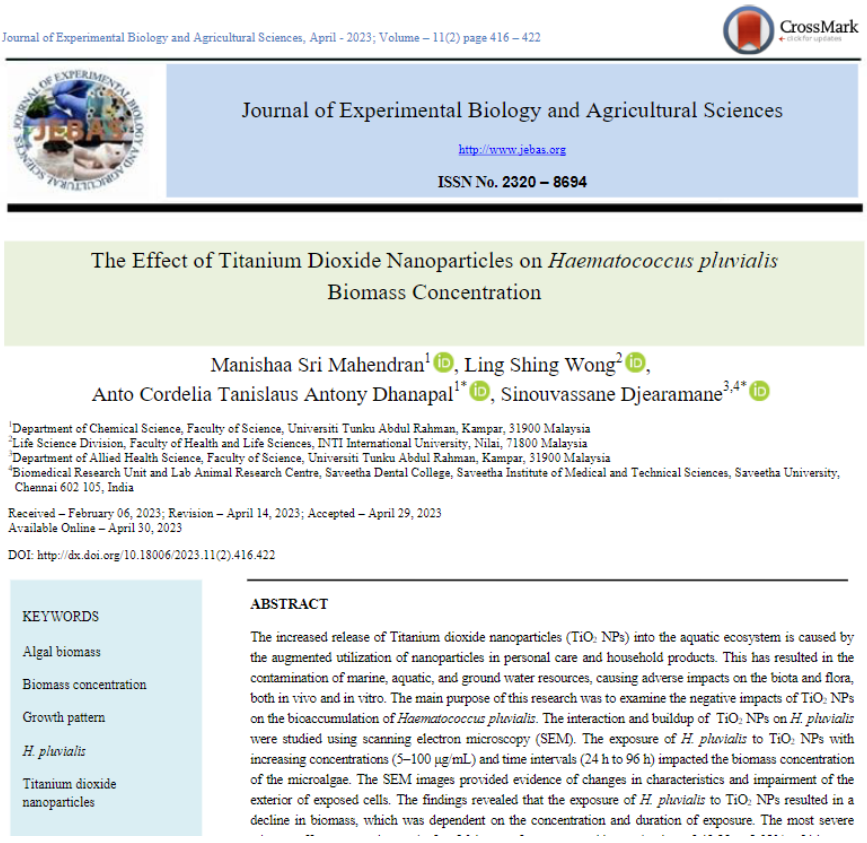

Journal of Experimental Biology and Agricultural Sciences, April - 2023; Volume – 11(2) page 416 – 422

Journal of Experimental Biology and Agricultural Sciences

http://www.jebas.org

ISSN No. 2320 – 8694

The Effect of Titanium Dioxide Nanoparticles on *Haematococcus pluvialis* Biomass Concentration

Manishaa Sri Mahendran[1], Ling Shing Wong[2], Anto Cordelia Tanislaus Antony Dhanapal[1*], Sinouvassane Djearamane[3,4*]

[1]Department of Chemical Science, Faculty of Science, Universiti Tunku Abdul Rahman, Kampar, 31900 Malaysia
[2]Life Science Division, Faculty of Health and Life Sciences, INTI International University, Nilai, 71800 Malaysia
[3]Department of Allied Health Science, Faculty of Science, Universiti Tunku Abdul Rahman, Kampar, 31900 Malaysia
[4]Biomedical Research Unit and Lab Animal Research Centre, Saveetha Dental College, Saveetha Institute of Medical and Technical Sciences, Saveetha University, Chennai 602 105, India

Received – February 06, 2023; Revision – April 14, 2023; Accepted – April 29, 2023
Available Online – April 30, 2023

DOI: http://dx.doi.org/10.18006/2023.11(2).416.422

KEYWORDS

Algal biomass

Biomass concentration

Growth pattern

H. pluvialis

Titanium dioxide nanoparticles

ABSTRACT

The increased release of Titanium dioxide nanoparticles (TiO_2 NPs) into the aquatic ecosystem is caused by the augmented utilization of nanoparticles in personal care and household products. This has resulted in the contamination of marine, aquatic, and ground water resources, causing adverse impacts on the biota and flora, both in vivo and in vitro. The main purpose of this research was to examine the negative impacts of TiO_2 NPs on the bioaccumulation of *Haematococcus pluvialis*. The interaction and buildup of TiO_2 NPs on *H. pluvialis* were studied using scanning electron microscopy (SEM). The exposure of *H. pluvialis* to TiO_2 NPs with increasing concentrations (5–100 µg/mL) and time intervals (24 h to 96 h) impacted the biomass concentration of the microalgae. The SEM images provided evidence of changes in characteristics and impairment of the exterior of exposed cells. The findings revealed that the exposure of *H. pluvialis* to TiO_2 NPs resulted in a decline in biomass, which was dependent on the concentration and duration of exposure. The most severe

2. Mahendran, M.S., Dhanapal, A.C.T.A., Wong, L.S., Kasivelu, G., Djearamane, S., 2021a. Microalgae as a Potential Source of Bioactive Food Compounds. *Curr. Res. Nutr. Food Sci*. J. 9, 917–927.

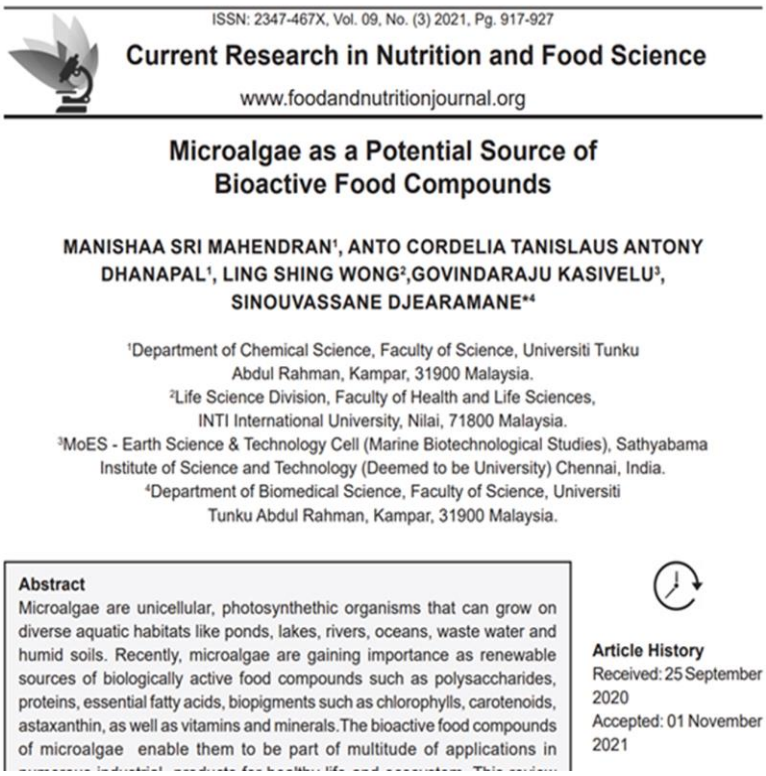

ISSN: 2347-467X, Vol. 09, No. (3) 2021, Pg. 917-927

Current Research in Nutrition and Food Science

www.foodandnutritionjournal.org

Microalgae as a Potential Source of Bioactive Food Compounds

MANISHAA SRI MAHENDRAN[1], ANTO CORDELIA TANISLAUS ANTONY DHANAPAL[1], LING SHING WONG[2],GOVINDARAJU KASIVELU[3], SINOUVASSANE DJEARAMANE*[4]

[1]Department of Chemical Science, Faculty of Science, Universiti Tunku Abdul Rahman, Kampar, 31900 Malaysia.
[2]Life Science Division, Faculty of Health and Life Sciences, INTI International University, Nilai, 71800 Malaysia.
[3]MoES - Earth Science & Technology Cell (Marine Biotechnological Studies), Sathyabama Institute of Science and Technology (Deemed to be University) Chennai, India.
[4]Department of Biomedical Science, Faculty of Science, Universiti Tunku Abdul Rahman, Kampar, 31900 Malaysia.

Abstract

Microalgae are unicellular, photosynthethic organisms that can grow on diverse aquatic habitats like ponds, lakes, rivers, oceans, waste water and humid soils. Recently, microalgae are gaining importance as renewable sources of biologically active food compounds such as polysaccharides, proteins, essential fatty acids, biopigments such as chlorophylls, carotenoids, astaxanthin, as well as vitamins and minerals.The bioactive food compounds of microalgae enable them to be part of multitude of applications in

Article History

Received: 25 September 2020

Accepted: 01 November 2021

3. Mahendran, M.S., Djearamane, S., Wong, L.S., Kasivelu, G., Dhanapal, A.C.T.A., 2021b. ANTIVIRAL PROPERTIES OF MICROALGAE AND CYANOBACTERIA. *J. Exp. Biol. Agric. Sci. 9*, S43–S48. https://doi.org/10.18006/2021.9(Spl-1 GCSGD_2020).S43.S48

Journal of Experimental Biology and Agricultural Sciences, March - 2021; Volume – 9(Spl-1- GCSGD_2020) page S43 – S48

Journal of Experimental Biology and Agricultural Sciences

http://www.jebas.org

ISSN No. 2320 – 8694

ANTIVIRAL PROPERTIES OF MICROALGAE AND CYANOBACTERIA

Manishaa Sri Mahendran[1], Sinouvassane Djearamane[2], Ling Shing Wong[3], Govindaraju Kasivelu[4], Anto Cordelia Tanislaus Antony Dhanapal[1*]

[1]Department of Chemical Science, Faculty of Science, Universiti Tunku Abdul Rahman, Kampar, 31900 Malaysia;
[2]Department of Biomedical Science, Faculty of Science, Universiti Tunku Abdul Rahman, Kampar, 31900 Malaysia
[3]Life Science Division, Faculty of Health and Life Sciences, INTI International University, Nilai, 71800 Malaysia;
[4]Centre for Ocean Research, MoES - Earth Science & Technology Cell (Marine Biotechnological Studies), Sathyabama Institute of Science and Technology (Deemed to be University), Chennai, 600119 India.

Received – July 18, 2020; Revision – September 17, 2020; Accepted – January 03, 2021
Available Online – March 25, 2021

DOI: http://dx.doi.org/10.18006/2021.9(Spl-1-GCSGD_2020).S43.S48

KEYWORDS

Microalgae

Cyanobacteria

Antiviral properties

Bioactive compounds

ABSTRACT

The recent outbreak of Corona Virus Disease (COVID-19) and the surge in accelerating the development of a vaccine to fight against the SARS-CoV-2 virus has imposed greater challenges to humanity worldwide. There is lack of research into the production of effective vaccines and methods of treatment against viral infections. As of now, strategies encompassing antiviral drugs and corticosteroids alongside mechanical respiratory treatment are in practice as frontline treatments. Though studies have reported that microalgae possess antiviral properties, only a few cases have presented the existence of antiviral compounds such as algal polysaccharides, lectins, aggluttinins, scytovirin, algal lipids such as sulfoquinovosyldiacylglycerol (SQDG), monogalactosyldiacylglycerides (MGDG) and

CONFERENCE PRESENTATIONS

1. Mahendran, M.S., Djearamane, S., Wong, L.S., Antony Dhanapal, A.C.T. "The Detrimental Effects of Titanium Dioxide Nanoparticles on *Haematococcus pluvialis*". *International Conference on Green Sustainable Technology and Management (ICGSTM) 2022* held by INTI International University on 10 – 11 June 2022. (Oral presentation)

2. Mahendran, M.S., Djearamane, S., Wong, L.S., Antony Dhanapal, A.C.T. “Impact of silver nanoparticles *Spirulina platensis*”. Global Congress on Sustainability for Growth & Development 2020 held by Einstein Research Academy on 18 July 2020. (Poster presentation)

APPENDIX A

Preparation of Chemical Reagents and Solvents

Culture medium for *H. pluvialis*

Sigma-Aldrich, Malaysia provided the culture medium for *H. pluvialis*. To make the working culture medium, 20ml of Basal bold medium (BBM) was mixed with 1L of distilled water that had been sterilized using autoclaving at 121°C for 30 minutes with 15 psi pressure. The chemical composition of BBM includes the following components and their corresponding amounts: $NaNO_3$ (0.25), $CaCl_2 \cdot 2H_2O$ (0.025), $MgSO_4 \cdot 7H_2O$ (0.075), $NaHCO_3$ (0.0126), K_2HPO_4 (0.075), KH_2PO_4 (0.175), NaCl (0.025), $Na_2EDTA \cdot 2H_2O$ (0.05), KOH (0.031), $FeSO_4 \cdot 7H_2O$ (0.005), $FeCl_3 \cdot 6H_2O$ (0.00315), H_3BO_3 (0.01142), $ZnSO_4 \cdot 7H_2O$ (0.00882), $MnCl_2 \cdot 4H_2O$ (0.00144), MoO_3 (0.00071), $Na_2MoO_4 \cdot 2H_2O$ (0.000006), $CuSO_4 \cdot 5H_2O$ (0.00157), $Co(NO_3)_2 \cdot 6H_2O$ (0.00049), and $CoCl_2 \cdot 6H_2O$ (0.00001) (Menezes et al., 2016).

Culture medium with (TiO_2 NPs)

Chemical Solution in Malaysia sold TiO_2 NPs which were used in this experiment. To prepare a stock culture solution of TiO_2 NPs at a concentration of 200 μg/mL, 0.14 g of TiO_2 NPs powder was added to 700 mL of BBM and then subjected to ultrasonication using a Tru-Sweep Ultrasonic Cleaner from Crest Ultrasonics in Malaysia, operating at 40 kHz until the NPs were evenly dispersed in the medium. Working concentrations of 100 μg/mL (1:2 dilution), 50 μg/mL (1:4 dilution), 25 μg/mL (1:8 dilution), 10 μg/mL (1:20 dilution), and 5 μg/mL (1:40 dilution) of TiO_2 NPs were then prepared by diluting the stock solution with BBM.

Phosphate buffered saline (PBS)

Sigma-Aldrich, Malaysia provided the initial solution of Phosphate Buffered Saline (PBS) at a concentration of 10 times (10x). To make a less concentrated solution, 1x PBS, a dilution was performed by mixing 100 mL of the 10x solution with 900 mL of distilled water.

Protein Assay

Bovine serum albumin (BSA, 100 μg/mL) powder was obtained from Sigma-Aldrich, Malaysia. NaOH and NaK tartrate·$4H_2O$ were purchased from Sigma- Aldrich, Malaysia, and Fisher Chemical, Malaysia, respectively. Folin-

Ciocalteu phenol reagent was provided by R&M Chemicals, Malaysia. The stock solution of BSA, 100 μg/mL was made by dissolving 5 mg of BSA powder in 50 mL of distilled water. The stock solution of BSA was then diluted with distilled water to prepare the working concentrations of 10, 20, 30, 40 and 50 μg/mL. Sodium hydroxide (NaOH, 0.5 N) solution was made by dissolving 20 g of NaOH pellet in 1000 mL distilled water. Lowry solution was mixed up afresh for every usage using Lowry reagents A (2% (w/v) Na_2CO_3 in 0.1 N NaOH), B (1% (w/v) NaK tartrate·$4H_2O$), and C (0.5% (w/v) $CuSO_4$·$4H_2O$) with the ratio of reagent A:B: C = 48:1:1. The preparation for Lowry reagent A, B, and C were as follows: Lowry reagent A: 2 g of sodium carbonate (Na_2CO_3) and 0.4 g of NaOH in 100 mL of distilled water; Lowry reagent B: 1 g of potassium sodium tartrate tetrahydrate (NaK tartrate·$4H_2O$) in 99 mL of distilled water; Lowry reagent C: 0.5 g of copper sulphate ($CuSO_4$) in 99.5 mL distilled water. Folin-Ciocalteu phenol reagent (FCR, 1 N) was prepared freshly by dissolving FCR with distilled water in a 1:1 ratio.

Lipid Assay

Chloroform was purchased from Fisher Chemical, Malaysia and methanol was purchased from RCI Labscan, Malaysia. Chloroform/methanol/water (1/2/0.8, v/v/v) was prepared by mixing 200 mL of chloroform, 400 mL of methanol, and 160 mL of distilled water to produce 760 mL of the solution.

Carbohydrate Assay

Glucose and hydrochloric acid (HCl, 2.5M) were obtained from Fisher Chemical, Malaysia, and QRë, Malaysia. By combining 5 mg of glucose powder with 50 mL of distilled water, a stock solution for glucose (100 g/mL) was created. To make the working concentrations of 10, 20, 30, 40, and 50 g/mL, distilled water was used to dilute the stock solution. 41 mL of 37% HCl were dissolved in 159 mL of clean water to create 2.5 N hydrochloric acid. 40 g of phenol were dissolved in 10 g of distilled water to create phenol (80%, w/w).

Chlorophyll-a and Carotenoid Assay

To get 1 L of 90% methanol solution, 900 mL of methanol was diluted in 100 mL of distilled water

Astaxanthin Assay

Acetone and hydrochloric acid (HCl, 2.5M) were obtained from Fisher Chemical, Malaysia and QRë, Malaysia.